CRANFIELD UNIVERSITY

SUBRAMANIAN JEYAKANDAN

DEVELOPMENT OF HYBRID LASER ARC WELDING PROCESS FOR AUTOMOTIVE STRUCTURAL APPLICATIONS

SCHOOL OF AEROSPACE, TRANSPORT AND MANUFACTURING
MRes Welding Engineering

MRes THESIS
Academic Year: 2018 - 2019

Supervisors: Dr. Supriyo Ganguly and Dr. Wojciech Suder
September 2019

CRANFIELD UNIVERSITY

SCHOOL OF AEROSPACE, TRANSPORT AND MANUFACTURING
MRes Welding Engineering

MRes THESIS

Academic Year 2018 - 2019

SUBRAMANIAN JEYAKANDAN

DEVELOPMENT OF HYBRID LASER ARC WELDING PROCESS FOR AUTOMOTIVE STRUCTURAL APPLICATIONS

Supervisors: Dr. Supriyo Ganguly and Dr. Wojciech Suder
September 2019

This thesis is submitted in fulfilment of the requirements for the degree of Master of Science

ABSTRACT

In today's world, two-wheelers (Motorcycles and Scooters) have become an indispensable part of people's lives. Customers are demanding high quality product with superior performance of the vehicle. Frame is one of the safety critical part of a two-wheeler which highly contributes to the functional and aesthetic quality of the vehicle. Predominantly, gas metal arc welding (GMAW) process is being used for the manufacturing of frame. Limited depth of penetration and low welding speed of GMAW process significantly hinders the quality and productivity. Moreover, high heat input of this process consequently results in larger distortion. High fusion zone and HAZ area leads to degradation of material properties. Better structural integrity and consistent frame dimensions are required to meet the functional and finish quality requirements of a vehicle. Hence, advanced laser welding processes were investigated as an alternative method to GMAW process in the facets of productivity, heat input, weld bead geometry, aesthetic quality, gap bridgeability and distortion. Typically two-wheeler frame is made of low carbon steel. Thus low carbon steel of S275 grade was used for the evaluation. The outcomes were compared with existing GMAW process to quantify the benefits of laser welding.

High power density of autogenous laser welding (ALW) process provided deeper penetration with significant improvement in productivity. When compared with GMAW process, productivity was improved by a factor of 8 times in 2 mm and 4 mm thick plates whereas 3 times improved productivity was achieved in 8 mm thick plates with complete penetration. However, lack of reinforcement and restricted part fit-up tolerance were found to be the critical limitations of ALW process. On the other hand, addition of filler metal using a GMAW arc in hybrid laser arc welding process (HLAW) ensured a better weld geometry and improved gap bridgeability of the process. Moreover, it was provided deeper penetration and significant improvement in productivity which is comparable to ALW process and far higher than GMAW process. Both HLAW and ALW processes produced ~75% and ~85% less distortion than GMAW process respectively.

Moreover, HLAW process improved the productivity with considerably less increase in hardness than ALW process. For instance, in 2 mm thick material, productivity was improved by 8 times than GMAW process with 55% and 17% increase in average fusion zone hardness in ALW and HLAW processes respectively. Moreover, substantial reduction in fusion zone and HAZ width was obtained in both HLAW and ALW processes. In mechanical strength standpoint, all three welding processes produced weld region stronger than base material. Therefore, fracture was occurred in the base material during tensile test. Overall, HLAW process combines the advantages of both individual processes and eliminates the limitations of them. Hence, hybrid laser arc welding process can be considered as the future of welding in the automobile sector.

Keywords

Productivity; weld bead geometry; gap bridgeability; distortion; mechanical properties; gas metal arc welding; autogenous laser welding; hybrid laser arc welding.

LIST OF PUBLICATIONS

- Subramanian, J., Ganguly, S., Mukherjee, D. and Shumshudeen, S. (2018) ‘Advanced welding processes for distortion reduction : A Review’, International Research Journal of Engineering and Technology (IRJET), 05(12), pp. 795–798.
- Subramanian, J., Ganguly, S., Suder, W. and Mukherjee, D. (2019) ‘Influence of welding processes on weld bead geometry’, International Research Journal of Engineering and Technology (IRJET), 06(01), pp. 635–639.

ACKNOWLEDGEMENTS

I would like to thank TVS Motor Company Ltd. for giving me the opportunity to pursue Masters in Welding engineering. I also wish to thank the members of Welding Engineering and Laser Processing Centre at Cranfield University.

I would like to express my deepest gratitude to my supervisors Dr. Supriyo Ganguly and Dr. Wojciech Suder for their extensive support and guidance throughout the course.

I want to express my utmost gratitude to Mr RM Chokkalingam, Mr S Saravanan and Mr Abhinay Choudary from TVS Motor Company Ltd. Special thanks to Mr Debajyoti Mukherjee from TVS Motor Company Ltd. for his guidance and valuable inputs during the discussions and reviews.

I offer my sincere thanks to Mr John Thrower, Mr Flemming Niselsen, Mr Nisar Shah, Mr Steve Pope, Mr Jarryd Braithwaite, Mr Ben Hopper and Mr Andrea Giampiccolo for taking time among their work to extend support during the experimentation and testing phases.

TABLE OF CONTENTS

LIST OF FIGURES

LIST OF TABLES

LIST OF EQUATIONS

NOMENCLATURE

1G	Flat welding position
ALW	Autogenous laser welding
AQ	Aesthetic quality
AQI	Aesthetic quality index
Ar	Argon
AWL	Applied weld load
BM	Base material
C-Mn	Carbon-Manganese
CMT	Cold metal transfer
CO_2	Carbon dioxide
Cpk	Process capability
CTWD	Contact tip to work distance
CW	Continuous wave
DC	Direct current
Df	Defocusing distance
DIC	Digital image correlation
d_{la}	Distance between laser and arc
E_{arc}	Energy of arc welding
E_{HLAW}	Energy of hybrid laser arc welding
E_{laser}	Energy of laser welding
E_{SP}	Specific point energy
fps	Frames per seconds
FQ	Functional quality
FZ	Fusion zone
GMA	Gas metal arc
GMAW	Gas metal arc welding

HAZ	Heat affected zone
He	Helium
HLAW	Hybrid laser arc welding
HSLA	High strength low alloy
HSS	High strength steel
I	Current
LBW	Laser beam welding
P_L	Laser power
q_p	Power density
SAW	Submerged arc welding
T_i	Interaction time
TIG	Tungsten inert gas
TS	Travel speed
TVSM	TVS Motor Company ltd.
U	Voltage of arc
V	Welding speed
WFS	Wire feed speed

1 Introduction

1.1 Background

In today's world, private mobility is no longer a privilege that only a select few can afford. Two-wheelers (Motorcycles and Scooters) have become an essential part of people's lives. The increase in range and variety of the products has further supported the growth of the business as customers are attracted by the choices. The growth in sales of two-wheelers has been phenomenal over the past few years as shown in Figure 1-1. Therefore to cope with increasing customer demand, automobile industries have ramped up their production rate over the past few years [1].

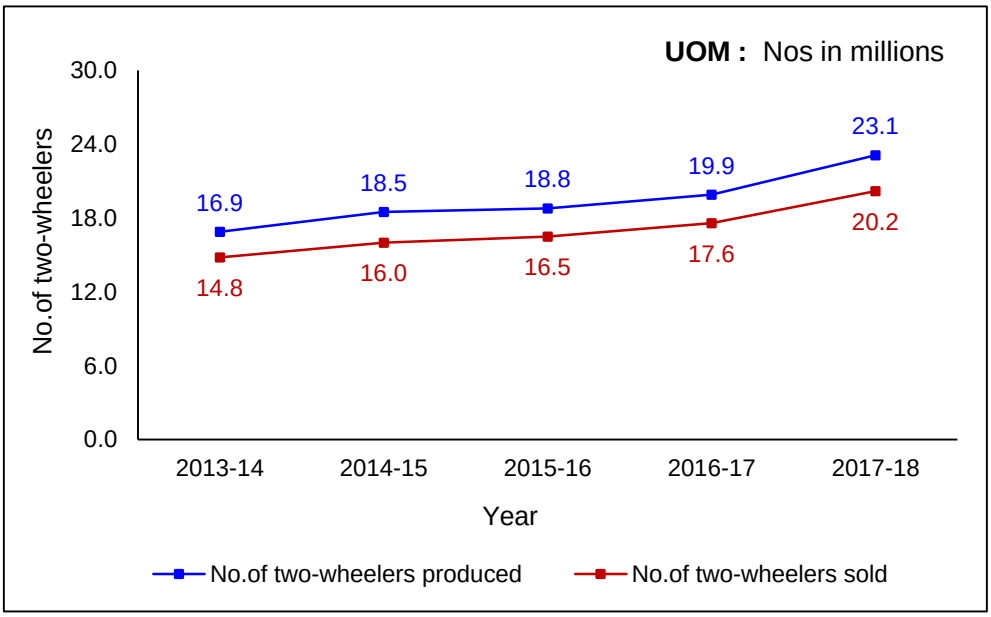

Figure 1-1 Two-wheelers domestic sales and production trend in India from 2013-2018 [1]

This ever-increasing demand stems the heavy competition in the market hence automobile industries strive to produce two-wheelers which can delight the customers through good functional and aesthetic quality. Customers are demanding vehicle with high quality and superior performance [2]. In a customer-driven market such as this, it is important to produce not just high quality but also cost-effective products to sustain in the market. Consequently, automotive

industries are keen to achieve excellence in manufacturing to meet the quality and production demand.

As mentioned earlier, the quality of a two-wheeler is defined in terms of functional and aesthetic quality. Functional quality (FQ) deals with the performance and safety related features of the vehicle whereas aesthetic quality (AQ) deals with the visual quality and aesthetic finish of the vehicle from customer perspective [3]. Typically, two-wheelers are consist of critical sub-systems as mentioned in Figure 1-2. Different sub-systems effect the performance of the vehicle by different means. Next, to the engine system, chassis system is the one that plays a crucial role in functional as well as the aesthetic quality of the two-wheelers. Enhancing the chassis quality is necessary to obtain better vehicle quality and performance.

Figure 1-2 Model of two-wheeler and its critical sub-systems [4]

Chassis or frame is one among the vital parts of two-wheelers [5,6]. As frame is a safety-critical part of a two-wheeler, it must withstand static and dynamic loads of the vehicle which includes weight of the components, braking force, acceleration force, load from riders and additional load they carry [5]. Moreover, time-varying loads lead to fatigue failure in the frame during service period [5]. Any failure in the frame can cause major damage to the vehicle and severely affect the rider. Therefore, frames are designed in such a way that they carry the

loads [5] and vibrations [6] in dynamic conditions. Strength of the frame depends on structural design, material properties and method of manufacturing. Steel is predominantly used as a parent material for two-wheeler frame [3,7]. However, depending on the requirements aluminium, carbon-fibre, magnesium, titanium, and composite materials are also have been used for frame [7]. The manufacturing process of the frame should be capable of meeting to the design requirement and achieving the stringent manufacturing targets in the aspects of productivity, quality and cost.

Gas metal arc welding (GMAW) process is being used in automotive industries for the manufacturing of frames which are made of low carbon steel with part thickness varying from 2 mm to 8 mm [3]. In that, structural and load-bearing members have a high thickness varying from 4 mm to 8 mm whilst the supporting members have a thickness ranging from 2 mm to 4 mm [3]. Different functional members of the frame are shown in Figure 1-3.

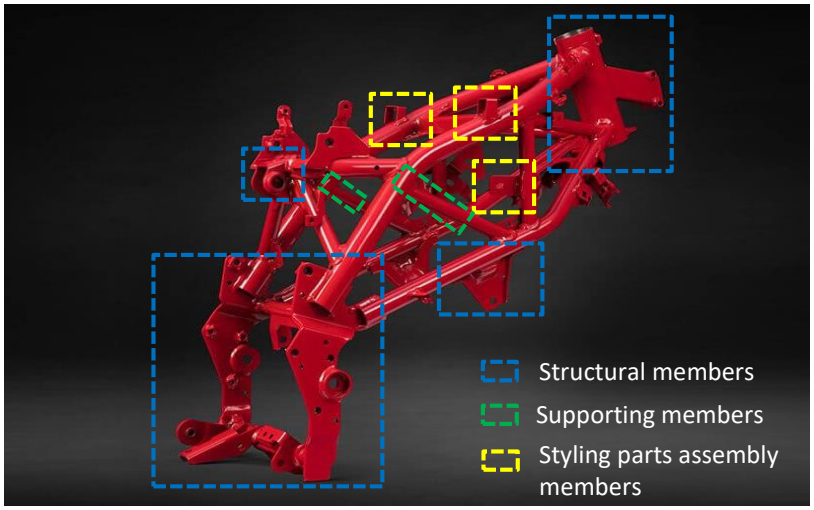

Figure 1-3 Model of Motorcycle frame [4]

Achieving the required weld penetration is the primary requirement as it decides the strength of the weld joint [8]. Better weld penetration, low distortion, and aesthetically attractive weld beads are the key considerations for deciding the quality of a frame which in turn results in customer appeal through desired functional performance and aesthetic quality of the vehicle [3].

1.2 Research motivation

Challenges that two-wheeler industries face are meeting the customer demand and providing satisfactory riding experience to the customers by means of superior performance of the vehicle. Performance of the vehicle also depends on quality of the frame because it is a backbone of the vehicle [5,6]. The characteristics of welding process determine the extent to which the required product characteristics can be achieved. Conventional arc welding processes are limited to a certain level of quality and productivity. The main limitations of GMAW process are high distortion [9], limited productivity [10], high fusion zone and heat affected zone area [11] and limitation on depth of penetration, especially in higher thickness materials. Moreover, to achieve the desired fit and finish in the vehicle, consistent frame dimensions are mandatory. Therefore, achieving process capability (Cpk) [12] of frame dimensions are really difficult in conventional arc welding process due to larger distortion.

With the advent of advanced welding processes like laser beam welding, there is a huge scope to overcome the challenges posed by conventional welding processes [13]. Low heat input of laser welding process provides an additional benefit of optimizing design as a lightweight structure with the application of high strength steels. Laser welding has thus far been applied successfully in four-wheeler industries for welding of automotive bodies [14,15]. Moreover, lasers are also being used to weld critical engine components and transmission parts [14]. Laser welding process provided benefits over conventional welding process in terms of less distortion, small HAZ area, high productivity and ease of automation [13,14]. However, it requires precise part fit-up [2] which will increase part manufacturing cost [16] nullifying the overall consumable and man power cost reduction which are expected through introduction of laser welding. This is where hybrid laser GMAW process comes into the picture. It is a trade-off between highly productive autogenous laser welding (ALW) process and good gap bridging GMAW process as it provides the benefits of both processes. Compared with conventional GMAW process currently in place, hybrid laser arc welding (HLAW) process delivered the following benefits to automotive industries [2].

- High welding speed
- Deep penetration
- Less consumption of filler wire
- Reduction in manpower cost

High productivity of this process can reduce the number of welding cells or lines which can significantly reduce the manpower. Therefore automobile industries have started to focus on autogenous laser welding and hybrid laser arc welding processes in order to reap the benefits.

1.3 Context of research

As GMAW is a low power density process, outcomes in terms of weld penetration range and level of welding speeds are limited which impacts the quality and productivity [2]. Larger distortion in GMAW process calls for revising and rework processes which are necessary to rectify the deviations [3]. The combination of lower welding speeds and high rework adversely affect the line capacity [3]. Loss in production directly translates to business opportunity loss.

Owing to this condition, to meet the production demand, multiple shift production is carried out which eventually increases product cost [3]. Laser beam welding process is the popular choice to replace conventional welding process [13]. However as mentioned before, laser welding is restricted to parts with precise fit-up which can be resolved by hybrid laser arc process [2]. In the context of moving on to these advanced welding processes, investigating the capability of ALW and HLAW processes as an alternative method for conventional GMAW process is the way forward. Evaluation is required in different facets of functional qualities such as weld penetration, bead geometries, mechanical properties and aesthetic quality of the weldment. Moreover, tendency of these processes towards distortion and gap bridgeability also needs to be evaluated.

Since meeting the production requirement without affecting quality is the key challenge for automobile industries [2], evaluating the trade-off between quality

and productivity of ALW and HLAW processes are mandatory to gauge the applicability of these processes for automotive industries.

1.4 Project scope

The scope of this project is to perform a fundamental evaluation of autogenous laser welding and hybrid laser GMAW processes as an alternative method for conventional GMAW process for the application in automotive industries. This would include:

- Developing an autogenous laser welding and hybrid laser GMAW methods for welding of low carbon steel with the specified requirements.
- Validating potential of autogenous laser welding and hybrid laser GMAW processes to meet the quality requirements of the two-wheeler frame.
- Recommend a suitable welding process or conditions for the intended application.

1.5 Aim and Objectives

The whole aim of this thesis is to evaluate the autogenous laser welding and hybrid laser GMAW processes and compare these processes with GMAW which is currently used for two-wheeler frame manufacturing.

The main objectives are,

- To assess the benefits of laser welding processes with respect to specified quality requirements of a two-wheeler frame.
- To study the productivity and quality levels of laser welding processes and compare with GMAW process in the aspects of weld penetration, bead geometry, welding speed and heat input.
- To evaluate the gap bridging capability of the laser welding processes.
- To evaluate the propensity of autogenous laser welding and hybrid laser GMAW processes on weldment distortion.
- To understand the metallurgical and mechanical properties such as microhardness and tensile strength of the laser welded samples.

- To examine the impact of laser welding processes on aesthetic quality of the welds.

1.6 Thesis structure

This thesis comprises of ten chapters as detailed in Figure 1-4. Chapter 1 gives a brief introduction to research background, aim and objectives. Chapter 2 deals with a comprehensive literature review on different welding processes such as GMAW, ALW, HLAW and its effects on weld characteristics. Chapter 3 defines research methodology and process flow which have been followed. Chapter 4 gives information about materials and experimental set-up were used in this research. In Chapter 5, the productivity and weld bead geometry details are discussed. Chapter 6 contains the evaluation of process' ability to bridge root gaps between joining material. Chapter 7 furnishes the details of distortion study conducted in the course of evaluation. In chapter 8, metallurgical and mechanical properties attained by the weldment are stated and discussed. Critical comparison of all three processes are discussed in Chapter 9. Chapter 10 gives a summary of the results obtained and conclusions arrived. At the end of this chapter, planned future work also stated.

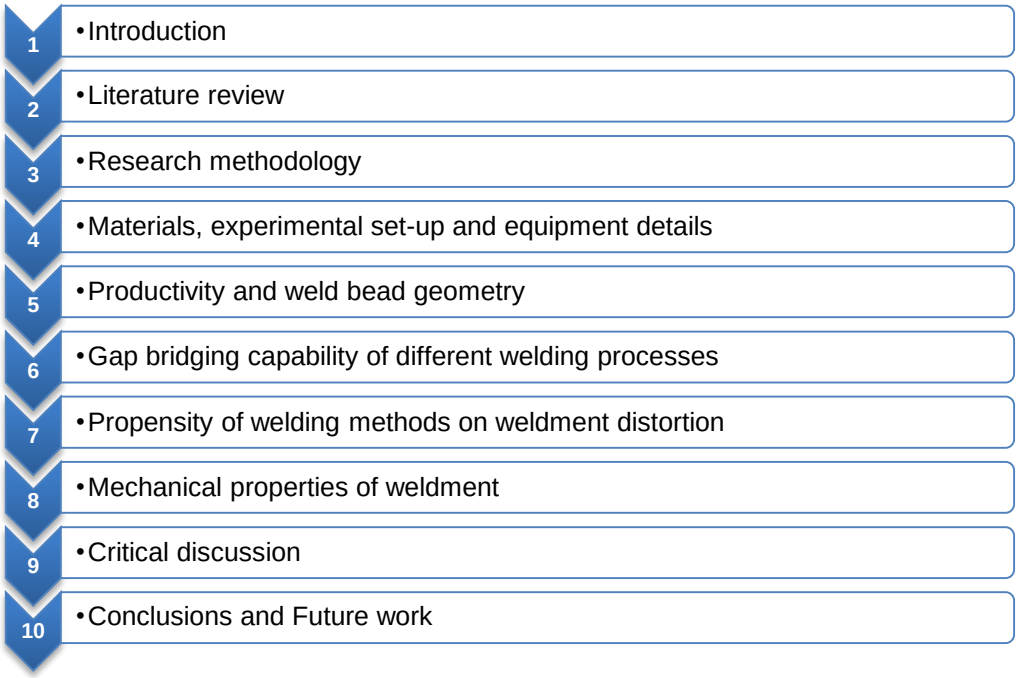

Figure 1-4 Structure of the thesis

2 Literature review

2.1 Introduction

A comprehensive literature review has been carried out to acquire the fundamental knowledge needed for this project. The motive was to study the propensity of Gas metal arc welding (GMAW), Autogenous laser welding (ALW) and Hybrid laser arc welding (HLAW) processes towards productivity, weld bead geometry, gap bridging capability, distortion, metallurgical and mechanical properties of the weldment. The entire chapter is divided into different sections as mentioned below.

- **Section 2.2** – Review of different welding processes
- **Section 2.3** – Study on productivity and weld bead geometry
- **Section 2.4** – Study of critical laser and hybrid laser welding parameters
- **Section 2.5** – Gap bridging capability of laser welding processes
- **Section 2.6** – Weldment distortion
- **Section 2.7** – Metallurgical and mechanical properties of weldment
- **Section 2.8** – Summary

2.2 Review of different welding processes

2.2.1 Challenges allied with the conventional arc welding process

The key challenges faced by automobile industries by conventional welding process are,

- Low productivity due to limitation on welding speed [2]
- Difficult to maintain trade-off between productivity and quality [2]
- High amount of distortion [9]

Low power density of GMAW process increases the heat input required to acquire desired depth of penetration [17] as shown in Figure 2-1. Heat input is always having a great influence on weld bead morphology, microstructure and mechanical properties of the weld [18]. Moreover, high heat input leads to larger distortion in the weldment [9]. As heat input is having a direct relation with depth

of penetration, meeting to the specification of other weld bead geometries without compromising depth of penetration is really a big challenge [3]. Therefore, moving on to the high power density processes should be the better way to eliminate these existing challenges.

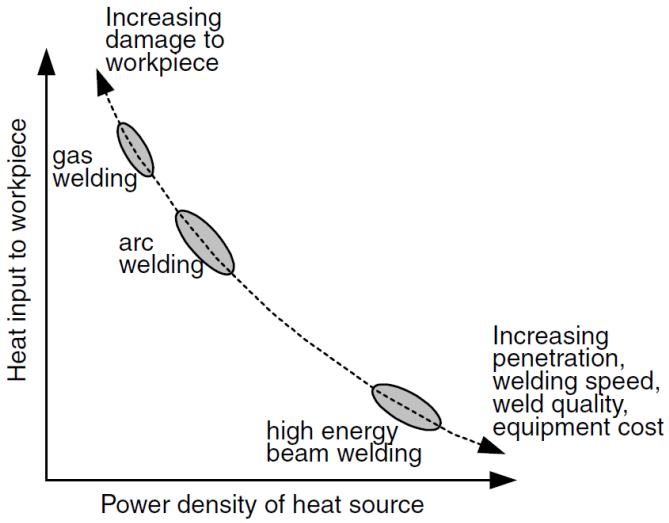

Figure 2-1 Relation between heat input and power density [17]

Laser welding process produces high power density in the range of 10^5 W/cm² to 10^7 W/cm² [19] which is ~4 times higher than conventional arc welding processes [20].

2.2.2 Autogenous laser welding process

The range of power densities associated with the laser beam welding process creates two distinctive regimes or modes [21,22]. Power density below 10^6 W/cm² results in conduction mode whereas power density more than 10^6 W/cm² results in keyhole mode [23]. Both modes are illustrated in Figure 2-2. In conduction mode substrate' temperature rises to a melting point and heat is transferred to the volume of material through conduction [21,24]. Whilst in keyhole mode, the temperature of the substrate rises to a vaporization point of the base material [19]. Consequently, a deep and narrow vapour cavity or keyhole is formed and multiple internal reflections of the laser beam inside the keyhole increases the absorption of laser beam [19,25].

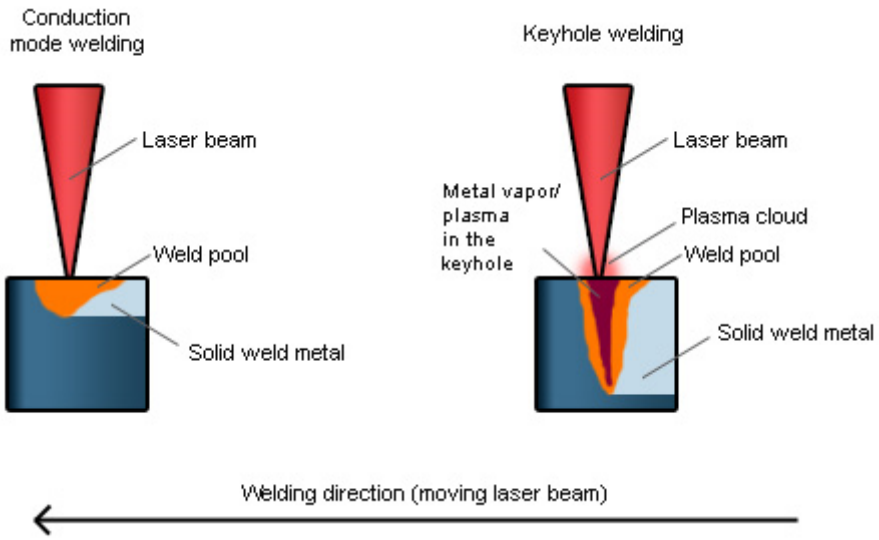

Figure 2-2 Conduction mode and Keyhole mode welding [26]

As conduction mode provides a limited depth of penetration [22], it could not be employed in structural welding where deep penetration is required. On the other hand, keyhole welding offers high-speed welding in thin sections [27] and complete penetration in thicker sections [27,28]. As two-wheeler frame consists of many structural joints, it requires deep penetration, low distortion and better structural integrity which can be fulfilled by the keyhole welding.

2.2.2.1 Advantages and limitations of laser welding process

Laser welding process provides benefits of deeper penetration [27,28] narrow HAZ [20] and less fusion zone area [29]. Extremely low heat input of laser welding process subsequently produces low distortion than conventional arc welding processes [29]. Nevertheless, faster cooling rate due to high welding speed results in formation of hard phases such as martensite in the weldment [30]. Excessive hardness reduces the toughness [31] of the weld. Moreover, due to focused laser spot, it needs precise part fitment [32] and it is really a challenge in series production industries.

In order to mitigate these limitations, laser welding with filler wire and hybrid laser arc welding processes [33,34] are developed.

2.2.3 Laser-assisted filler wire welding

Incorporation of filler wire with laser beam provides benefits of better gap bridgeability and allows one to modify the composition of fusion zone to enhance metallurgical and mechanical properties of the weld [35]. This process is more complex than autogenous laser welding due to the interaction among laser beam, filler wire, and base material. Therefore, precise wire positioning is required to obtain better weld quality [35,36]. Generally, the efficiency of laser with filler wire welding is lower than autogenous laser welding because the given input power is also being used to melt the wire [36]. Consequently, this loss of heat input needs to be compensated either by increasing laser power or reducing the travel speed [36]. Additionally, the reflection of a laser beam by filler wire [35] also hinders the process efficiency.

The following are the key challenges in laser-assisted filler wire welding process,

- Reduction of welding speed compared with autogenous laser welding [36]
- Some part of laser energy is being used to melt the wire [36]
- Stringent wire positioning is required [35]
- Improper wire mixing behaviour in the weld metal [35]

2.2.4 Hybrid laser arc welding process

Hybrid laser arc welding (HLAW) process combines both laser energy and arc energy in the same weld pool which mutually assists each other [37]. The secondary heat source increases the absorption of laser energy [38] and laser-induced plasma assist the arc for faster droplet transfer at high welding speed [39]. The hybridization effect of this process compensating the limitations associated with both the individual processes [38]. Hybrid laser arc welding process configuration is illustrated in Figure 2-3. Due to the additional arc energy, higher welding speed can be achieved than autogenous laser welding [40]. Moreover, it decreases the hardness in the fusion zone [30] and addition of filler wire improves the part fit-up tolerance [36]. Formation of keyhole resulted in deep penetration and the deposition of filler wire provides better weld bead profile as

shown in Figure 2-4 [36]. However, incorporation of both laser and arc makes this process more complex because of the increase in number of process parameters [41]. Precise optimization of parameters are required for better weld quality [38].

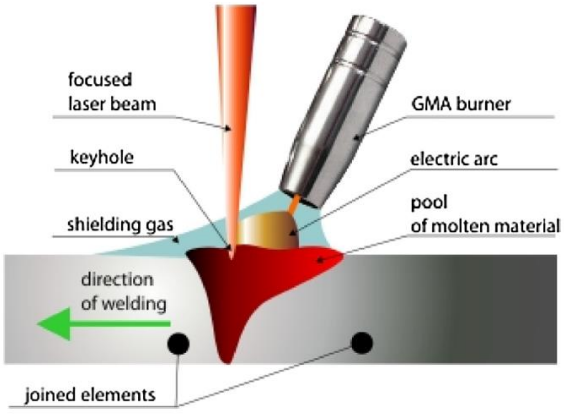

Figure 2-3 Representation of hybrid laser arc welding process [42]

Comprehensive benefits of hybrid laser arc welding process are [2,16]

- High productivity in thick section welding
- Low distortion
- Good tolerance fit-up
- Better weld bead profile

Gap bridgeability of hybrid laser welding process extended its application in welding of automotive parts [34]. Therefore, hybrid laser welding process appears to be a promising technology for industrial applications [2,43].

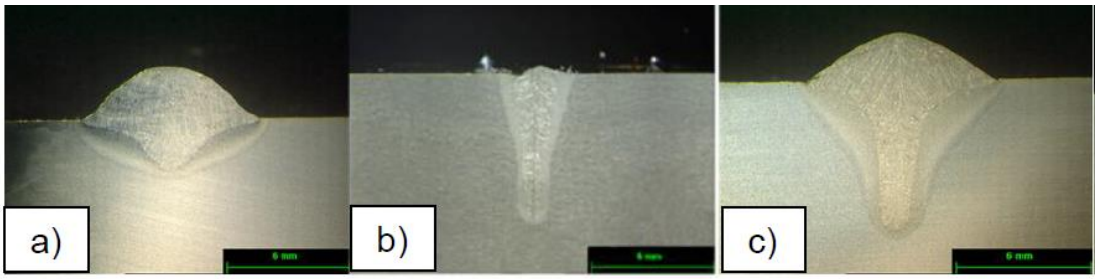

Figure 2-4 Weld bead profile in various welding processes (a) GMAW (b) Autogenous laser welding (c) Hybrid laser GMAW [16]

2.2.5 Keyhole mechanism in laser welding process

The applied laser energy is absorbed by conduction free electrons at the metal surface through Fresnel absorption [44]. If the applied power density is adequate to vaporize the material then keyhole is generated [25]. Vapour pressure or recoil pressure causes the formation of narrow and deep keyhole [25] which is illustrated in Figure 2-5. Thus the laser beam can penetrate the material through the keyhole and multiple reflections of laser beam inside the keyhole increases the absorption efficiency [25,45]. Eventually, it results in increase of penetration depth and produces weld with high aspect ratio [25]. Moreover, the ionized vapour plasma absorbs the power through inverse bremsstrahlung absorption [19]. The degree of this absorption depends on laser wavelength, laser irradiation and molecular species in the plasma [19]. The presence of ionized vapour, defocuses the laser beam which eventually reduces the power density [27]. This negative effects of plasma are most common in CO_2 laser welding whereas it is negligible in fibre laser welding [16,32] Therefore during CO_2 laser welding, shielding gas is used for plasma suppression [19]. Pure Ar and He or mixture of Ar and He are being used for plasma suppression [19].

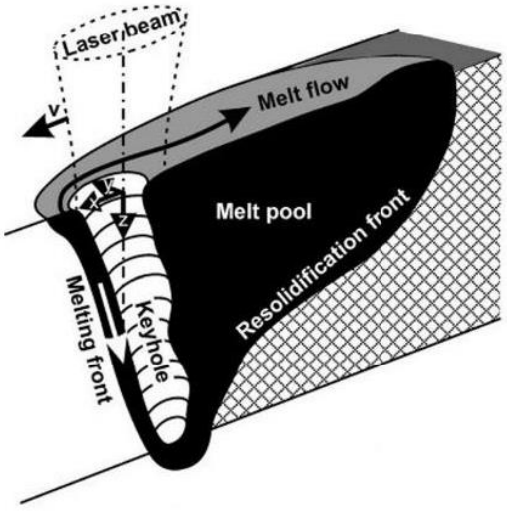

Figure 2-5 Keyhole mechanism in laser welding [46]

2.2.6 Laser–arc interaction in HLAW process

Typically in the GMAW process, welding at high speed leads to the formation of weld imperfections [10]. However in the HLAW process, laser assists the droplet transfer which provide uniform beads even at higher welding speeds [34,39]. As per the current waveforms shown in Figure 2-6 of both the processes, reduction of fluctuation in current and increase of frequency improves the stability of droplet transfer in hybrid laser arc welding [39].

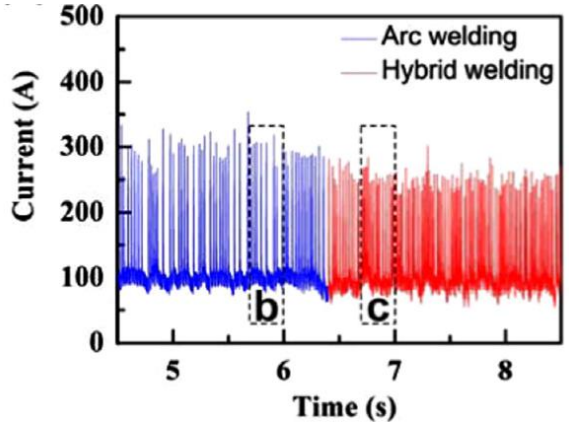

Figure 2-6 Comparison of current waveforms in arc welding and hybrid laser arc welding processes [39]

Droplet transfer frequency was increased from 33.3 Hz to 56.7 Hz which reduces the droplet transfer time from 30.1 ms to 18.1 ms in short-circuit mode [39]. Almost droplet transfer time is reduced by 40% [39]. This is attributed by an increase in electromagnetic force and plasma drag force due to the large angle and more conduction zone area respectively which are illustrated in Figure 2-7 [39]. Compared with arc plasma, the low ionization potential of laser-induced plasma attracted arc plasma and provides more electrical conductivity in the droplet transfer zone [39,47].

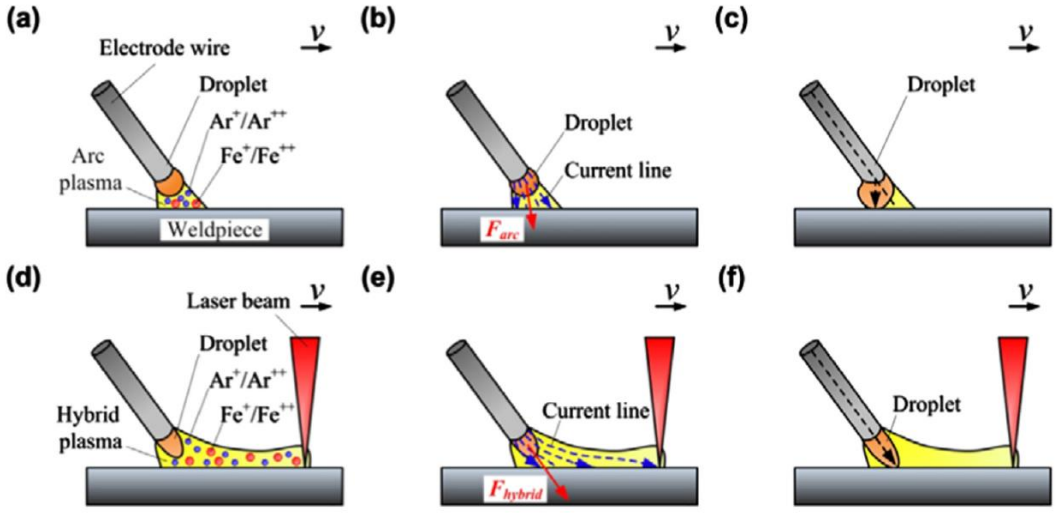

Figure 2-7 Comparison of droplet transfer in short-circuit mode in (a) to (c) - arc welding, (d) to (f) - hybrid laser arc welding [39]

2.2.7 Cold metal transfer (CMT)

Cold metal transfer (CMT) is a unique welding technology which was invented by Fronius international [48]. Alternating thermal arc pool of CMT makes this process extremely cold i.e. arc pool is hot during an initiation of arc and cold once the arc is extinguished [49]. The minimum current of CMT arc is less than the regular dip arc transfer [49] as shown in Figure 2-8. Thus, droplet transfer is being carried out at extremely low current than other conventional metal transfer modes [49].

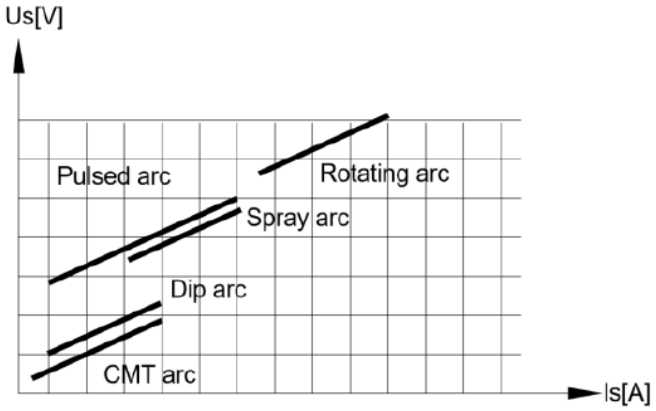

Figure 2-8 Comparison of current and voltage in different modes of metal transfers [49]

The peculiar characteristic of CMT technology is a method of droplet detachment which is illustrated in Figure 2-9. Once the electrode tip makes an interaction with molten pool, the arc is extinguished and the wire is retracted by the digital process control [48,49]. This retraction of wire leads to detachment of the droplet. Therefore, droplet detachment is happening nearly at zero current [48] whereas in the conventional process it occurs at circuit phase which means at high thermal energy [50]. This unique droplet detachment leads to low heat input, less spatters, and better aesthetic quality of the weld bead [51].

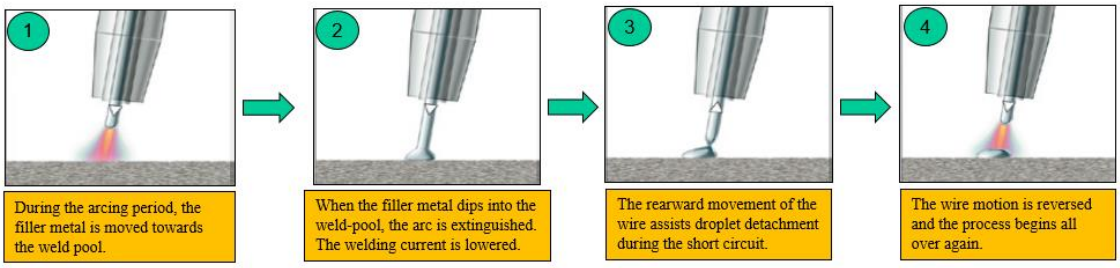

Figure 2-9 CMT welding process sequence [49]

Synergic lines of CMT technology made this process more user-friendly. Moreover, it comprises of various arc modes such as CMT pulse, CMT advance, CMT pulse advance, and CMT dynamic [50] which can be employed depending on the requirement of weld quality. Compared with conventional pulse welding, CMT showed extensive benefits of less fusion zone area, bead width, HAZ width [52] and low distortion [29]. However, limited depth of penetration of CMT is restricting its application to thin structures.

2.3 Study on productivity and weld bead geometry

Productivity of the welding process can be determined by deposition rate in heavy welding applications and attributed by welding speed in sheet metal welding applications [53]. Hence, welding speed is the primary measuring stick for the productivity in two-wheeler frame welding process. Weld quality is having a great influence on integrity of the structure [54] and it is significantly varying with welding speed. Therefore, in the present competitive industrial environment maintaining the trade-off between productivity and quality is mandatory to sustain

in the market [10,53]. Implementation of advanced welding processes with maximized welding speeds can provide significant improvement in productivity and quality [10].

In the GMAW process, increase in productivity often requires an increase in welding speed [55]. However, to achieve sufficient heat input to obtain the desired penetration, arc power also needs to be increased [55]. Moreover, high welding speed causes critical defects which are mainly undercut and humping [10]. The presence of undercut lowers the fatigue and fracture strength of the welded structure [10]. In the case of humping, depth penetration will be the same in both valleys and humping beads whereas the reinforcement height significantly varies [10]. Both undercut and humping exhibits an adverse effects on integrity of the welded structure [10]. Moreover the aesthetic quality of the weld bead also greatly compromised. Therefore, these defects are mainly limiting the application of high welding speed in GMAW process which eventually hinders the productivity [10]. In thick sections, complete penetration can be achieved by groove preparation with multi-pass welding in GMAW [56]. Nevertheless, it requires additional processing and cost [56].

Weld bead geometry is a key factor which determines the mechanical properties [57] and aesthetic quality of the weld joint. Typically, high heat input in the GMAW process has an adverse effect on weld bead geometry. It increases bead width [11], HAZ width [11] and produces excess reinforcement which consequently increases the metallurgical damage to the base material. Nevertheless, a sufficient amount of heat input must be delivered to avoid incomplete penetration in the weld joint. Lack of penetration significantly affects the fatigue life of the welded structure [58].

High power density of the laser beam welding process delivers low heat input to the substrate which reduces the microstructural degradation of parent material [20]. In laser welding, heat input shows a near-linear relation with penetration depth as shown in Figure 2-10. At low heat input of 10 to 100 J/mm, due to

conduction mode, less increase in penetration was observed whereas significant increase was observed in keyhole mode [59].

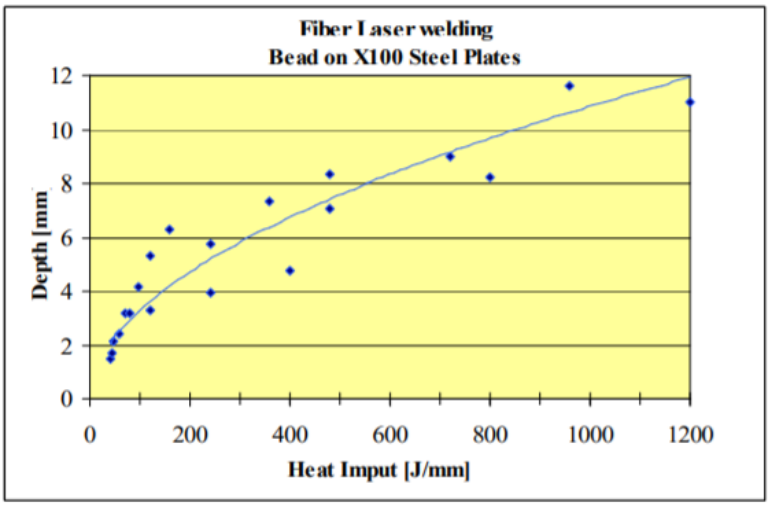

Figure 2-10 Depth of penetration versus heat input for fibre laser welding [59]

Compared with the GMAW process, ALW process can produce complete penetration at low heat input along with narrow fusion zone and HAZ [11]. This was proved by [11] through experimentation on micro alloyed C-Mn steel, thickness of 5 mm with groove preparation. Complete penetration was achieved in laser welding with 78% less heat input than GMAW process along with improved productivity of more than 10 times. Also, laser welding process has shown significant reduction in bead width and HAZ width than GMAW by the factor of ~3 to 7 times and ~4 to 5 times respectively. This is attributed by the formation of keyhole at a high power density of ALW process [11]. Weld bead appearances and macro sections of both laser and GMAW processes are compared in Figure 2-11. Low power density of GMAW process provided a wide thermal effect which results in larger fusion zone area [11].

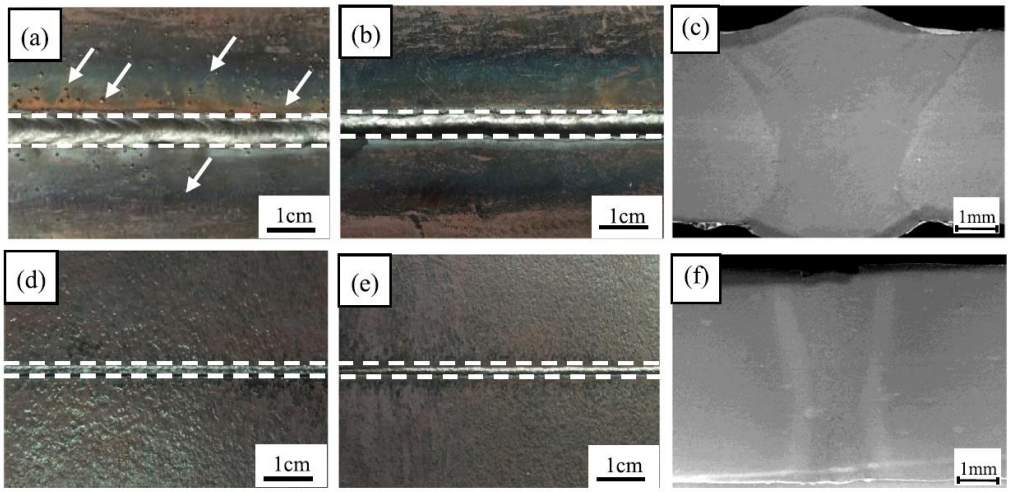

Figure 2-11 Bead appearances and macro-sections of welded joints (a) top bead of GMAW, (b) bottom bead of GMAW, (c) macro-section of GMAW, (d) top bead of LBW (e) bottom bead of LBW, (f) macro-section of LBW [11]

In another investigation by [9] showed that ALW process produced 70% narrow weld bead than CO_2 gas arc welding. As the laser welding process exhibits less impact to the material adjacent to weld bead which controls the width of HAZ [20]. Therefore, 10 times reduced HAZ width was produced by ALW process than arc welding [20].

The net heat input of hybrid laser arc welding process is higher than autogenous laser welding process due to the addition of arc energy. Therefore, it can be operated at higher welding speed than ALW which results in an improvement of productivity [40]. Moreover, comparatively with laser welding, a hybrid laser arc process produced more fusion zone and HAZ area [30]. However, higher power density and much lower heat input of HLAW process than GMAW process lead to achieve complete penetration even in higher thickness materials with narrow HAZ [43].

2.4 Study of critical laser and hybrid laser welding parameters

The critical laser and hybrid laser arc welding parameters and their effects on weld quality are discussed here. Hybrid laser arc welding process comprises of parameters from both the individual processes as well as the laser and arc

interaction parameters [41]. The optimized parameters of each individual processes may not be the optimized condition for hybrid process [33]. Therefore, process setting of hybrid laser arc welding is more complex due to this incorporation of numerous parameters [41]. More complexity [41] and high investment [33] are the two main factors limiting the industrial application of the hybrid laser arc welding process.

2.4.1 Laser power, welding speed, and beam diameter

Laser power and welding speed are the most influential parameters in depth of penetration where laser power is having a direct relation with penetration and travel speed exhibits an inverse relation [59] with penetration as shown in Figure 2-12.

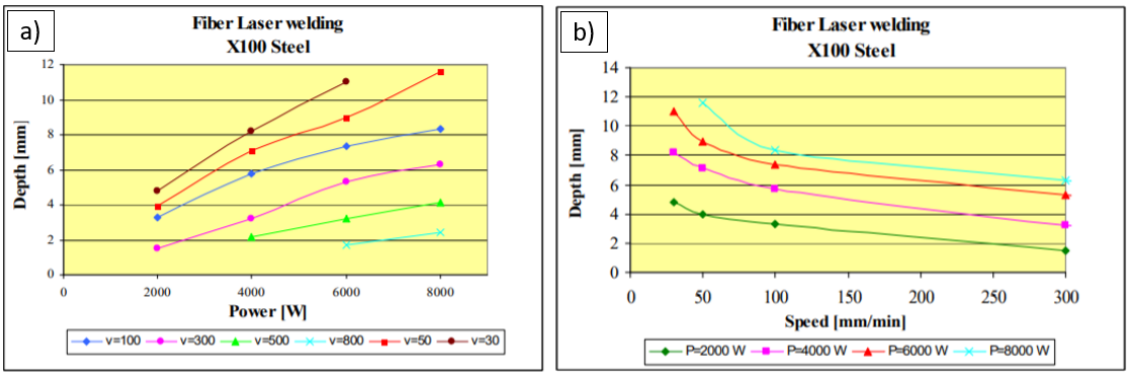

Figure 2-12 a) Variation of penetration with laser power b) Variation of penetration with welding speed [59]

Increase in welding speed decreases the amount of heat input delivered to the workpiece which eventually reduces the penetration [60]. Conversely, an increase in laser power increases the heat input which results in deeper penetration [60,61]. Both of these parameters exhibits a similar effect on bead width as well [15,61]. High power density of ALW process results in deep penetration, low distortion, narrow fusion zone and HAZ area [56].

Beam diameter is another influential parameter of weld bead geometry as it controls the power density for the given power [19]. At the same laser power and welding speed, beam diameter exhibits an inverse relation with penetration [32].

Figure 2-13 shows that effects of welding speed and beam diameter on penetration depth and other weld imperfections. At constant laser power and travel speed, an increase in beam diameter increases the bead width and reduces the penetration depth [15]. The relationship between weld bead geometry and basic laser system parameters are shown in Table 2-1.

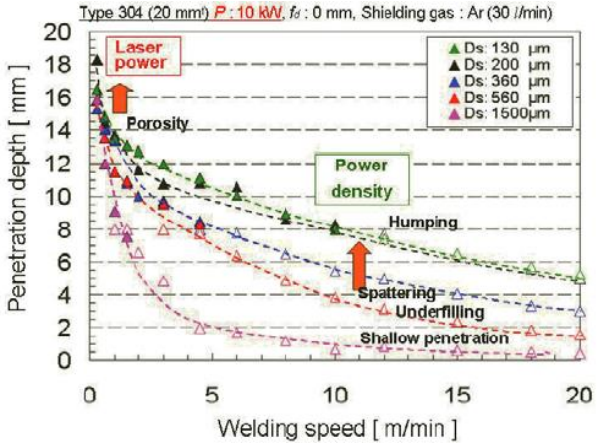

Figure 2-13 Variation of penetration depth with beam diameter and welding speed [32]

Table 2-1 Relation of laser welding parameters with weld bead geometry [15,61]

Parameters	Depth of penetration	Fusion zone width	HAZ width
Laser power	Positive	Positive	Positive
Welding speed	Negative	Negative	Negative
Beam diameter	Negative	Positive	Positive

2.4.2 Focal position

Defocusing distance decides the laser spot size which eventually determines the power density [60]. Therefore the change in defocusing distance alters the weld bead geometry as shown in Figure 2-14. A focal point on the workpiece surface leads to high power density as the beam diameter is smaller which produces complete penetration [60]. The longer the distance between laser head and the workpiece the shallower the penetration depth [32]. At constant laser power and welding speed, a focal plane on the workpiece surface produced full penetration

with less concavity in the top bead whereas full penetration with more concavity was observed at -2 mm focus position [60]. Defocusing to -3 mm causes incomplete penetration as shown in Figure 2-14, c).

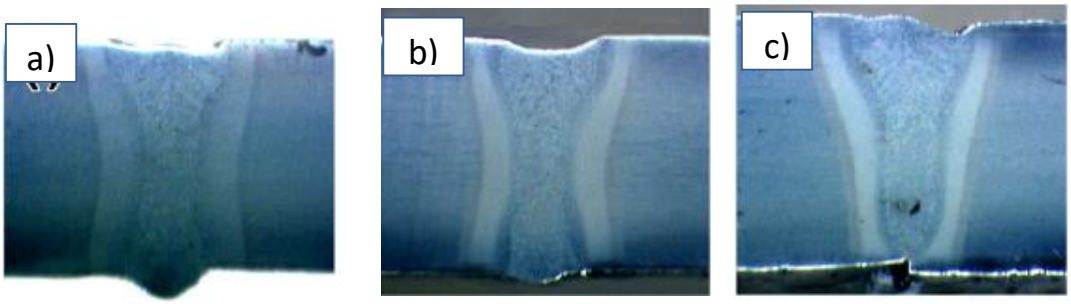

Figure 2-14 Variation of penetration depth with defocusing distance at P_L = 3 kW, V = 1.2 m/min a) Df = 0 mm, b) Df = -2 mm, c) Df = -3 mm [60]

Along with laser power and welding speed, defocusing distance also influences the bead width. The decrease in welding speed and defocused beam eventually increases the bead or fusion zone width [61].

Control of weld quality in laser welding process becomes complex due to these numerous parameters and it is difficult to determine the suitable combination of these laser system parameters. Moreover, transfer of parameters among laser systems also limited due to the variation of laser properties and optics system [62]. Thus the power factor model through laser interaction parameters [62] has been developed which simplifies the selection of process parameters and enables the transfer of parameters among laser systems [62].

2.4.3 Power factor model

The influence of laser optics parameters on weld penetration can be eliminated through the application of this model [62] because laser optics controls the beam diameter and it varies for each system [62]. For particular laser power and welding speed, change in beam diameter changes the penetration depth [62]. The brief about laser interaction parameters are shown in Table 2-2.

Table 2-2 Laser interaction parameters [63]

Parameter	Definition	Formula	Critical effect
Power density (q_p)	The ratio of laser power to the area of laser spot on the surface	$q_p = \frac{P}{A_s}\ (W\ m^{-2})$ **(2-1)** P- Laser power (W) A_S – Area of laser spot on the surface (m²)	Control of penetration depth
Interaction time (T_i)	This is the exposure time of a particular point on the surface to the laser beam	$T_i = \frac{d}{v}\ (s)$ **(2-2)** d – Spot size (mm) v – Welding speed (mm/s)	Control of weld width
Specific point energy (E_{SP})	The product of power density, interaction time and area of laser spot on the surface	$E_{sp} = q_p . T_i . A_s = P\ . T_i\ (J)$ **(2-3)**	Control of penetration depth

The flow of parameter selection as per the full version of power factor model is shown in Figure 2-15, a). Interaction time and travel speed needs to be selected based on the weld bead geometry and productivity requirement respectively [62]. Then, model will give the suitable beam diameter and corresponding power factor to be chosen with respect to the requirement of penetration depth from Figure 2-16 [62]. Finally, the suitable laser power with respect to the power factor and beam diameter will be suggested by the model [62].

Moreover, the simplified version of power factor model also can be used to calculate the laser power requirement to acquire desired depth of penetration for a given travel speed and beam diameter [62]. Simplified version of power factor model is shown in Figure 2-15, b). At constant beam diameter and travel speed, interaction time can be calculated whereas power factor depends on penetration depth requirement as shown in Figure 2-15, b) [62]. Then with respect to the power factor and beam diameter suitable laser power can be determined [62].

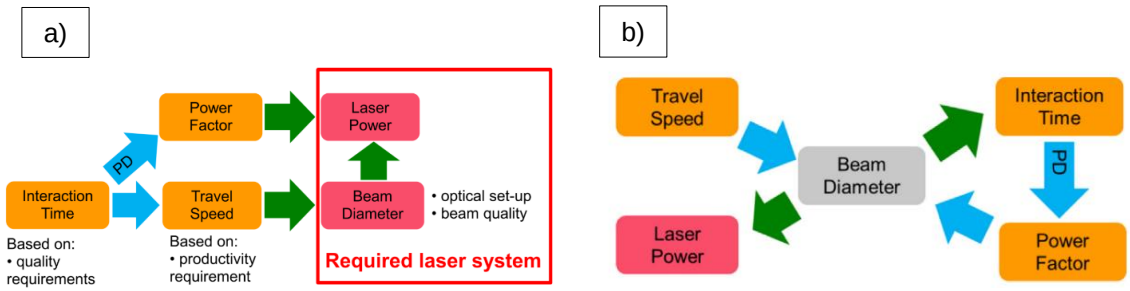

Figure 2-15 Application of power factor model for parameter selection a) Full version b) Simplified version [65]

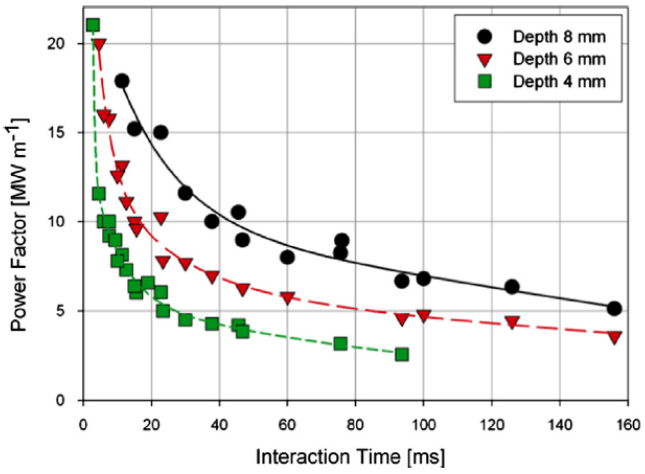

Figure 2-16 Depth of penetration achievement with different combination of power factor and interaction time for a range of beam diameter between 0.38 mm and 0.78 mm [62]

Therefore, application of power factor model is the simplest and effective method to determine the parameters in laser welding process.

2.4.4 Laser power and arc power in HLAW process

Addition of arc energy in the hybrid laser arc welding process increases the amount of heat input delivered to the substrate. Therefore, overall weld energy in HLAW process can be calculated by the following equation (2-4) [37],

$$E_{HLAW} = E_{arc} + E_{laser} = \frac{U * I * 60}{V} + \frac{P_L * 60}{V} \quad \textbf{(2-4)}$$

E_{HLAW} – Energy of hybrid laser arc welding (kJ/mm), E_{arc} – Energy of arc welding (kJ/mm), E_{laser} – Energy of laser welding (kJ/mm), U – Voltage of arc (V), I – Current of arc (I), V – Welding speed (mm/min), P_L – Laser power (W)

Moreover, the heat input ratio of laser and arc greatly influences the weld bead geometry [64] as shown in Figure 2-17. Equal heat input ratio of laser and arc (basic specimen) produced almost equal amount of top and root reinforcement as shown in Figure 2-17. High fraction of laser heat input (laser emphasis specimen) causes high root reinforcement with minor undercut on top surface whereas high fraction of arc heat input (arc emphasis specimen) produces large top reinforcement [64]. Increase in overall energy in HLAW process reduces the hardness and it also affects the aesthetic quality of the weld [37]. Moreover a decrease in the fraction of arc energy results in a decrease in the fusion zone area [64]. However, it is difficult to correlate the fraction of arc energy directly with the weld properties [37].

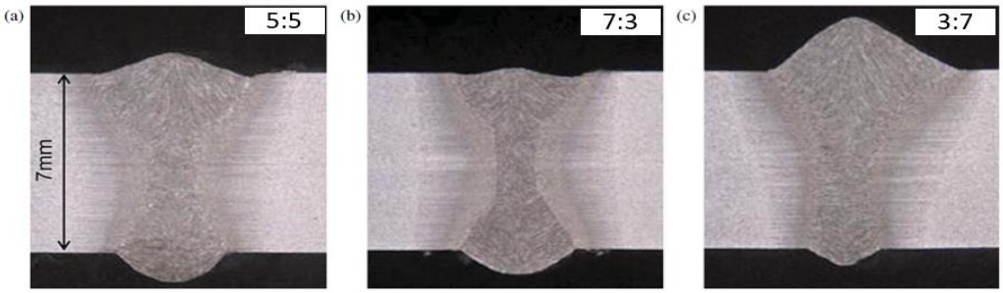

Figure 2-17 Macrographs of welds at different heat input ratio of laser and arc a) basic specimen b) laser emphasis specimen c) arc emphasis specimen [64]

This result implies that in the HLAW process, laser is dominating in the root region due to keyhole effect and arc energy is controlling the top reinforcement [65]. Therefore the ratio of laser and arc power controls the weld bead reinforcement [65]. However, the increase in overall heat input in HLAW process, correspondingly increases the fusion zone and HAZ width and eventually decreases the depth to width ratio [66] as shown in Figure 2-18. Moreover, at high welding speed, optimization of wire feed speed is required because molten

filler wire cannot be deposited completely to fill the groove which leads to the formation of concavity in the top bead [66] (Refer Figure 2-18 a).

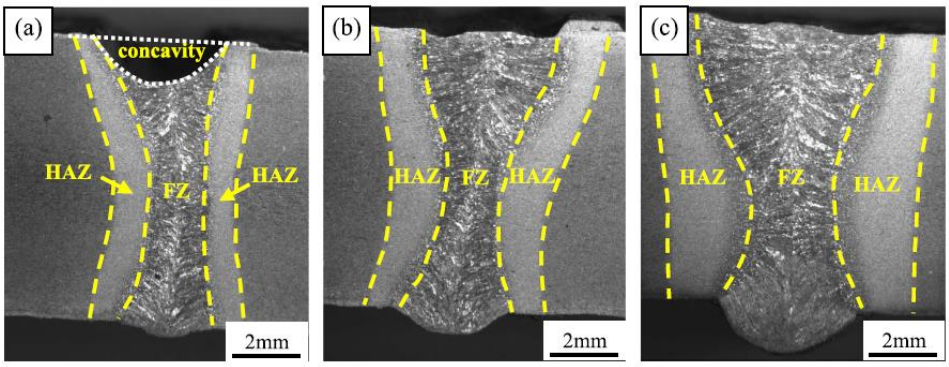

Figure 2-18 Macrographs of welds at different heat input in HLAW process a) 3.90 kJ/cm b) 5.20 kJ/cm c) 7.75 kJ/cm [66]

However, laser power should be high enough for the formation of proper keyhole on the root side in order to avoid root sagging and also process becomes more stable when laser power is higher [37].

2.4.5 Process orientation

Typically in the hybrid laser arc welding process, laser head is positioned perpendicular to the workpiece surface to obtain the deep penetration [42]. Arc torch will be positioned either front or behind the laser beam which is called arc leading or laser leading respectively [38,42]. Both configurations are shown in Figure 2-19.

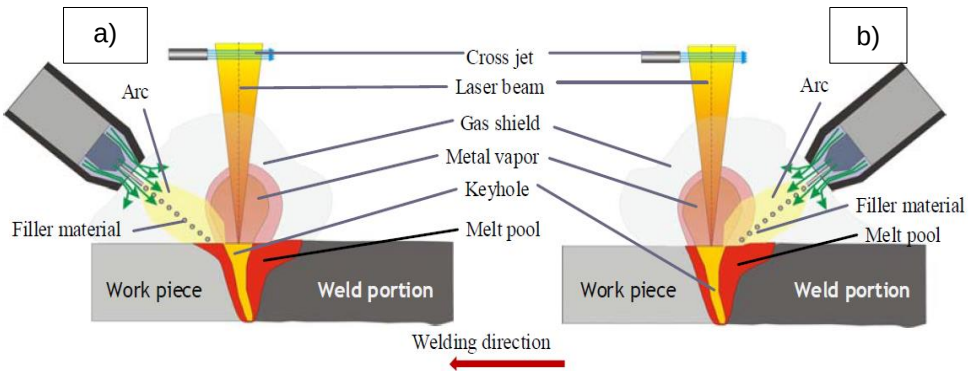

Figure 2-19 Schematic representation a) arc-leading configuration, b) laser-leading configuration [38]

Arc leading process orientation, increases the penetration due to the effect of preheating and laser irradiation on molten pool increases the absorption of laser energy [67]. Investigation by [67] showed that laser leading produces deep penetration at shorter process separation and arc leading is suitable for longer process distance. Comparatively, higher stability of keyhole in laser leading configuration results in a more stable arc than in an arc leading configuration [42]. In the comparative study between these two process orientations, laser leading produced more uniform and better quality of weld bead whereas arc leading produced non-uniform weld bead with spatters and oxidation of weld metal [43]. Moreover, as shown in Figure 2-20 arc leading produced high depth of underfill due to strong evaporative loss and protrusion of excessive weld on the root side [43]. Therefore the wire feed speed needs to be optimized to avoid underfill [43]. Also, laser leading produced more acceptable weld beads than arc leading even at the presence of root gaps [68].

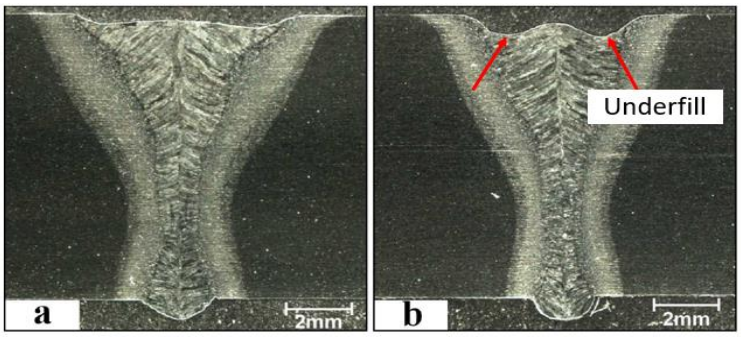

Figure 2-20 Macrographs of welds a) laser-leading configuration and b) arc-leading configuration [43]

2.4.6 Process separation

In HLAW process, process separation (d_{la}) is defined as the distance between laser spot and filler wire [37] as represented in Figure 2-21. It greatly affects solidification morphology and microstructure of the weld [19,42]. Moreover, it is an important parameter to control the depth of penetration [33].

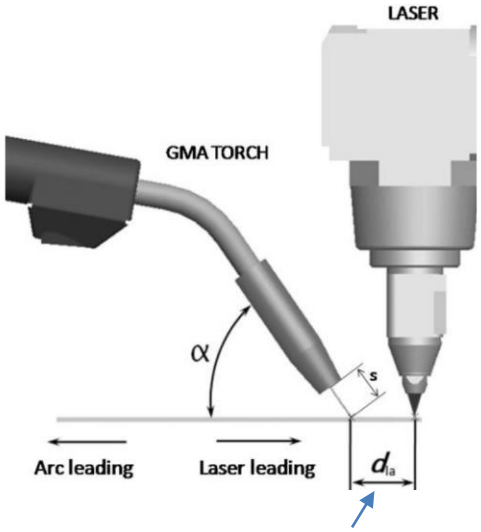

Figure 2-21 Laser-arc distance [33]

Generally, the range of process separation varies from 0 mm (Co-axial arrangement) to 5 or 6 mm (Paraxial arrangements) which depends on the material, laser power, travel speed and process orientation [19,42]. Synergic effect of laser and arc will be lost if the process distance is too high [33,38]. On the other hand, very short distance causes the absorption of laser energy by arc plasma which eventually results in low penetration depth [33]. Optimal process distance is required for better penetration. Moreover, it affects the metal transfer mode as well because the laser-induced plasma transfers heat to the electrode and changes the droplet transfer mode [69,70]. It was found to be advantageous when laser-plasma changes the globular transfer mode to projected transfer mode with increasing the process separation [70]. Also, changing the process distance correspondingly changes the weld bead shape [70] and symmetry of the fusion zone [40]. Weld morphology is changing from cocktail cup shape to cone-head shape when the range of distance is changing from 0 to 2 mm to 2 to 6 mm [70]. The optimal process distance of 2 mm can provide deep penetration [38].Lateral displacement (b) of arc torch more than 1.5 mm results in asymmetrical fusion zone [40] as shown in Figure 2-22.

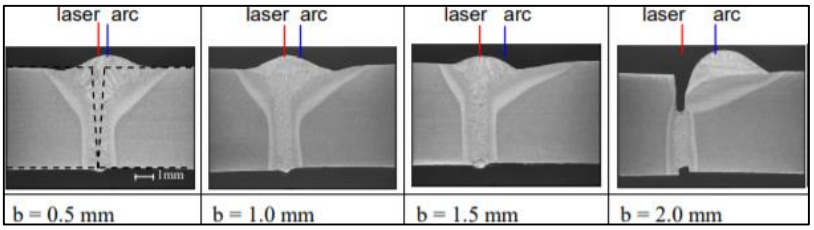

Figure 2-22 Cross-sections of welds with a lateral displacement (b) of the arc torch, TS = 1.8 m/min, WFS = 8 m/min, Voltage = 32 V [40]

2.5 Gap bridging capability of laser welding processes

Gap bridgeability of welding process is one of the primary requirement in automotive industries [2]. Conventional arc welding processes are less sensitive to joint gaps [2]. Even though autogenous laser welding process is known for its high power density, high welding speed and low distortion, the gap bridging capability of this process is always questionable due to small spot size of laser beam [36]. This restricts the application of laser welding process in an automotive industries [2]. However advancements of laser welding processes opens the way to resolve this problem. Processes such as laser welding with filler wire and hybrid laser arc welding provide better gap bridgeability [36] due to the addition of filler wire.

Many researchers investigated the gap bridgeability of these three welding methods which are detailed in Table 2-3.

Table 2-3 Reviewed gap bridging capability of different welding processes

Processes/ Authors	Autogenous laser welding	Laser with filler wire	Hybrid laser arc welding
(Shi and Hilton, 2005) [36]	✓	✓	✓
(Sun and Kuo, 1999) [35]		✓	
(Kong *et al*., 2013) [71]		✓	✓
(Möller *et al*, 2014) [72]			✓
Lamas, Frostevarg and Kaplan, 2015 [73]			✓

[36] investigated the gap bridging ability of autogenous laser welding, laser welding with cold filler wire and hybrid CO_2 laser-MAG welding processes. Autogenous laser welding process produced acceptable welds up to 0.2 mm root gap at full penetration condition with a beam diameter of 0.3 mm. Laser welding with filler wire exhibited better gap bridging capability than ALW process with compromise on productivity. This is due to the given laser power being consumed to melt the filler wire which eventually reduces heat input delivered to the base material [36]. Therefore, welding speed was reduced by ~33% at the same laser power and wire feed speed in order to acquire the complete penetration. Conversely, hybrid laser arc welding process exhibited better gap bridgeability even at the same travel speed of autogenous laser welding. It produced acceptable welds up to 1.6 mm of joint gap however, gap above ~1.2 mm is required an optimization of wire feed speed or reduction in travel speed [36] to avoid the formation of incompletely filled groove. Acceptable joints produced by each processes at maximum root gap are shown in Figure 2-23. HLAW process exhibited a wide window of part fit-up tolerance than the other two processes as shown in Figure 2-24.

Condition	Autogenous laser welding	Laser welding with filler wire	Hybrid laser MAG welding
Zero root gap condition	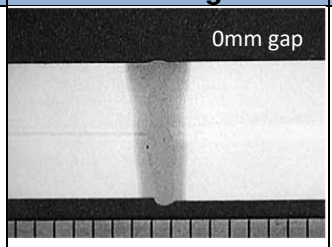	-	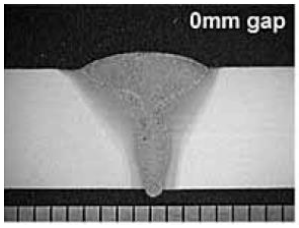
Maximum root gap condition	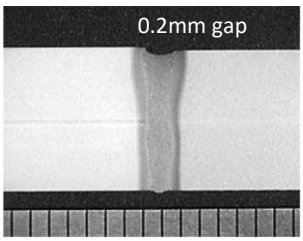	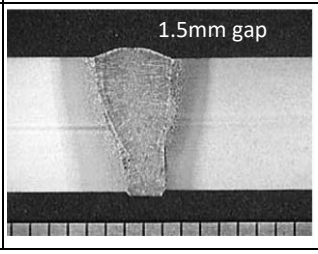	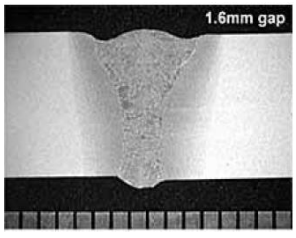

Figure 2-23 Macro sections of acceptable welds produced by different welding processes at different root gaps [36]

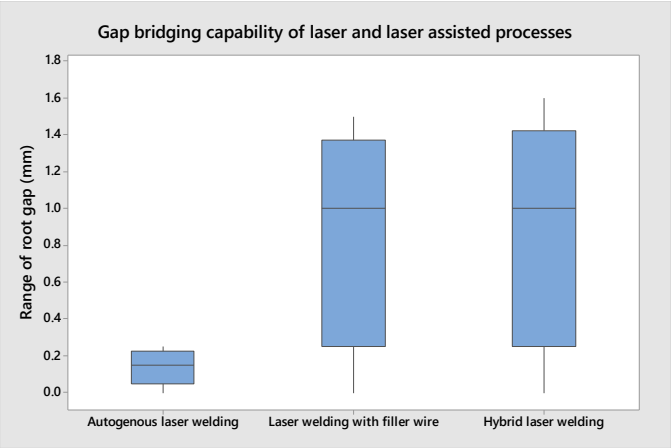

Figure 2-24 Range of root gaps accompanied by laser and laser-assisted welding processes [36]

According to the study by [40], the hybrid laser arc welding process can produce acceptable welds at maximum gap of 2 mm in square butt joints and it can be welded with maximum welding speed until a gap of 1 mm.

Moreover, in HLAW process, different metal transfer modes also exhibits different gap bridging behaviour [73]. CMT mode and pulse mode were extensively compared at similar basic process conditions for gap bridgeability in butt joint configuration where the gap is linearly varying from 0 mm to 1.3 mm [73]. However, slight adjustment in parameters was carried out to obtain acceptable welds in both the modes [73]. As root gap increases, more volume of molten metal flows through the gap which led to the reduction of reinforcement followed by the formation of undercut (at 0 to 0.6 mm gap) and underfill (at 0.6 to 0.8 mm gap) [73]. Narrower arc and gouge of CMT mode causes less undercut than pulse mode [73]. Additionally, smooth droplet transfer in CMT led to less root sagging than pulse mode [73]. However, at wider gaps from 0.8 mm to 1.3 mm, both the modes exhibited top bridging effects with partial penetration [73]. This is due to, insufficient interaction of the laser beam with the sidewalls of the lower region of the joint leading to improper wetting [73]. Therefore, in upper region arc melts the edges of the sidewalls and forms a bridge. For even wider gap, arc fails to bridge the gap [73]. Comparatively, laser with CMT mode showed a better gap bridgeability with few weld imperfections. These investigations showed that the

hybrid laser arc welding process can be a better alternative method for the conventional welding processes in an industrial application [73].

Moreover, the presence of a small gap helps for the better interaction of laser and arc in HLAW process [38]. At zero-gap condition, molten metal cannot flow through the groove therefore, accumulation of excess molten metal can block the keyhole whereas in the existence of a small gap, arc penetrates more [38]. It leads to better interaction of laser and arc [38]. This deep flow of molten metal increases the depth of penetration. Moreover, in order to fill the gap, correspondingly wire feed speed needs to be increased [40]. Hence, welding speed can be increased in the presence of root gap [40]. However, welding speed cannot be increased linearly because it is limited by the gap width and weld imperfections [40]. As shown in Figure 2-25 reduction in welding speed is required above the certain range to obtain better weld profile at high root gap conditions [40].

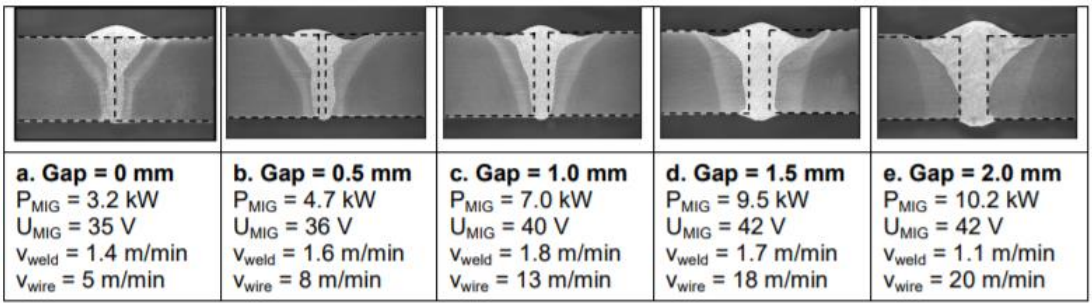

Figure 2-25 Macrographs of butt joints with different root gaps [40]

The maximum welding speed can be achieved up to a gap of 1 mm [40] as shown in Figure 2-26 which demonstrates the relation of welding speed and wire feed speed as a function of root gap. Further increase in root gap requires high heat input for the deposition of more molten filler metal [40]. In addition, mixing of filler wire with base material is also improved during the presence of tolerable root gap [68].

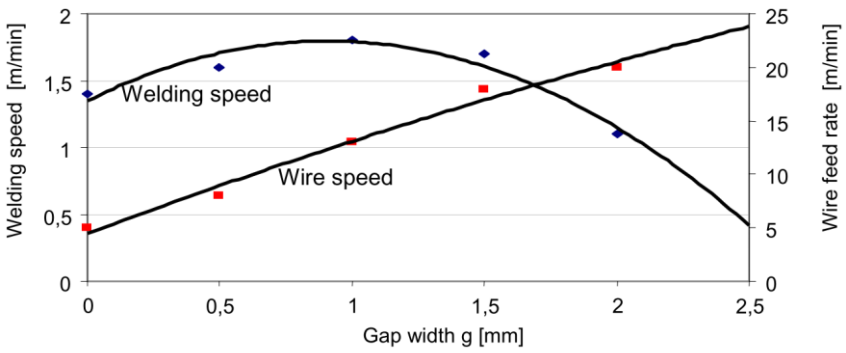

Figure 2-26 Welding speed and wire feed speed as a function of root gap in HLAW process [40]

However, the presence of excessive root gap has an adverse effects on mechanical properties of the weldment [71]. Effect of root gap on mechanical strength was investigated by [71] in laser with cold filler wire welding. Increase in gap reduces the tensile strength of the weldment as shown in Figure 2-27. During tensile test, fracture occurred at fusion zone in the specimen welded with a gap of 1.25 mm [71]. Increase in gap tends to move the fracture location from base metal to fusion zone [71]. As gap increases, formation of severe undercut and reduction in load-bearing area causes the failure in fusion zone [71].

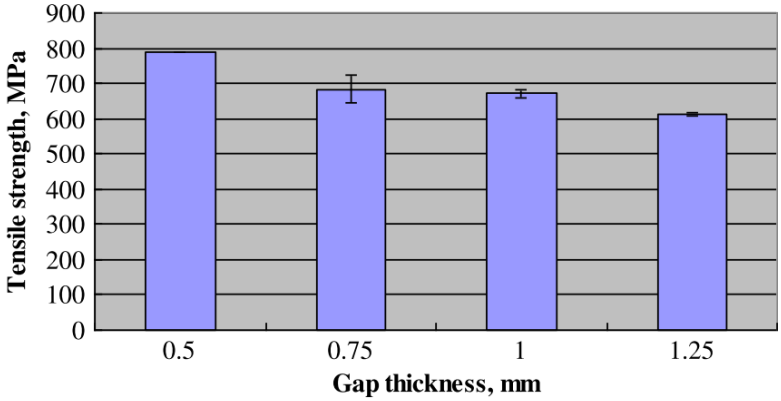

Figure 2-27 Tensile strength exhibited by specimen welded by laser-assisted filler wire welding process at various root gaps [71]

2.6 Weldment distortion

Distortion and residual stresses are the two key issues in any welding processes and both are interrelated phenomena [29,74]. Locked up stresses or residual stresses are formed during the welding process and structure tends to deform when some of these stresses are relieved [29,74]. Distortion exhibits negative effects on performance of the welded structure during variable loading conditions and reduces the buckling strength of the structure [75]. Moreover, distortion leads to dimensional deviation in the welded component [76]. Therefore, welded structure will fail to satisfy the purpose for which it has been designed [77]. Particularly in welding of thin structures, distortion is a key challenge [9]. Lack of rigidity in thin structures causes more shrinkage [75]. It will create issues in assembly processes and adversely affects the functional performance of the product [9].

Residual stress distribution on the weldment is shown in Figure 2-28. Residual stresses are either in the form of tensile or compressive, where the tensile residual stresses are detrimental and compressive residual stresses are improves the component quality [78]. The compressive residual stresses prevent the initiation and propagation of fatigue cracks and improve the fatigue strength of weld components [78]. On the other hand, tensile residual stresses causes brittle fracture [78].

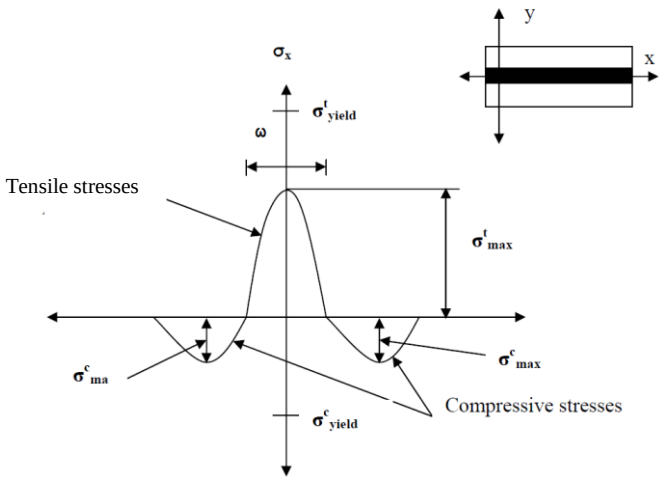

Figure 2-28 Residual stresses on the weldment [79]

It has been emphasized to determine the residual stresses in terms of applied weld load (AWL) [29]. AWL is the load imposed by longitudinal residual stress [80] which can be calculated from the following equation (2-5) [29].

$$AWL = Average\ tensile\ stress\ (\sigma^t max)\ X\ Width\ of\ the\ tensile\ region\ (\omega) \quad \textbf{(2-5)}$$

Distortion occurs if the magnitude of AWL goes beyond the critical buckling load of the structure [29]. In order to reduce the magnitude of AWL, it is necessary to reduce the tensile peak or reduce the tensile stress region [29]. Stress engineering can be employed for the reduction of peak tensile stress wherein employing of low heat input processes, reduces the tensile stress region [29].

High power density of laser welding process produces desired penetration with low heat input which results in lower residual stress generation than conventional arc welding process [81]. Comparatively with CO_2 gas arc welding process, laser beam welding process produced 97% less distortion in 2.3 mm thick low carbon steel [9]. Complete penetration was produced in LBW process with 65% less heat input than GMAW process with narrow fusion zone width and HAZ width [9]. Moreover, the narrow fusion zone and HAZ reduces the thermal contraction which eventually lowers the residual stress and distortion [56]. High weld aspect ratio does not cause for an uneven volume of material in top and root of the weld which controls the angular distortion in butt joints [56].

[29] demonstrated the effects of different welding processes on residual stress formation and distortion. In that autogenous laser welding exhibited lower distortion and followed by hybrid laser arc welding process due to very low heat input of these processes. Residual stress measurement across welds of different welding processes (Figure 2-29) showed that width of tensile stress region increases with heat input [29].

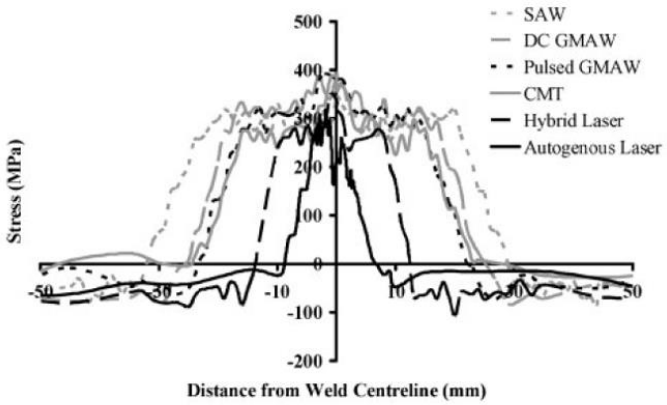

Figure 2-29 Measured longitudinal residual stress across the welds of six different processes [29]

Also, distortion index and fusion zone area showed a near-linear relation with heat input [29] as shown in Figure 2-30. As laser welding is a high power density process, which results in comparatively lower distortion than other processes. Moreover, hybrid laser arc welding process also exhibited relatively lower distortion than conventional arc welding processes.

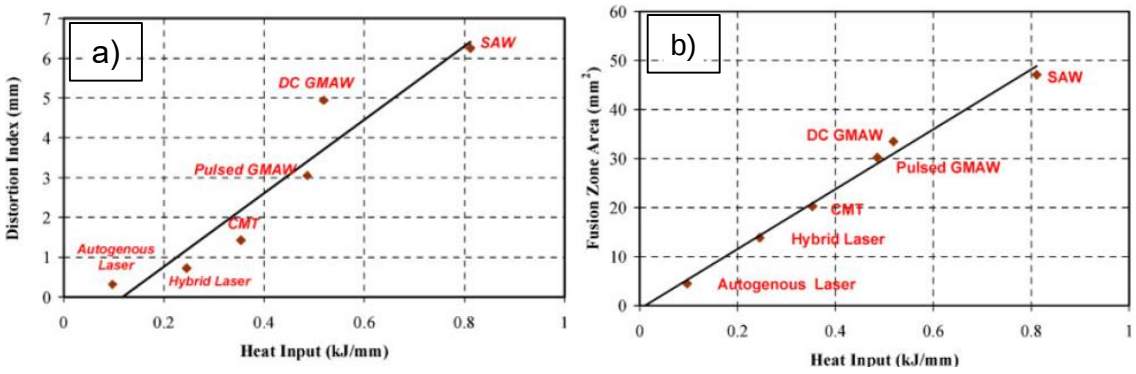

Figure 2-30 a) Variation of distortion index with heat input in different welding processes b) Variation of fusion zone area with heat input in different welding processes [29]

In HLAW process, the heat input ratio of laser and arc also influences the range of angular distortion in butt joint configuration [64]. Variation in the top and root reinforcement has tendency to change the magnitude and direction of angular distortion in butt joint configuration which is represented [64] in Figure 2-31. As

arc heat input dominated specimen (A.E) produced large amount of top reinforcement, it increased the magnitude of distortion as high as 2 mm. Conversely, equal heat input ratio specimen (Basic) and laser heat input dominated specimen (L.E) produced 0.28 mm and 0.52 mm distortion respectively [64].

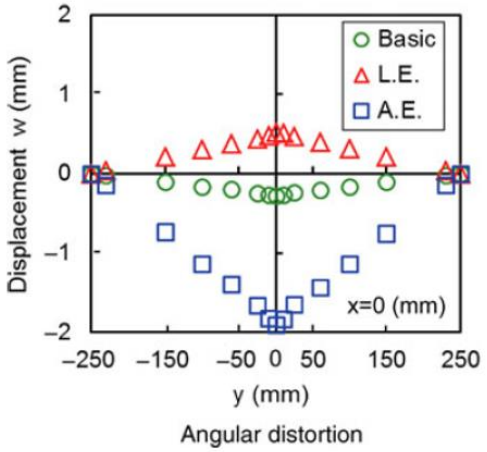

Figure 2-31 Angular distortion of hybrid laser-welded specimen at different heat input ratio of laser and arc [64]

2.7 Metallurgical and mechanical properties of weldment

2.7.1 Microhardness of weldment

Weld bead is a non-homogenous part of the structure [82] which shows different metallurgical and mechanical properties compared to parent metal as it is subjected to heating and cooling process. The amount of heat input delivers to the substrate is varies in different welding processes. This variation in heat input results in different mechanical and metallurgical characteristics [11,30] among laser, GMAW and hybrid laser GMAW processes. Moreover, low heat input results in higher cooling rate and vice-versa [11]. The cooling rate affects the formation of different microstructures in the weldment [11,83]. Microstructural changes in fusion zone and heat affected zone of the weldment in different welding processes are detailed in Table 2-4.

Table 2-4 Microstructural changes in fusion zone and HAZ in different welding processes

Base material	Process	Microstructure of Base material	Microstructure of Fusion Zone	Microstructure of HAZ	Ref.
HSLA - SA516 grade 70	HLAW	Ferrite and pearlite	Acicular ferrite	Ferrite and austenite	[30]
	ALW		Martensitic structure	Martensite with austenite	
HSLA 65 Steel	HLAW	Ferrite and pearlite	Acicular ferrite	Martensite	[43]
C-Mn steel micro-alloyed	GMAW	Ferrite and pearlite	Acicular ferrite & fine-grained ferrite	Granular bainite	[11]
	ALW		Lath martensite	Lath martensite	
HSS HY – 80	GMAW	Granular bainite, ferrite and martensite	Acicular ferrite	Granular bainite, ferrite and martensite	[84]

It can be inferred from the Table 2-4 that ferrite and pearlite microstructure of the parent metal is changed into acicular ferrite and martensite in fusion zone of GMAW and laser welded joints respectively in the experimented conditions. Microstructure of the weld region decides the range of hardness [11,85]. Depends on cooling rate and the composition of filler metal, fusion zone of GMAW weldment may exhibit lower hardness than HAZ [84]. For instance, in multi-pass GMAW in 8 mm thick HY-80 steel, the root zone of the weld joint experienced less heat input than an upper zone of the weld joint which led to high hardness in the root zone [84]. Hardness distribution in top and root region are shown in Figure 2-32. Moreover, HAZ showed higher hardness than fusion zone due to the presence of granular bainite, ferrite and martensite mixture whereas fusion zone consisted of acicular ferrite [84].

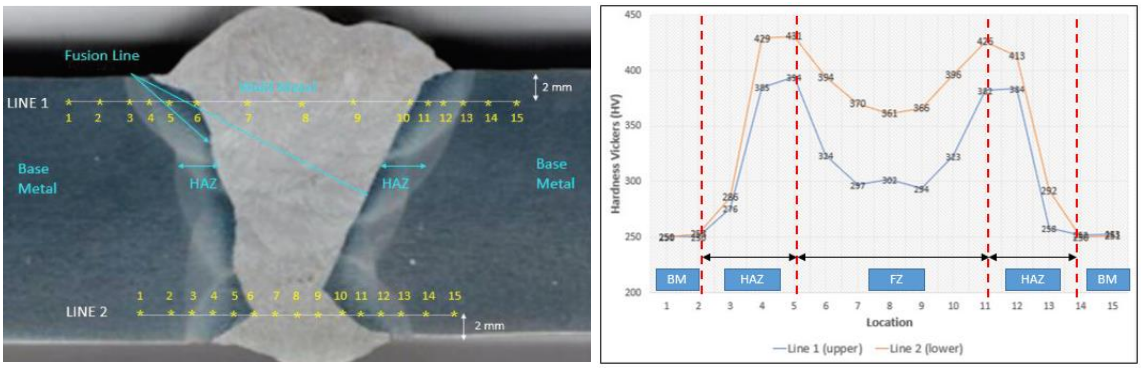

Figure 2-32 Hardness distribution profile of HY-80 steel of 12 mm thick plate in GMAW multi-pass welding [84]

Extremely high cooling rate of steel associated with laser welding process results in high hardness in the weld region [11,28]. Thus, laser welded joints showed higher hardness than GMAW and hybrid laser GMAW joints [11,30] as shown in Figure 2-33 and Figure 2-34 respectively. Increase in hardness, increases the strength of the weld metal [86]. However an excessive hardness is undesirable [28] as it reduces the toughness of the weld metal [31]. In the hybrid laser arc welding process, additional heat input due to arc energy and incorporation of filler wire causes the reduction of hardness in the weld region [30]. Fusion zone of laser-welded joint exhibited 41% more hardness than hybrid laser GMAW joint [30]. Similarly, 1.4 times higher hardness was observed in the fusion zone of the laser-welded joint than GMAW joint [11].

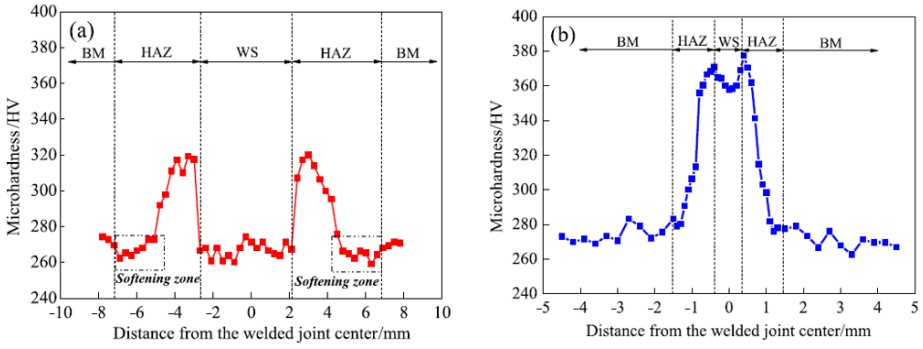

Figure 2-33 Distribution of microhardness in micro alloyed C-Mn high strength steel welded by two different welding processes (a) GMAW (b) ALW [11]

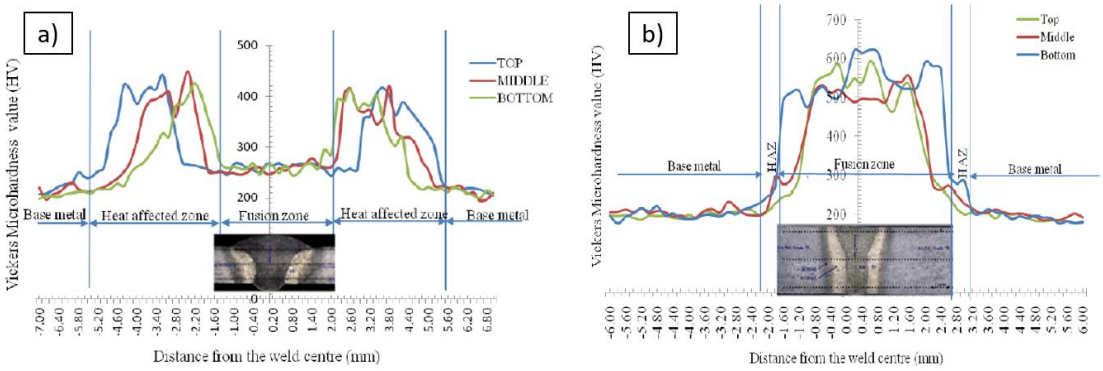

Figure 2-34 Distribution of microhardness in HSLA-SA516 grade 70 steel welded by two different welding processes (a) hybrid laser-GMAW (b) laser welding [30]

As shown in Figure 2-33-a) the softening zone was observed in HAZ of GMAW welded joint whereas both laser [11] and hybrid laser arc welding [30,43] processes were not exhibited any softening zone. Moreover, increase of welding speed increases the fusion zone hardness in both laser [28] and hybrid laser arc welding processes which can be attributed by increase in cooling rate [43].

2.7.2 Strength of weldment

Extremely low heat input and high power density of laser welding processes almost leaves the strength of the parent metal is unaffected and produces very narrow HAZ [20]. As filler metal is not being used in the laser welding process, the composition of weld metal remains the same [20]. Laser weld produces a martensite phase with high hardness due to high cooling rate [30]. Therefore, laser welded joints exhibits greater strength than base metal [20]. Yield strength and ultimate tensile strength of the weldment is greater than the strength of base material. Therefore, fracture occurs in base material during tensile test [30]. However, high hardness in the welded region results in lower impact toughness than base material [30]. In the perspective of mechanical strength, both laser and hybrid laser-GMAW processes exhibits greater tensile strength than base material [30]. High hardness in fusion zone and HAZ than the base material, leads to localization of excessive strain on the base material and eventually fracture occurs at base material [43].

Fatigue strength of the welded joints mainly affected by external discontinuities and internal discontinuities in the weld [87]. External discontinuities such as excess weld reinforcement and uneven transition between weld toe and base metal [87]. Excess weld reinforcement can be controlled by adjusting the weld metal deposition and weld toe can be smoothened either by grinding or TIG dressing process [87]. Internal discontinuities are lack of penetration, lack of fusion, weld cracks and porosity [87]. Optimal process parameters and desired process conditions are required to avoid these defects. According to the investigation of [8] during a fatigue test, in full penetrated joints crack initiated at weld toe and propagated to the HAZ whereas in partially penetrated joints, crack initiated at the lack of penetration section and propagated into the weld metal or weld toe. Partially penetrated joints exhibited considerably lower strength [8]. Hence, better weld geometry and desired depth of penetration enhance the fatigue life of the welded structure.

2.8 Summary

The key points from the literature review are,

- Depth of penetration is limited in GMAW process due to low power density and much higher heat input is required to obtain the required penetration. Moreover, high heat input results in increase of fusion zone and HAZ area.
- Productivity of the GMAW process is limited by low power density and high speed fusion defects such as undercut and humping whereas laser welding can improve the productivity significantly.
- High power density of laser welding processes enhances deep penetration even at low heat input with high weld aspect ratio, less fusion zone and HAZ area.
- However, stringent fit-up tolerance, excessive hardness and lack of reinforcement were found to be the key limitations of autogenous laser welding process.

- Synergic effect of laser and arc in HLAW process enhances the deep penetration with improved part fit-up tolerance and addition of filler metal supports to alter the properties of fusion zone.
- Laser–arc interaction ensures the smooth droplet transfer even at high welding speed and precise combination of laser power and arc power is mandatory to obtain better weld bead geometry which also plays a major role in distortion of the weldment.
- Combination of laser with CMT is preferable over laser with pulse mode for better gap bridgeability with control of weld imperfections.
- Low heat input of laser welding processes reduces the width of the tensile stress region which consequently controls the distortion.
- High cooling rate of laser welding processes, increases the hardness in weld region higher than base material thus both ALW and HLAW joints exhibits higher tensile strength than base material. However an excessive hardness in the autogenous laser welded joints lowers the impact toughness of the weld than the base material.

3 Research methodology

Research methodology has been established based on the main theme of evaluating two advanced laser welding processes and comparing the outcomes with existing GMAW process in different facets for the application in two-wheeler frame. Research has been categorized into four main phases as shown in Figure 3-1. The research scope and objectives are stated in define phase. Experimentation and validation phases were carried out to evaluate the mentioned welding processes in various aspects. Finally, based on the comparative analysis results, a suitable welding process or conditions are recommended in conclusion phase. The detailed research strategy is illustrated in Figure 3-2.

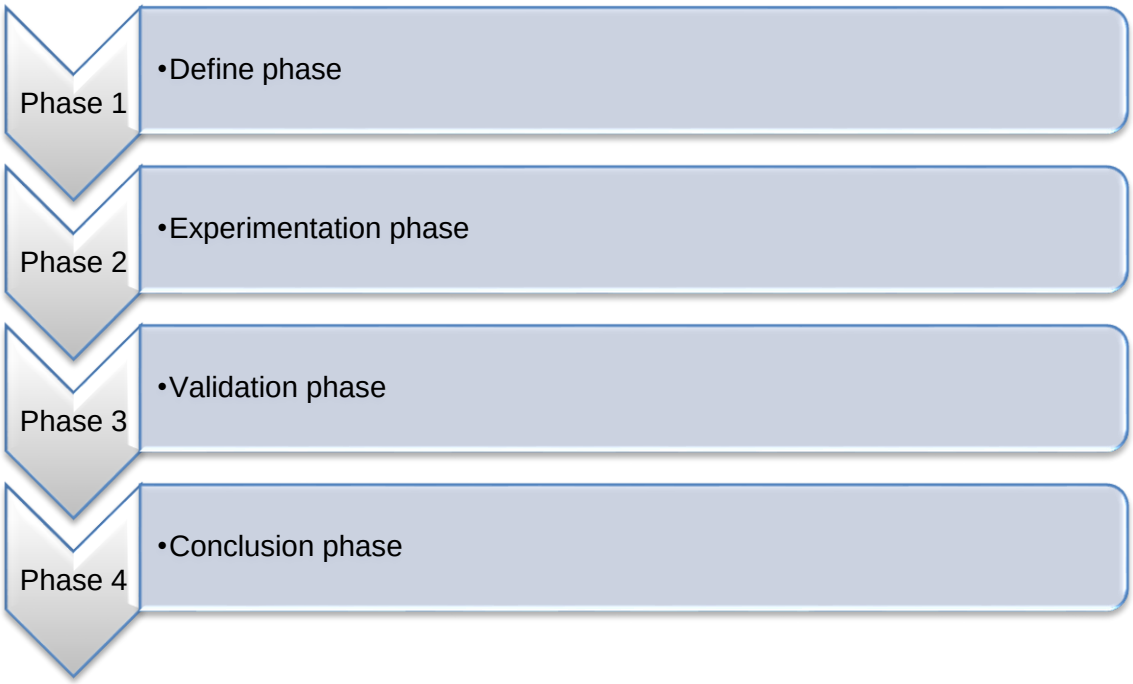

Figure 3-1 Different phases of research

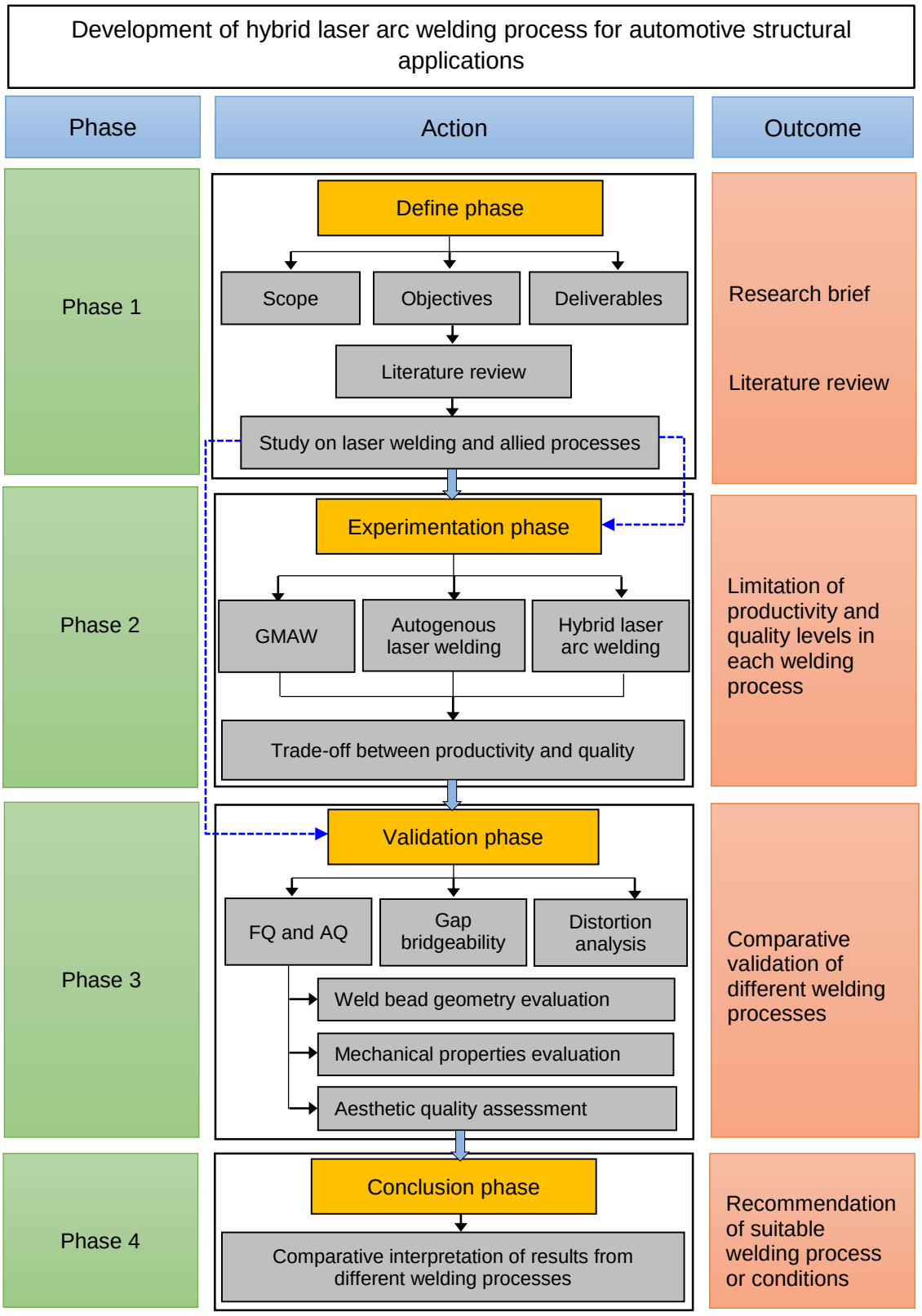

Figure 3-2 Research methodology

4 Materials, experimental set-up, and equipment details

4.1 Introduction

The experimental set-up and equipment used for the research are presented in this chapter. This mainly includes an autogenous laser welding (ALW) system, gas metal arc welding (GMAW) system, and hybrid laser arc welding (HLAW) system. In addition, the details of clamping set-up, joint configuration and arc characterisation equipment also presented. Chemical composition and mechanical properties of both base material and filler wire along with critical sample preparation procedure also described.

4.2 Autogenous laser welding system

IPG-YLR 8 kW CW multimode fibre laser system with beam parameter product of 16 mm.mrad was used for the laser welding experiments carried out throughout this thesis. Set-up of autogenous laser welding system is shown in Figure 4-1. The laser beam was delivered through 300 µm diameter optical fibre with focal lengths of collimating lens and focusing lens of 125 mm and 250 mm respectively.

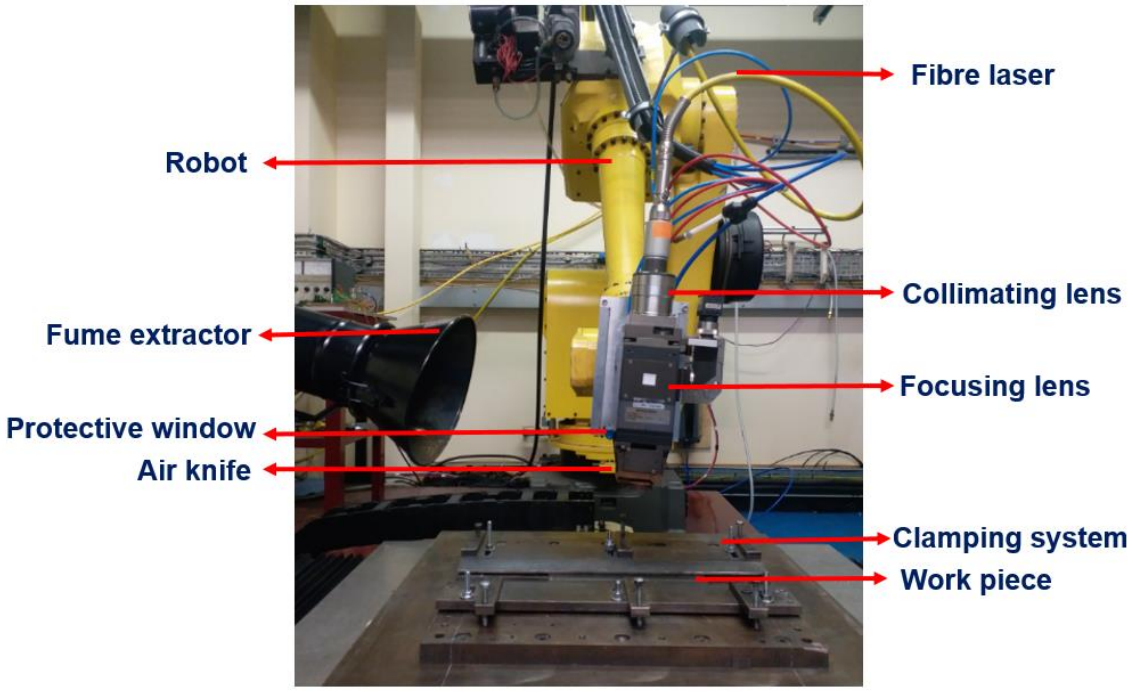

Figure 4-1 Experimental set-up – Autogenous laser welding system

Air knife was used to protect the optics system from spatters. Laser head was mounted in articulated 6 axis Fanuc robot and robot was moved in a linear axis to make a weld seam and the worktable was fixed. Laser head inclination angle was set as 5º as shown in Figure 4-2 to avoid the damage of optics due to back reflection of laser beam.

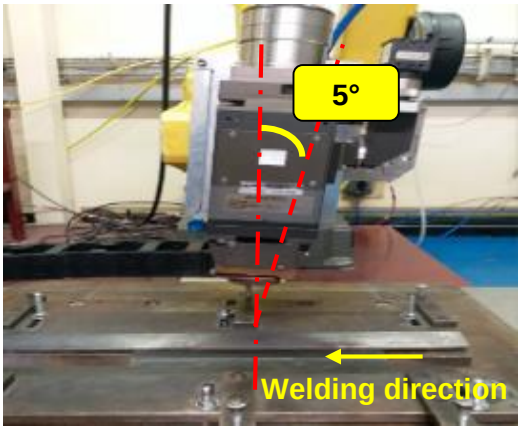

Figure 4-2 Inclination angle of laser head

4.2.1 Clamping set-up

All autogenous laser and hybrid laser arc welding samples were clamped over the entire length and no backing bar was used. The clamping system is shown in Figure 4-3.

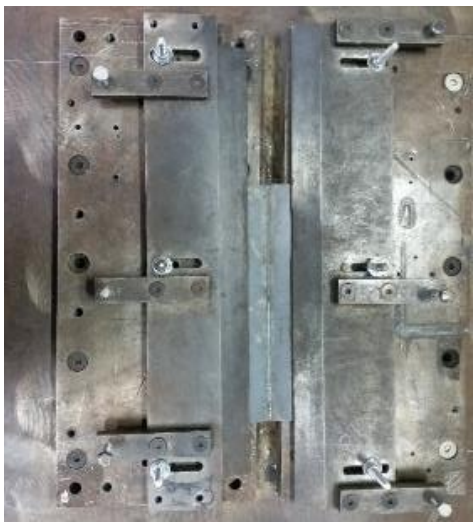

Figure 4-3 Clamping set-up

4.3 Gas metal arc welding system

Gas metal arc welding trials were carried out with Transpuls synergic 5000 CMT R welding machine. IRB 2400-10 model 6 axis ABB robot was interfaced with the welding machine. The experimental set-up of GMAW system is shown in Figure 4-4. Suitable synergic lines were selected based on the welding mode requirement including CMT, pulse and CMT pulse. All the parameters are pre-set with respect to wire feed speed. Therefore, different wire feed speeds were selected based on the required experimental conditions.

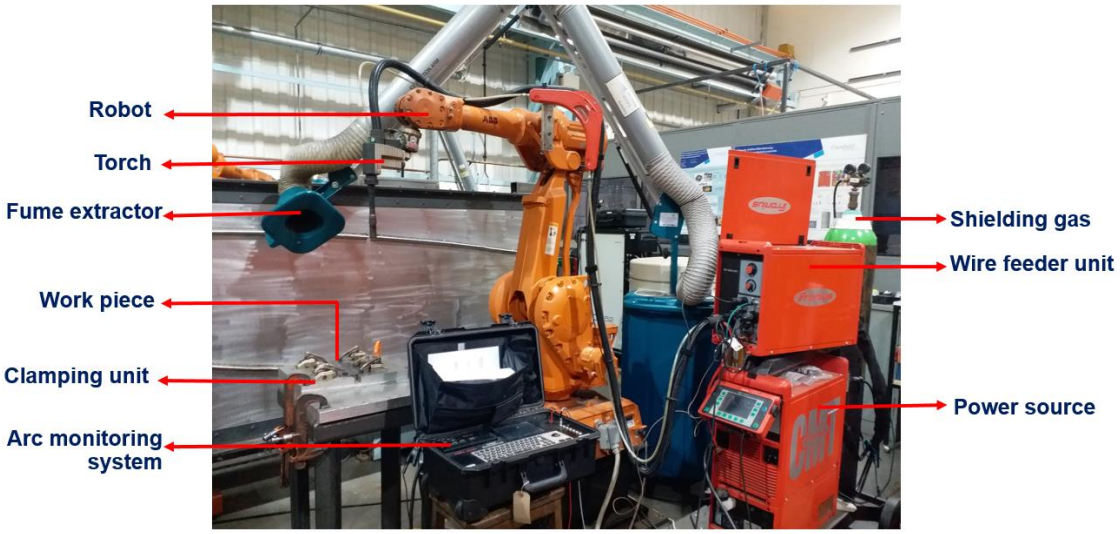

Figure 4-4 Experimental set-up – Gas metal arc welding system

4.3.1 Clamping set-up

The substrate was clamped using the system shown in Figure 4-5. Tack welds were provided to maintain proper fit-up of parts. Copper backing bar was used in GMAW process trials as complete penetration trials were planned.

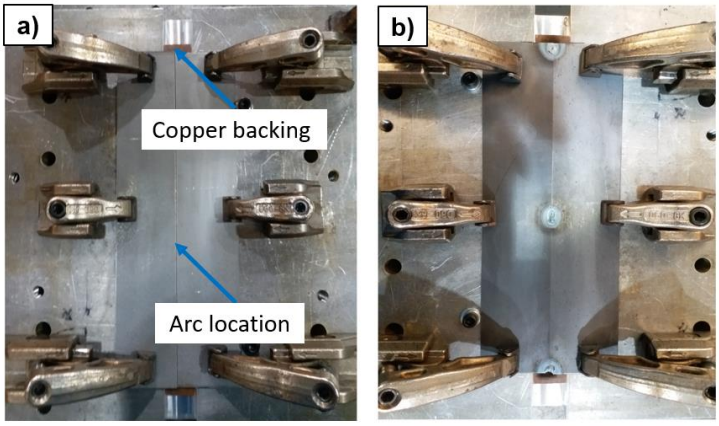

Figure 4-5 Substrate in a) Clamped condition b) Tack welded condition

4.3.2 Torch angle and CTWD

Robot angle was set perpendicular to the substrate and contact tip to work distance (CTWD) was maintained as 11 mm throughout all the GMAW trials as represented in Figure 4-6.

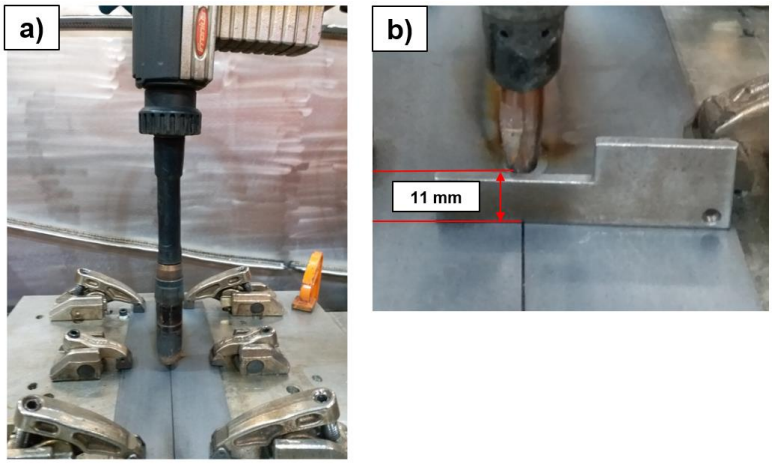

Figure 4-6 a) Torch angle used for welding b) CTWD

4.3.3 Equipment for arc characterisation

The arc energy delivered to the substrate and waveform of arc current and arc voltage were recorded using AMV 4000 data logger which is shown in Figure 4-7. The sample rate used for the accusation was 20 kHz. Waveform from the middle block was taken for heat input calculation [16]. Instantaneous arc power is calculated from the following equation (4-1) [88].

$$P_{AI} = \sum_{i=1}^{n} \frac{I_i V_i}{n} \quad \textbf{(4-1)}$$

Figure 4-7 Arc monitoring system used for arc characterisation

Heat input in all three welding processes are calculated as a theoretical heat input which is the ratio between input power to welding speed [88] and the process efficiency factor was not included.

4.4 Hybrid laser–GMAW system

Fronius Transpuls synergic 5000 CMT R welding machine was interfaced with a Fanuc 6 axis robot where the laser head was mounted. Triangular cut-out has been taken in the nozzle to avoid the collision of laser beam with nozzle. The process separation between laser spot and filler wire was maintained approximately as 2 to 3 mm. Laser leading configuration was used for all the HLAW trials. Figure 4-8 shows the integrated set-up of hybrid laser GMAW system.

4.4.1 Torch angle and CTWD

The laser head and GMAW torch are positioned as shown in Figure 4-9. Laser head was positioned perpendicular to the workpiece wherein GMAW torch was positioned 30° of inclination angle from the laser head [16]. The contact tip to work distance was maintained as 13.5 mm in all the hybrid laser welding experiments.

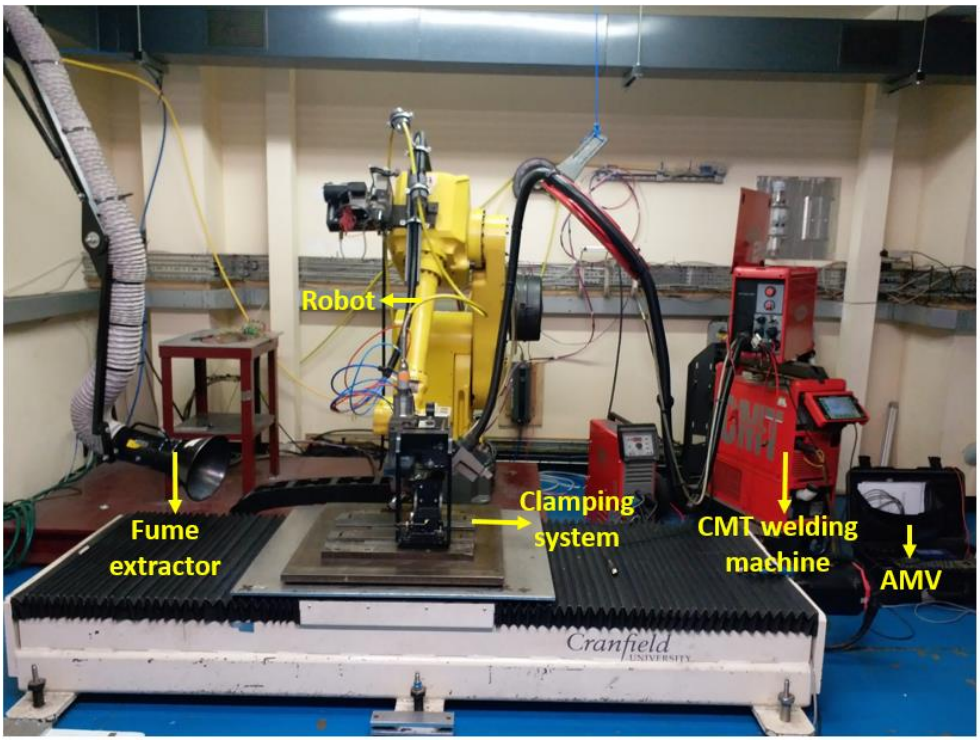

Figure 4-8 Experimental set-up – Hybrid laser GMAW system

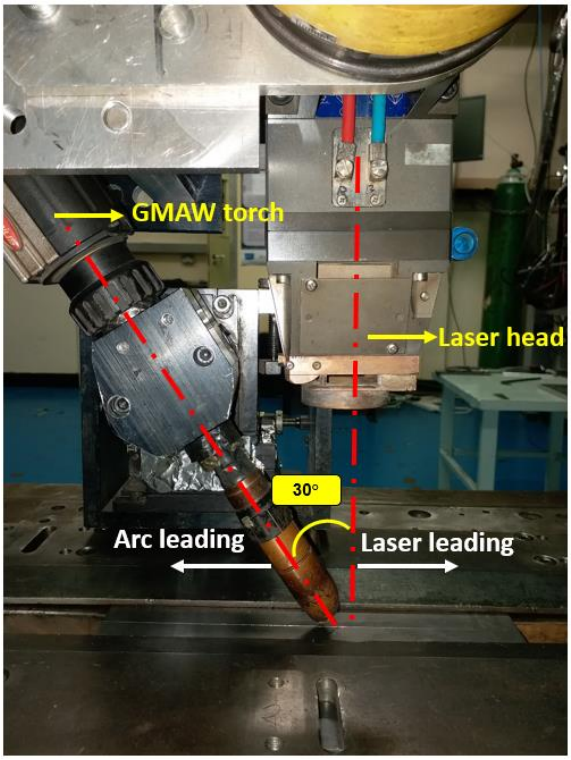

Figure 4-9 Configuration of GMAW torch and laser head (Laser leading was used)

4.5 Material composition

4.5.1 Base material

The low carbon steel of S275 was used for the experiments and dimensional details of the specimen are mentioned in Table 4-1. Three different thicknesses were selected based on the minimum to maximum thickness range typically used in the two-wheeler frame [3]. Chemical composition and mechanical properties of base material are described in Table 4-2 and Table 4-3 respectively. Carbon equivalent of the steel was calculated by using the following equation (4-2) [89].

$$CE = C + \frac{Mn}{6} + \frac{(Cr + Mo + V)}{5} + \frac{(Ni + Cu)}{15} \quad \textbf{(4-2)}$$

Table 4-1 Size of specimen used for experiments

Steel grade	Thickness (mm)	Length (mm)	Width (mm)
Low carbon steel - S275	2	250	50
	4	250	50
	8	250	50

Table 4-2 Chemical composition of base material (% wt)

Element	% wt (2 mm)	% wt (4 mm)	% wt (8 mm)
C	0.140	0.150	0.163
Si	0.021	0.030	0.016
Mn	0.790	0.790	0.940
P	0.011	0.014	0.018
S	0.011	0.002	0.003
Cr	0.040	0.010	0.020
Mo	0.005	0.000	0.001
Ni	0.050	0.000	0.008
Cu	0.060	0.010	0.005
V	0.003	0.002	0.001
Al	0.060	0.046	0.048
Nb	0.002	0.001	0.001
N	0.005	0.005	0.005
CE	**0.289**	**0.285**	**0.325**

The above mentioned chemical compositions of both base material and filler wire were taken from material certificates which were provided by the manufacturer.

Table 4-3 Mechanical properties of base material

#	Properties / Thickness	2 mm	4 mm	8 mm
1	Yield strength (N/mm²)	392	329	362
2	Tensile strength (N/mm²)	490	440	489

4.5.2 Filler wire

The applied filler wire for GMAW and HLAW experiments was AWS ER70S6 grade, Supra-MIG Ultra (Lincoln Electric) filler wire of 1 mm diameter. Chemical composition and mechanical properties of the filler wire are shown in Table 4-4 and Table 4-5 respectively.

Table 4-4 Chemical composition of filler wire (% wt)

Element	C	Mn	Si	S	P	Cr	Mo	Ni	Cu	V	Al	Ti	Zr
% wt.	0.08	1.67	0.94	0.02	0.01	0.04	0.010	0.01	0.01	0.006	0.003	0.010	0.002

Table 4-5 Mechanical properties of filler wire

#	Properties	Value
1	Yield strength (N/mm²)	538
2	Tensile strength (N/mm²)	595

4.6 Shielding gas

The shielding gas composition, flow rate and delivery methods used in the experiments are shown in Table 4-6. The combination of shielding gas was selected to achieve better arc stability, low spatter and improved weld bead profile [79].

Table 4-6 Shielding gas parameters

Process	Gas composition	Gas flow rate	Delivery
Gas metal arc welding	80% of Ar + 20% of CO_2	20 l/min	Arc torch
Autogenous laser welding	-	-	-
Hybrid laser-GMA welding	80% of Ar + 20% of CO_2	20 l/min	Arc torch

4.7 Joint configuration

Square butt joint configuration was used in all the experiments and the specimen size are shown in Figure 4-10. All the weld bead geometry evaluation and gap bridgeability trials were carried out with this dimension of the specimen. Two different weld seams were made in each plate in all the experimental trials except distortion study.

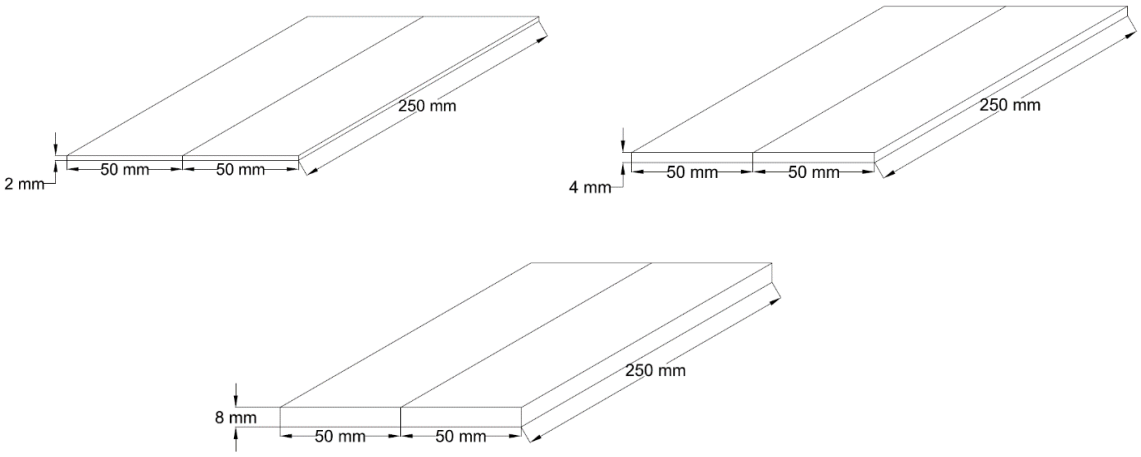

Figure 4-10 Joint configuration

4.8 Distortion measurement and mechanical testing systems

4.8.1 Specimen preparation and clamping set-up

Distortion analysis was carried out in samples welded by all three welding processes. Square butt joint configuration with dimensions of 250 mm x 100 mm size in two different thicknesses of 2 mm and 4 mm are used for the experimentation. Joint configuration is shown in Figure 4-11. Edges of the plates were machined for a proper fit-up. Two ends of the plates were tack welded using

gas tungsten arc welding process. Welding was done over the entire length of the specimen with start and stop plates. Root gap was maintained as zero in all the experiments. Figure 4-12 shows the clamping set-up used for the distortion analysis experiments in all three welding processes without a backing bar.

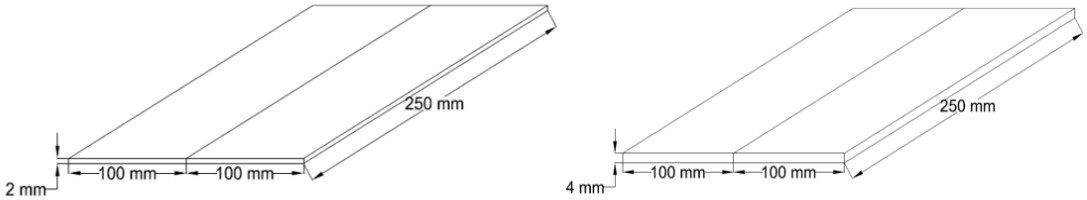

Figure 4-11 Joint configuration - Distortion study

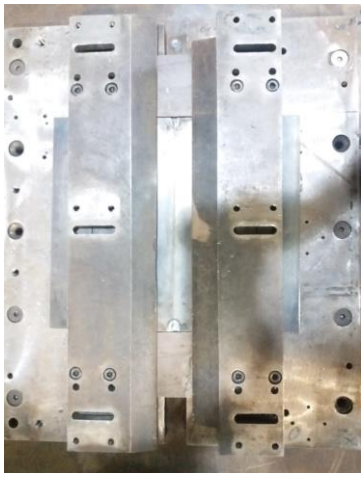

Figure 4-12 Clamping set-up - Distortion study

4.8.2 Distortion measurement jig

The jig used for distortion measurement is shown in Figure 4-13. Four digital dial indicators were mounted on the jig with the interval distance of 50 mm. The large sheet which contains two rails were positioned on the surface table and fixed by using C-Clamps at all the four corners. The jig was positioned on the rail which provided continuous movement of dial indicators over the surface of welded sample.

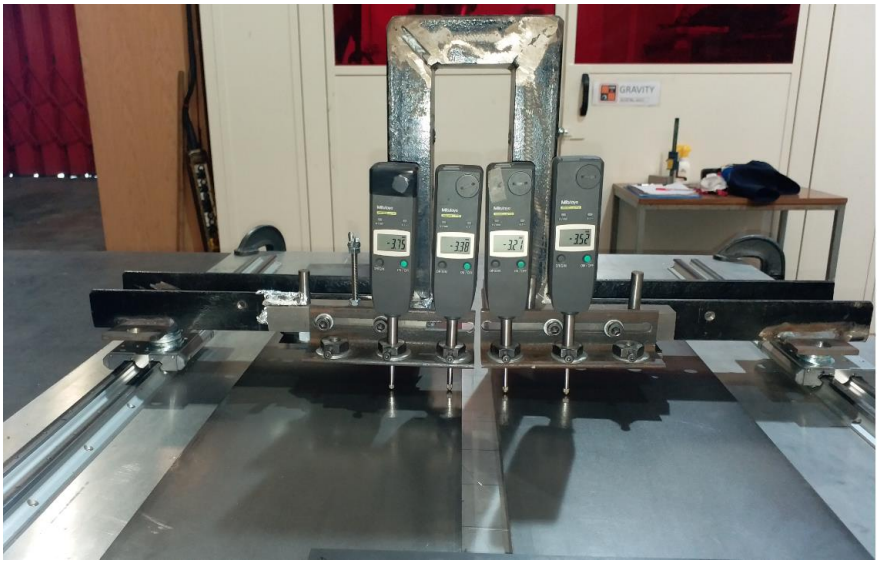

Figure 4-13 Distortion measurement set-up

4.8.3 Microhardness test

Microindentation hardness test was carried out to determine the range of hardness in different zones of weldment such as fusion zone, heat affected zone, and base material as per ASTM E384-17 standard. Zwick/Roell ZHV microhardness equipment was used with a pyramidal diamond indenter which is shown in Figure 4-14. In all the tests, 0.3 kg load was applied for dwell time of 15 sec [71].

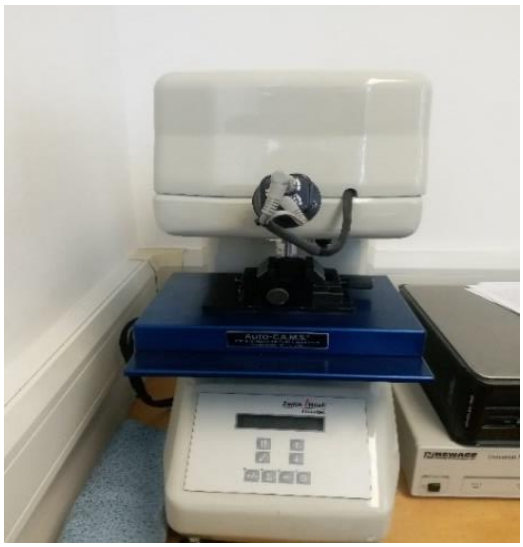

Figure 4-14 Vickers microindentation hardness tester

4.8.4 Tensile strength test

Tensile properties of the weldment were investigated as per ASTM E8/E8M-16a standard. The test was performed by using an electro-mechanical equipment Instron 5500R with a load cell of 30 kN. Dantec 3D Digital Image Correlation (DIC) system was used to measure the distribution of strain on the specimen. The whole deformation process was recorded by the stereoscopic cameras which were mounted perpendicular to the testing surface. All the deformations were captured at 1 fps. The set-up of DIC system is shown in Figure 4-15.

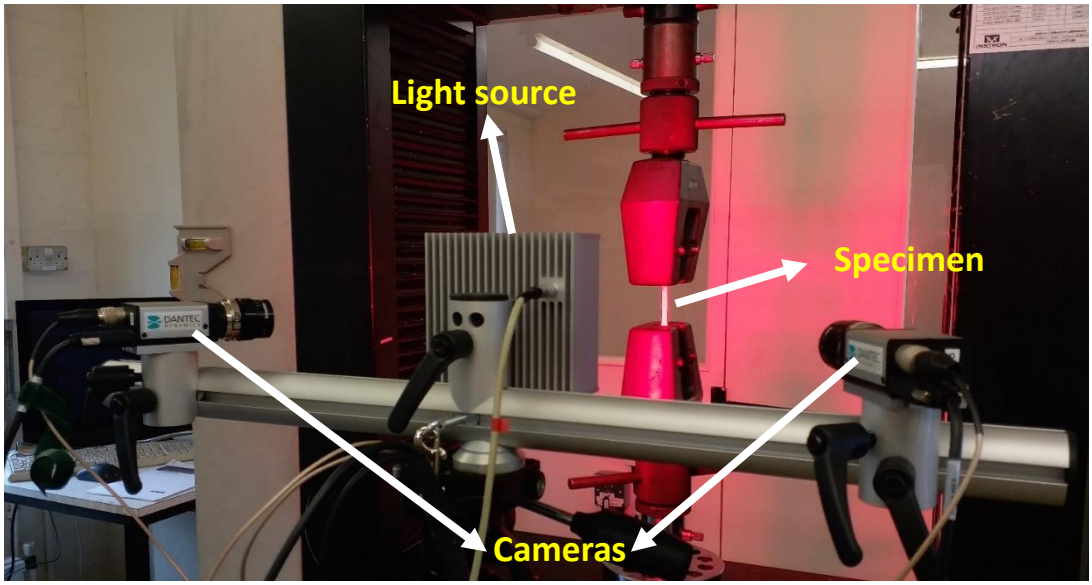

Figure 4-15 Digital image correlation system set-up

4.9 Preparation of samples and quality acceptance criteria

4.9.1 Before welding

Top and bottom surfaces, as well as machined faces of the samples were cleaned by acetone prior to welding.

4.9.2 Preparation for macroscopic evaluation

Welded joints were prepared for macroscopic inspection. The process flow of sample preparation is shown in Figure 4-16.

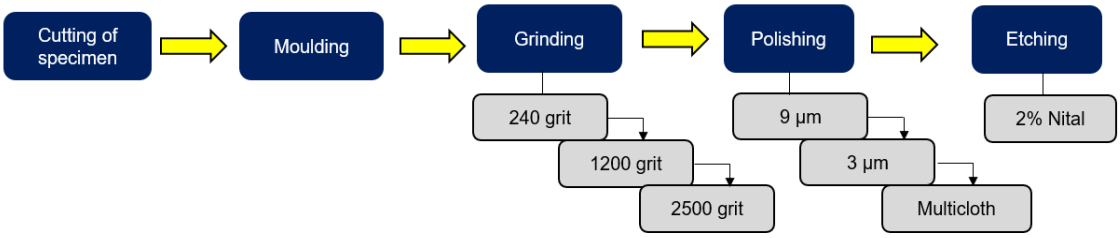

Figure 4-16 Process flow of sample preparation for macroscopic examination

All the welded samples were sectioned at the middle and cold mounted using the mixture of epoxy resin and hardener in the proportion of 25 g and 3 g respectively. Mounted specimen were assembled in the holder to carry out the grinding and polishing operations in the automatic machines. The grinding process was started with 240 grit followed by 1200 grit and 2500 grit were used. Then, samples were taken for polishing operation with different grades of polishing pads including 9 µm and 3 µm used with diamond suspension. Final polishing was done by using multicloth of 0.05 µm pad with silica suspension. Polished samples were etched with 2% or 5% of nital (2% or 5% Nitric acid + 98% or 95% Ethanol) solution for 10 sec to differentiate the base metal, fusion zone and HAZ for macroscopic evaluation. Macrostructures of the joints were captured by using stereo microscope of LEICA E23. Fusion zone area and HAZ area were measured using Carl Zeiss Axio vision 4.8 image analysis software [16].

4.9.3 Criteria for the evaluation of weld bead geometry and aesthetic quality

Weld bead geometries such as depth of penetration, bead width, fusion zone area and weld bead profile were measured and comparative analysis has been carried out among all three welding processes such as GMAW, ALW and HLAW. BS EN ISO 5817:2014 standard was referred for the analysis.

However, the main focus was on studying the effects of process parameters over critical weld bead geometries in all three welding processes where merits and demerits of each process in the aspect of weld bead geometry has been investigated.

Aesthetic quality of the weld beads was quantitatively analysed through AQI (Aesthetic quality index) scoring method as shown in Figure 4-17. Each defect was scored based on the severity of the defect in different aspects including aesthetic issues, structural issues and rework or scrap related issues. Critical weld defects are rated as high, medium or low based on severity in each aspects and scored accordingly as shown in Figure 4-17. For instance, defect concerned with safety including weld offset and burnthrough will have a high score whereas least severe defect like glass bead (Silica deposition) will be scored low. Lower the AQI score better the aesthetic quality.

Risk	Aesthetic issues			Structural issues			Rework/Scrap issues			Overall score for defect
Severity	High	Medium	Low	High	Medium	Low	High	Medium	Low	
Rating/Score	**6**	**4**	**2**	**6**	**4**	**2**	**6**	**4**	**2**	
Glass bead	-	-	2	-	-	-	-	-	-	2
Uneven weld bead	-	4	-	-	-	-	-	-	-	4
Weld spatter	-	4	-	-	-	-	-	4	-	8
Blow hole / Porosity	-	4	-	-	4	-	-	4	-	12
Undercut	-	4	-	-	4	-	-	4	-	12
Underfill	-	4	-	-	4	-	-	4	-	12
Weld offset	6	-	-	6	-	-	6	-	-	18
Incomplete weld	6	-	-	6	-	-	6	-	-	18
Burnthrough	6	-	-	6	-	-	6	-	-	18

Figure 4-17 Scoring criteria for aesthetic quality evaluation

5 Productivity and weld bead geometry

5.1 Introduction

In this chapter, critical evaluation of different welding methods on productivity, weld bead geometry and aesthetic quality of the weld beads are presented. Experimental results of autogenous laser welding (ALW) and hybrid laser arc welding (HLAW) processes were compared with the outcomes of gas metal arc welding (GMAW) process and the effects were analysed. Characteristics of different arc modes such as CMT standard, CMT pulse and pulse mode of GMAW process were also studied. Moreover, the combination of laser with CMT and laser with pulse mode were also experimented and the effects were evaluated.

5.2 Experimental procedure

GMAW, ALW and HLAW process trials were carried out with a different combination of travel speed and power. Travel speed is the measuring factor for productivity in two-wheeler frame welding. Therefore, limitation on productivity was evaluated mainly with respect to travel speed and depth of penetration. In addition, other weld bead geometries and aesthetic quality of the weld beads were also taken as the determining factors for evaluation. The following trials were done in square butt joint configuration with zero root gap. Gap bridging capability of these three welding processes also evaluated which are explained in Chapter 6.

5.2.1 Experimentation matrix for manufacture of baseline GMAW welds

The base line GMAW process parameters includes wire feed speed (WFS) and travel speed (TS) for each thickness of materials were taken from existing process conditions which are shown in Table 5-1. Those parameters are taken as a reference and different combination of parameters were derived to evaluate the limitation on productivity. Optimal quality of the weld was obtained at lower travel speed conditions which significantly hinders the productivity

Table 5-1 Base line GMAW process parameters for various thickness of materials

#	Thickness (mm)	Arc Mode	WFS (m/min)	TS (m/min)
1	2	CMT	5.6	0.3
2	4	CMT	8.2	0.3
3	8	Pulse	10.2	0.3

In order to study the trade-off between productivity and quality of GMAW process, experimentation matrix was formed based on different conditions as follows,

- Different travel speeds at constant wire feed speed
- Different wire feed speeds and travel speeds at constant WFS to TS ratio

Predominantly, Cold metal transfer (CMT) mode was used for the experimentation of 2 mm and 4 mm thick materials, as it produces less spatters and aesthetically good weld beads [51]. Pulse mode was used for welding of 8 mm thick plates to achieve the desired weld penetration. Comparative study of CMT standard mode and pulse mode at same wire feed speed and travel speed were experimented in 4 mm thick plates. Also in a similar way, CMT pulse mode was compared with pulse mode. Influence of these modes on depth of penetration, bead geometry and aesthetic quality of the weld beads were studied. The detailed list of process parameters used in the GMAW trials are described in Table 5-2. Contact tip to work distance (CTWD) was maintained as 11 mm in all the GMAW experiments. Depth of penetration is measured as a percentage of depth to which metal is penetrated in the thickness. The experiment number is mentioned on the macroscopic images for ease of interpretation

Table 5-2 List of experimental parameters used for evaluation of GMAW process

GMAW Process parameters					
Exp.No.	**Thickness (mm)**	**Arc mode**	**WFS (m/min)**	**TS (m/min)**	**WFS/TS ratio**
G – 1	2	CMT	5.6	0.3	18.7
G – 2				0.4	14.0
G – 3				0.5	11.2
G – 4				0.6	9.3
G – 5				0.8	7.0
G – 6				1.0	5.6
G – 7			7.4	0.4	18.5
G – 8			9.3	0.5	18.6
G – 9	4	CMT	8.2	0.3	27.3
G – 10				0.5	16.4
G – 11		Pulse		0.3	27.3
G – 12				0.5	16.4
G – 13		CMT pulse	13.6	0.5	27.2
G – 14		Pulse	13.6	0.5	27.2
G – 15	8	Pulse	10.2	0.3	34.0
G – 16				0.5	20.4
G – 17			17.0	0.5	34.0
Filler wire diameter = 1 mm					

5.2.2 Experimentation matrix for ALW process

In ALW process, power factor model [62] was used to calculate the laser parameters. Productivity was evaluated with different range of travel speeds varying from 0.5 m/min to 5 m/min. At each travel speed, approximately corresponding laser power was calculated using power factor model for the constant beam diameter of 0.6 mm. Table 5-3 shows the parameters used for the experimentation of autogenous laser welding.

Table 5-3 List of experimental parameters used for evaluation of ALW process

Autogenous laser welding process parameters							
Exp.No.	**Thickness (mm)**	**P_L (W)**	**TS (m/min)**	**Heat input (J/mm)**	**q_p (MW/cm²)**	**T_i(ms)**	**E_{SP} (J)**
L – 1	2	1000	0.5	120	0.35	72.00	72.00
L – 2		1200	1	72	0.42	36.00	43.20
L – 3		1600	2	48	0.57	18.00	28.80
L – 4		2000	3	40	0.71	12.00	24.00
L – 5		2300	4	35	0.81	9.00	20.70
L – 6		2600	5	31	0.92	7.20	18.72
L – 7	4	2100	0.5	252	0.74	72.00	151.20
L – 8		2800	1	168	0.99	36.00	100.80
L – 9		3700	2	111	1.31	18.00	66.60
L – 10		4500	3	90	1.59	12.00	54.00
L – 11		5200	4	78	1.84	9.00	46.80
L – 12		5800	5	70	2.05	7.20	41.76
L – 13	8	5100	0.5	612	1.80	72.00	367.20
L – 14		6400	1	384	2.26	36.00	230.40
L – 15		7600	1.5	304	2.69	24.00	182.40
Beam diameter = 0.6 mm							

5.2.3 Experimentation matrix for HLAW process

Hybrid laser-GMA welding trials were carried out with a different combination of wire feed speed, travel speed, and laser power. Table 5-4 describes the experimental parameters used for hybrid laser GMAW trials. The following conditions are used to form the experimentation matrix for HLAW process,

- Different wire feed speeds and travel speeds at constant WFS to TS ratio
- Different wire feed speeds at constant laser power and travel speed
- Comparison between laser with CMT mode and laser with pulse mode at same wire feed speed, travel speed and laser power

Table 5-4 List of experimental parameters used for evaluation of HLAW process

Hybrid laser GMAW process parameters						
Exp.No	**Thickness (mm)**	**Arc mode**	**Laser power (W)**	**WFS (m/min)**	**TS (m/min)**	**WFS/TS ratio**
H – 1	2	CMT	1000	2	0.5	4
H – 2			1200	2	1	2
H – 3			1600	4	2	
H – 4			2000	6	3	
H – 5			2300	8	4	
H – 6			2600	9.4	5	
H – 7			1200	4	1	4
H – 8			1200	6	1	6
H – 9			1200	8	1	8
H – 10		Pulse	1200	2	1	2
H – 11			1600	4	2	
H – 12	4	CMT	2100	2	0.5	4
H – 13			2800	2	1	2
H – 14			3700	4	2	
H – 15			4500	6	3	
H – 16			5200	8	4	
H – 17			5800	9.4	5	
H – 18			2800	4	1	4
H – 19			2800	6	1	6
H – 20		Pulse	2800	2	1	2
H – 21			3700	4	2	
H – 22	8	CMT	5100	2	0.5	4
H – 23			6400	2	1	2
H – 24			7600	3	1.5	
H – 25			6400	4	1	4
H – 26			6400	6	1	6
H – 27		Pulse	6400	2	1	2
H – 28			7600	3	1.5	
Beam diameter = 0.6 mm, Filler wire diameter = 1 mm						

Different of travel speed was selected based on the level of productivity from low to high which was ranging from 0.5 m/min to 5 m/min. Corresponding laser power was calculated by using power factor model and wire feed speed was selected from minimum to maximum range at constant WFS to TS ratio.

5.3 Results

5.3.1 Evaluation of productivity and weld bead geometry in thin structure

In a preliminary experiment from G-1 to G-6 as shown in Table 5-2, limitation on productivity of GMAW process in 2 mm thick sheets were evaluated at a constant wire feed speed of 5.6 m/min and at different travel speeds. Travel speed has been increased from 0.3 m/min to 1 m/min. Macrographs of these welds are presented in Figure 5-1. The data indicates that there is an optimum welding speed for a given wire feed speed and current. Travel speeds of 0.4 m/min and 0.5 m/min have produced better weld penetration profile than the other lower and higher travel speed conditions as shown in Figure 5-1, G-2 and G-3.

TS = 0.3 m/min	**TS = 0.4 m/min**	**TS = 0.5 m/min**
	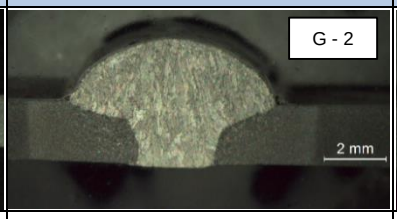	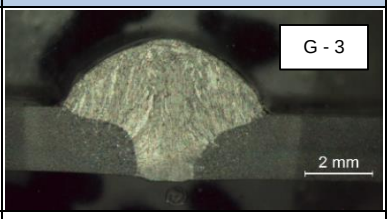
Depth of fusion = 100%	Depth of fusion = 100%	Depth of fusion = 100%
TS = 0.6 m/min	**TS = 0.8 m/min**	**TS = 1 m/min**
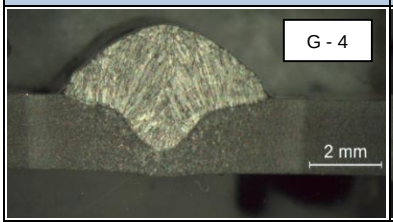	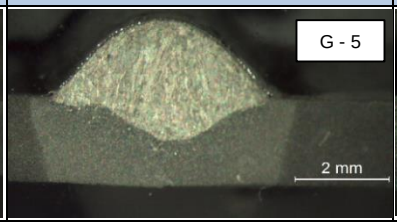	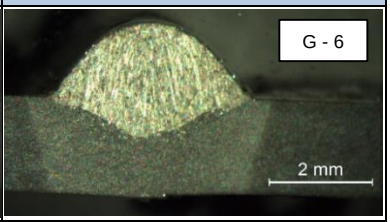
Depth of fusion = 75%	Depth of fusion = 51%	Depth of fusion = 41%

Figure 5-1 Macrographs of GMAW joints at constant WFS of 5.6 m/min and different travel speeds in CMT standard mode – 2 mm thickness

It is apparent from Figure 5-1 and Figure 5-2 that, increase in travel speed beyond 0.6 m/min at constant wire feed speed, reduces the penetration. Productivity of the process is limited to 0.5 m/min because complete penetration was not achieved above the travel speed of 0.5 m/min. Reduction of heat input due to increase in travel speed at constant arc power reduces the penetration. Moreover, it decreases weld bead width and top bead reinforcement as shown in Figure 5-3. Increase in travel speed from 0.3 m/min to 1 m/min at constant wire feed speed, decreases the penetration approximately by 59% and decreases the bead width and top bead reinforcement by 44% and 34% respectively. Therefore comparatively, travel speed has a minimal effect on top bead reinforcement [52].

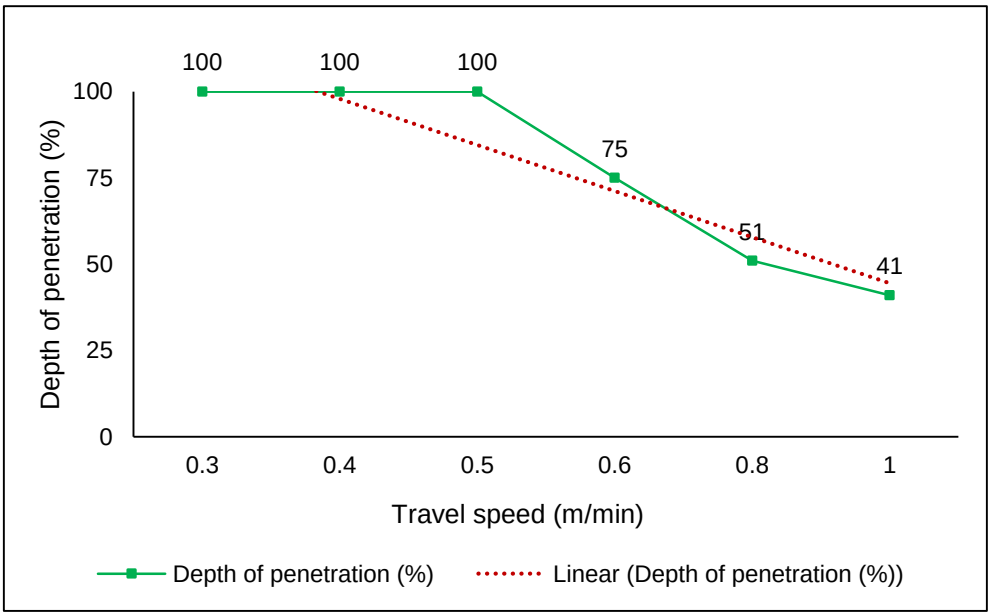

Figure 5-2 Depth of penetration achieved at constant wire feed speed of 5.6 m/min and different travel speeds – 2 mm thickness

Result presented in Figure 5-2 shows that CMT process can produce complete penetration in 2 mm thick sheet up to welding speed of 0.5 m/min and this is the baseline for comparison with other processes.

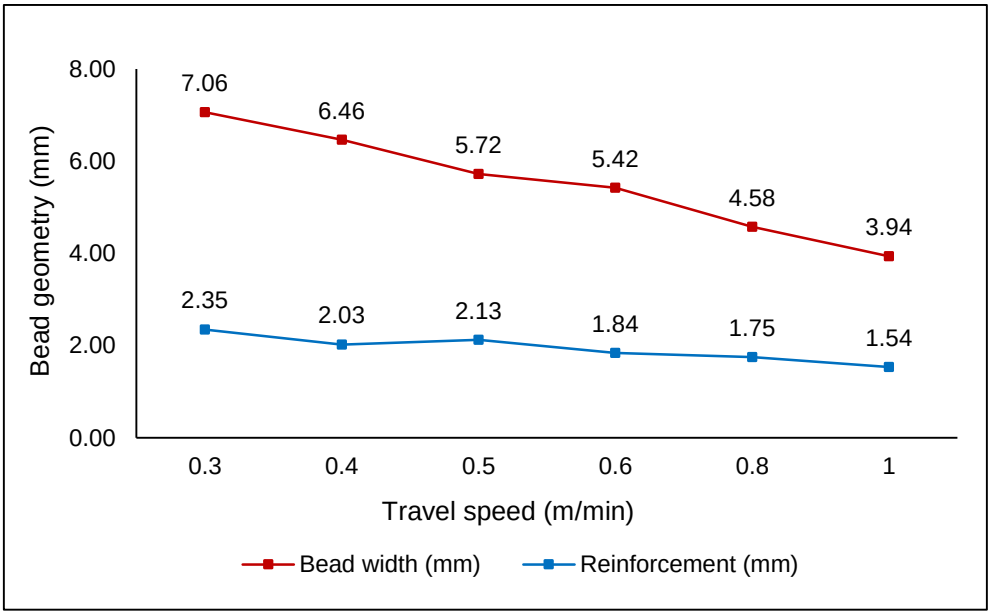

Figure 5-3 Effect of travel speed on weld bead width and reinforcement at constant WFS of 5.6 m/min

In the main experiment, all three welding processes were evaluated in the combination of different power and travel speed. Travel speeds used in the range of 0.3 m/min to 0.5 m/min in GMAW and 0.5 m/min to 5 m/min in ALW and HLAW processes. Macrographs of 2 mm thick joints welded by all the three welding processes are shown in Figure 5-4. In GMAW process, at constant WFS to TS ratio, both WFS and TS was increased until the formation of major non-conformance in the weld. Complete penetration was obtained at 0.4 m/min and 0.5 m/min conditions as shown in Figure 5-4, G-7 and G-8. However, weld burnthrough was observed at TS of 0.5 m/min and WFS of 9.3 m/min. CMT could produce complete penetration at a travel speed of 0.5 m/min and it was difficult to control penetration depth and root profile. On the other hand, ALW could produce complete penetration up to travel speed of 5 m/min however, acceptable root profile was achieved at maximum travel speed of 4 m/min. Due to the lack of filler metal, it is more difficult to achieve sufficient reinforcement. Moreover, precise control of laser power is required to ensure complete penetration without excessive material loss. HLAW process provided welds with complete penetration up to travel speed of 5 m/min along with the control of bead profile.

Process	Macrographs of welds – 2 mm thickness		
GMAW - CMT	WFS = 5.6 m/min TS = 0.3 m/min	WFS = 7.4 m/min TS = 0.4 m/min	WFS = 9.3 m/min TS = 0.5 m/min
	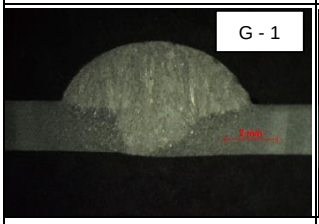	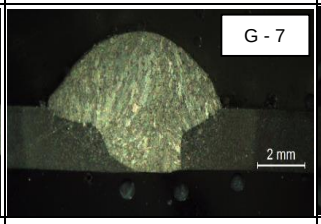	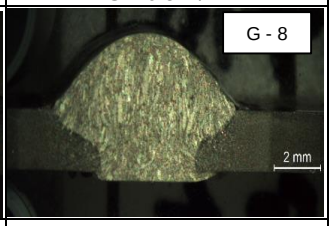
	Depth of fusion = 100%	Depth of fusion = 100%	Depth of fusion = 100%
Autogenous laser welding	P_L = 1000 W, TS = 0.5 m/min	P_L = 1200 W, TS = 1 m/min	P_L = 1600 W, TS = 2 m/min
	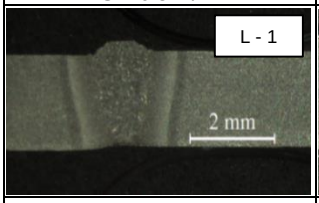	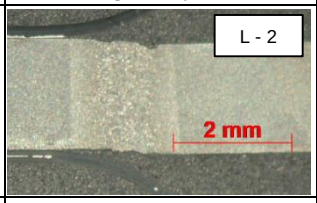	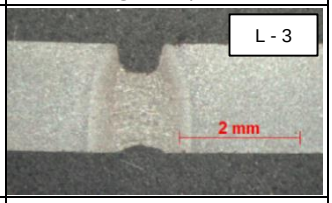
	Depth of fusion = 100%	Depth of fusion = 100%	Depth of fusion = 100%
	P_L = 2000 W, TS = 3 m/min	P_L = 2300 W, TS = 4 m/min	P_L = 2600 W, TS = 5 m/min
	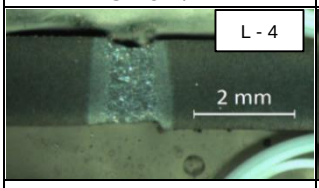	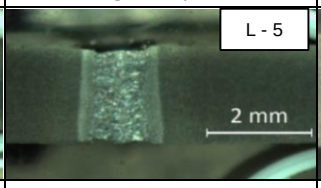	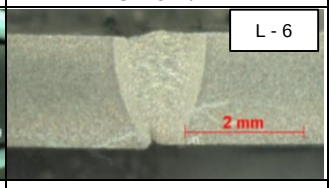
	Depth of fusion = 100%	Depth of fusion = 100%	Depth of fusion = 87%
HLAW – Laser+CMT	P_L = 1000 W, TS= 0.5 m/min, WFS = 2 m/min	P_L = 1200 W, TS = 1 m/min, WFS = 2 m/min	P_L = 1600 W, TS = 2 m/min, WFS = 4 m/min
	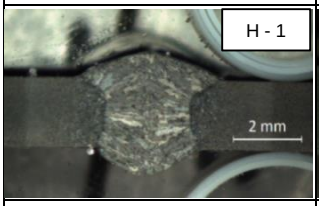	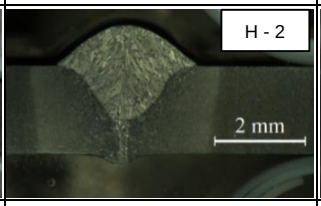	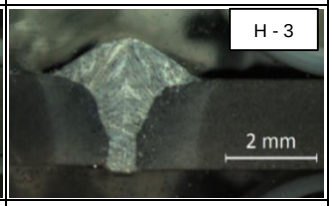
	Depth of fusion = 100%	Depth of fusion = 100%	Depth of fusion = 100%
	P_L = 2000 W, TS = 3 m/min, WFS = 6 m/min	P_L = 2300 W, TS = 4 m/min, WFS = 8 m/min	P_L = 2600 W, TS = 5 m/min, WFS = 9.4 m/min
	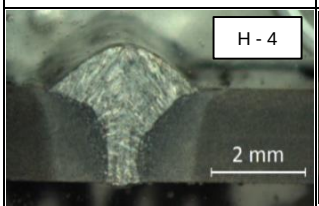	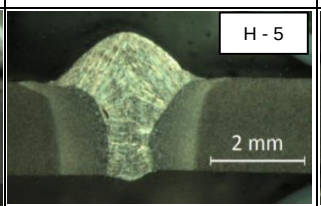	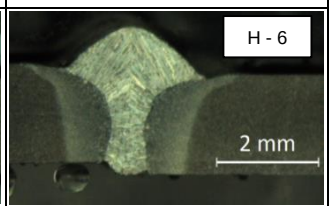
	Depth of fusion = 100%	Depth of fusion = 100%	Depth of fusion = 100%

Figure 5-4 Macrographs of specimen welded by different welding processes – 2 mm thickness

In GMAW process, as shown in Figure 5-3, it is apparent that at constant wire feed speed with increase in travel speed limiting the productivity to 0.5 m/min and in complete penetration condition. At the same time, at constant WFS to TS ratio, increasing both of these parameters increases the heat input marginally. Weld burnthrough occurred at a travel speed of 0.5 m/min where the heat input was 491 J/mm as shown in Figure 5-5. In this case, productivity is limited to 0.4 m/min. This indicates that it is difficult to control penetration depth independently in GMAW process. Achievement of weld penetration in GMAW process at different parametric conditions are presented in Figure 5-6.

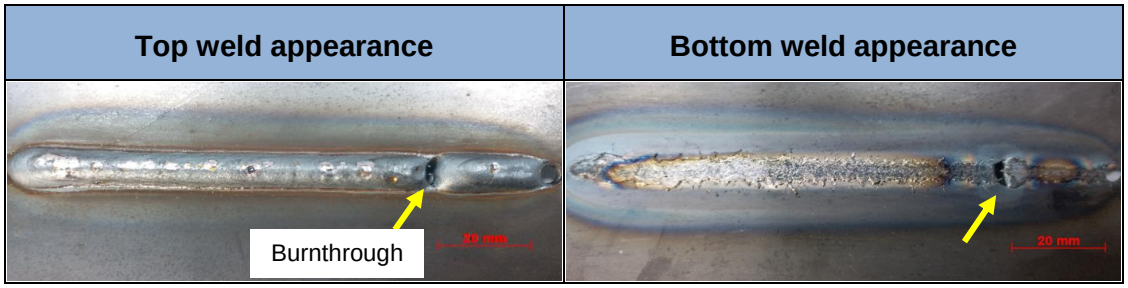

Figure 5-5 Top and bottom weld appearances of specimen welded at WFS = 9.3 m/min, TS = 0.5 m/min in CMT mode – 2 mm thickness

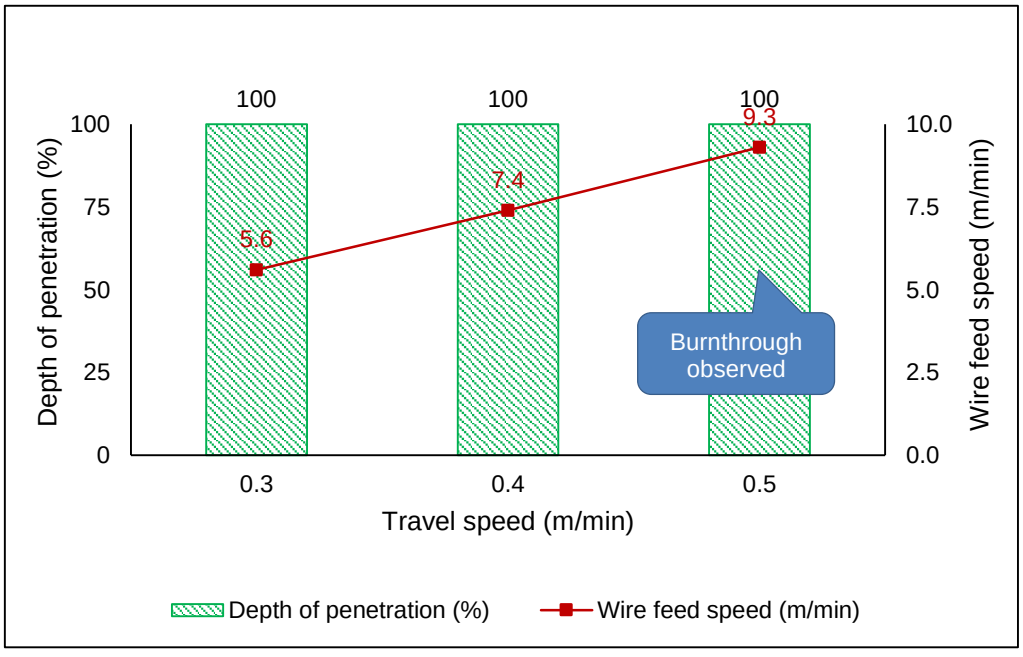

Figure 5-6 Depth of penetration achieved in GMAW process at different parametric conditions - 2 mm thickness

A marginal increase in heat input has minor effects on weld bead width and top bead reinforcement as shown in Figure 5-7. An almost equal amount of reinforcement shows that uniform amount of weld metal deposited at constant wire feed speed to travel speed ratio [90].

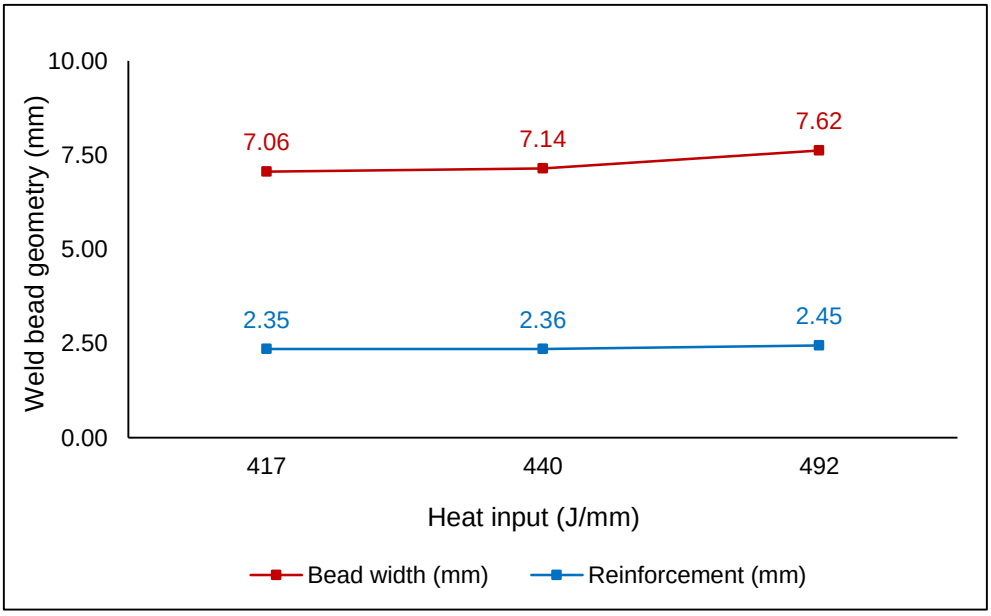

Figure 5-7 Effect of heat input on weld bead geometry – GMAW process

Overall in GMAW process in order to achieve complete penetration at both the conditions such as constant wire feed speed with increase in travel speed condition and increase in WFS and TS at constant WFS to TS ratio, productivity is limited to maximum travel speeds of 0.5 m/min and 0.4 m/min respectively.

Autogenous laser welded joints are shown in Figure 5-4. L-1 to L- 6. Maximum depth of fusion was achieved at all the travel speed conditions except at 5 m/min where lack of fusion was observed. Weld penetration attainment with corresponding process parameters are shown in Figure 5-8. High power density of the laser welding process, produced better penetration with less fusion zone area and narrow HAZ [11]. As there is no filler metal, it is difficult to control top and root reinforcement in laser welding process which can be seen in Figure 5-4, L-3 and L-6. Lack of reinforcement was found to be the limitation in ALW process as it may affects the fatigue life of the welded structure [91].

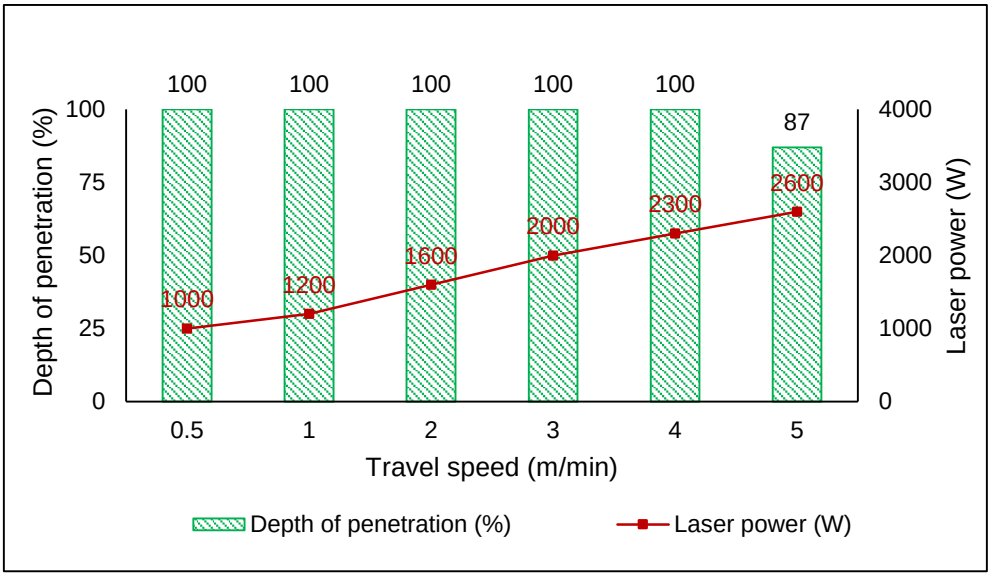

Figure 5-8 Depth of penetration achieved by ALW process at different parametric conditions – 2 mm thickness

Hybrid laser arc welded joints are shown in Figure 5-4, H-1 to H-6 which exhibited the benefits of both GMAW and ALW processes, such as better weld bead profile and complete penetration respectively. It was obtained in all the range of travel speeds from 0.5 m/min to 5 m/min. Nevertheless, in Experiment H-2 where the incomplete distribution of filler wire was observed as shown in Figure 5-9. This is attributed to an improper ratio between laser power and arc power. It may cause non-homogeneity in the fusion zone. Excluding this, all other parametric conditions were produced acceptable welds.

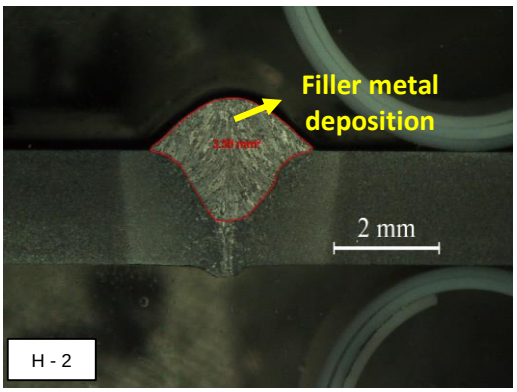

Figure 5-9 Filler metal distribution in HLAW process at P_L = 1200 W, TS = 1 m/min, WFS = 2 m/min

Achievement of weld penetration in HLAW process at different parametric conditions including travel speed with both laser power and arc power are presented in Figure 5-10. Complete weld penetration was achieved in all the experimented travel speeds ranging from 0.5 m/min to 5 m/min.

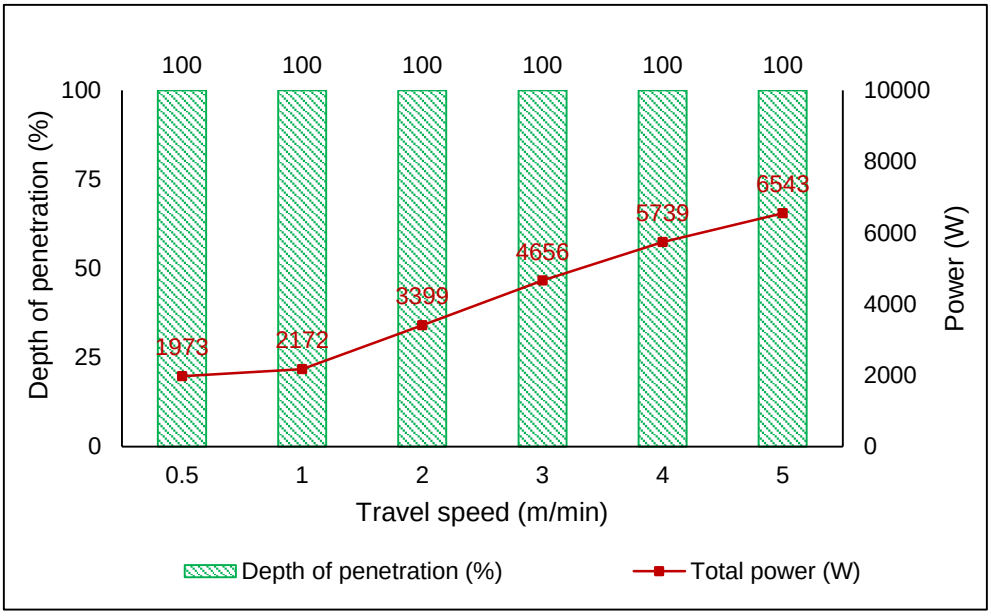

Figure 5-10 Depth of penetration achieved by HLAW process at different parametric conditions – 2 mm thickness

Addition of filler wire in HLAW process produced weld bead profile with the large semi-hemispherical shape at the top and small semi-hemispherical shape in the root as shown in Figure 5-11 [31]. It indicates that arc has more influence on the top region whereas laser dominating in the root region [65] for the given laser power and arc power. Moreover, the slow rate of flow of molten metal causes less reinforcement in the bottom [30]. Similar results were inferred by [30].

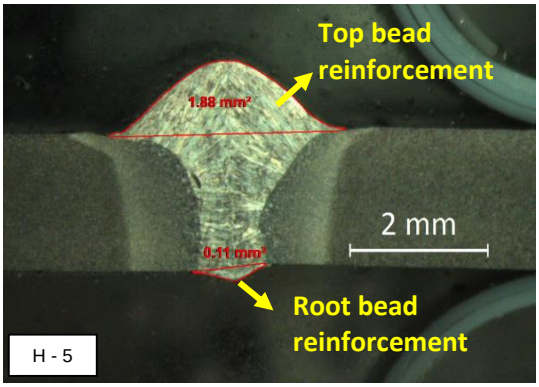

Figure 5-11 Top and root bead reinforcement in HLAW process at P_L = 2300 W, TS = 4 m/min, WFS = 8 m/min

In thin materials, GMAW process also can produce complete weld penetration. Nevertheless, low heat input and high welding speed of ALW and HLAW processes can reduce the distortion and improve the productivity significantly. HLAW process was found to be easiest in terms of control of penetration as well as bead reinforcement.

5.3.2 Evaluation of productivity and weld bead geometry in thick structures

As similar to the experiments on 2 mm thick sheets, experimentation on 4 mm and 8 mm thick plates also have been carried out. Macrographs of the 4 mm thick joints are shown in Figure 5-12. In GMAW process on 4 mm thick plates, CMT mode was used with constant WFS and increase in TS condition. At constant WFS of 8.2 m/min, increase in travel speed from 0.3 m/min to 0.5 m/min reduced the penetration as shown in Figure 5-12, G-9 and G-10. As CMT standard mode was limited to WFS of 9.4 m/min for the 1 mm diameter of filler wire, CMT pulse mode was employed to increase the WFS further. It was difficult to achieve complete penetration in CMT. However, 99% of penetration was achieved with CMT pulse mode along with more bead width and reinforcement. ALW process produced fully penetrated welds up to travel speed of 4 m/min whereas penetration depth of 89% was observed at the speed of 5 m/min. Controlled bead profile with complete penetration was achieved in HLAW process up to travel speed of 5 m/min. However, undercut was observed at the speed of 5 m/min.

Process	Macrographs of welds – 4 mm thickness		
GMAW	WFS = 8.2 m/min TS = 0.3 m/min, Mode - CMT	WFS = 8.2 m/min TS = 0.5 m/min, Mode - CMT	WFS = 13.6 m/min TS = 0.5 m/min, Mode – CMT Pulse
	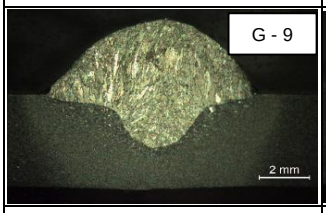	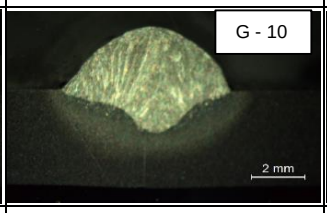	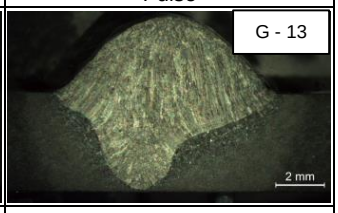
	Depth of fusion = 59%	Depth of fusion = 46%	Depth of fusion = 99%
Autogenous laser welding	P_L = 2100 W, TS = 0.5 m/min	P_L = 2800 W, TS = 1 m/min	P_L = 3700 W, TS = 2 m/min
	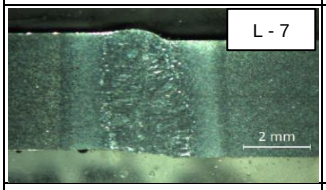	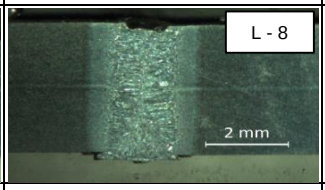	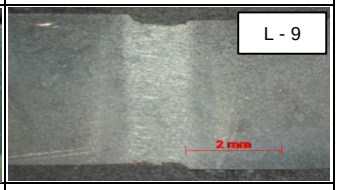
	Depth of fusion = 100%	Depth of fusion = 100%	Depth of fusion = 100%
	P_L = 4500 W, TS = 3 m/min	P_L = 5200 W, TS = 4 m/min	P_L = 5800 W, TS = 5 m/min
	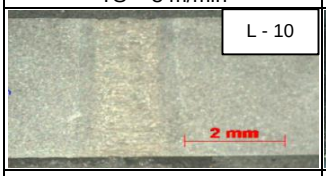	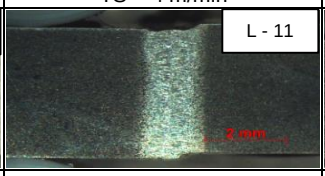	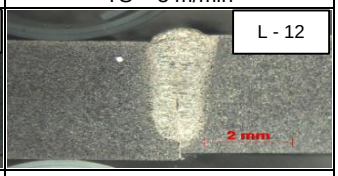
	Depth of fusion = 100%	Depth of fusion = 100%	Depth of fusion = 89%
HLAW – Laser+CMT	P_L = 2100 W,TS= 0.5 m/min, WFS = 2 m/min	P_L = 2800 W,TS = 1 m/min, WFS = 2 m/min	P_L = 3700 W, TS = 2 m/min, WFS = 4 m/min
	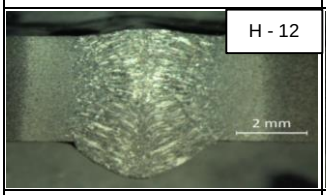	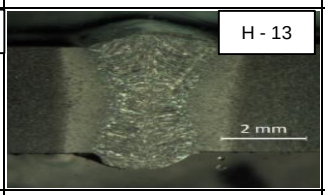	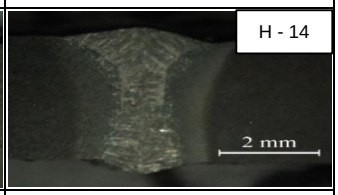
	Depth of fusion = 100%	Depth of fusion = 100%	Depth of fusion = 100%
	P_L = 4500 W,TS = 3 m/min, WFS = 6 m/min	P_L = 5200 W, TS = 4 m/min, WFS = 8 m/min	P_L = 5800 W,TS = 5 m/min, WFS = 9.4 m/min
	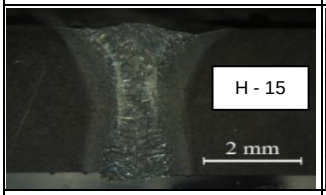	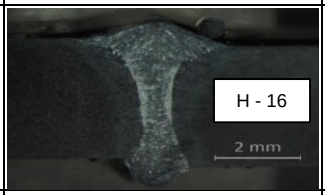	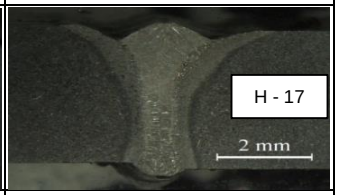
	Depth of fusion = 100%	Depth of fusion = 100%	Depth of fusion = 100%

Figure 5-12 Macrographs of specimen welded by different welding processes – 4 mm thickness

In GMAW process, much higher heat input was required to achieve deep penetration in higher thickness materials. Nevertheless, high heat input increases the fusion zone area and deposition of filler metal as well. ALW process produced complete penetration at different travel speeds ranging from 0.5 m/min to 4 m/min with a lack of reinforcement. However, complete penetration with controlled top and root bead reinforcement without any weld imperfections was obtained in HLAW process at travel speeds ranging from 0.5 m/min to 4 m/min.

CMT pulse synergic line was used in the condition of increased wire feed speed and travel speed at constant WFS to TS ratio in GMAW. It produced 99% depth of penetration as shown in Figure 5-12, G-13. CMT mode produced low penetration and aesthetically good weld bead without spatters. In case of CMT pulse mode, a combination of CMT and pulse cycles improved the penetration with few spatters on the surface. Parametric conditions and depth of penetration achieved by GMAW process in 4 mm thick plates are shown in Figure 5-13.

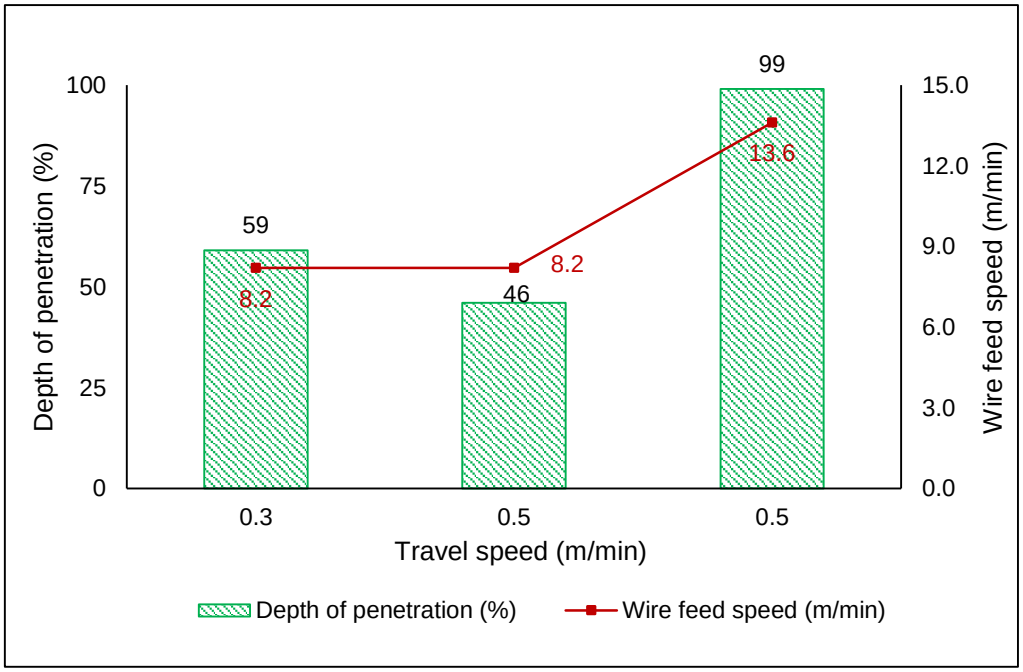

Figure 5-13 Depth of penetration achieved by GMAW process at different parametric conditions – 4 mm thickness

Weld penetration achievement in 4 mm thick joints by ALW process is shown in Figure 5-14. Complete weld penetration was achieved with narrow fusion zone and HAZ width in a wide range of travel speeds from 0.5 m/min to 4 m/min as shown in Figure 5-12, L-7 to L-11. Incomplete penetration was observed at travel speed of 5 m/min which can be referred in Figure 5-12, L-12.

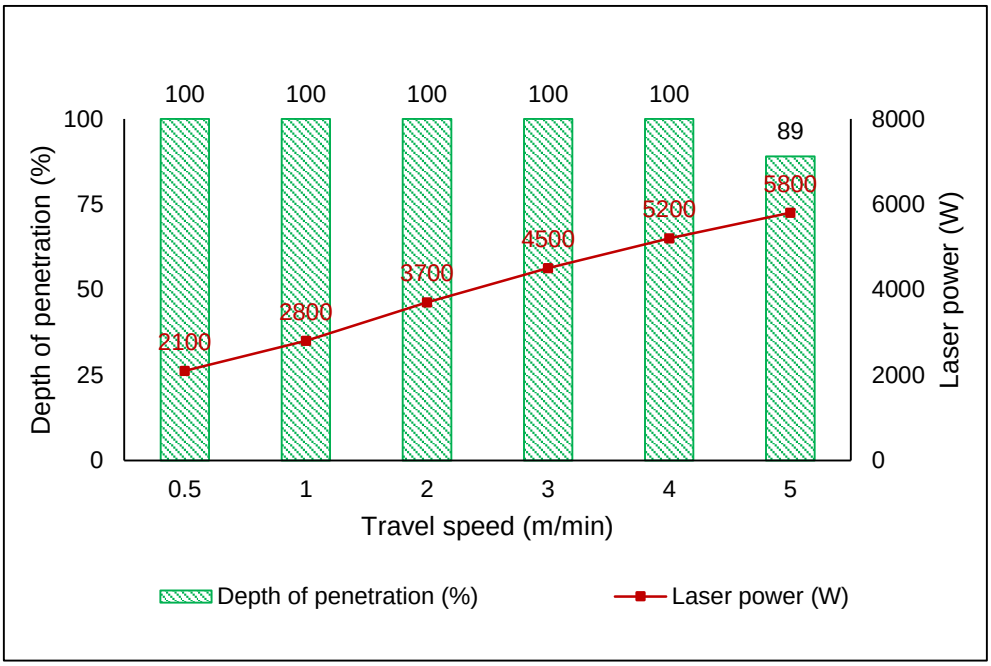

Figure 5-14 Depth of penetration achieved by ALW process at different parametric conditions – 4 mm thickness

Hybrid laser welded joints produced complete penetration with better weld bead geometry as shown in Figure 5-12, H-12 to H-17. Complete penetration was obtained in all the range of travel speeds from 0.5 m/min to 5 m/min. At high travel speed of 5 m/min, surface undercut was observed with complete penetration as shown in Figure 5-12, H-18. Figure 5-15 shows that acquired weld penetration and corresponding parametric conditions by HLAW process in 4 mm thick joints.

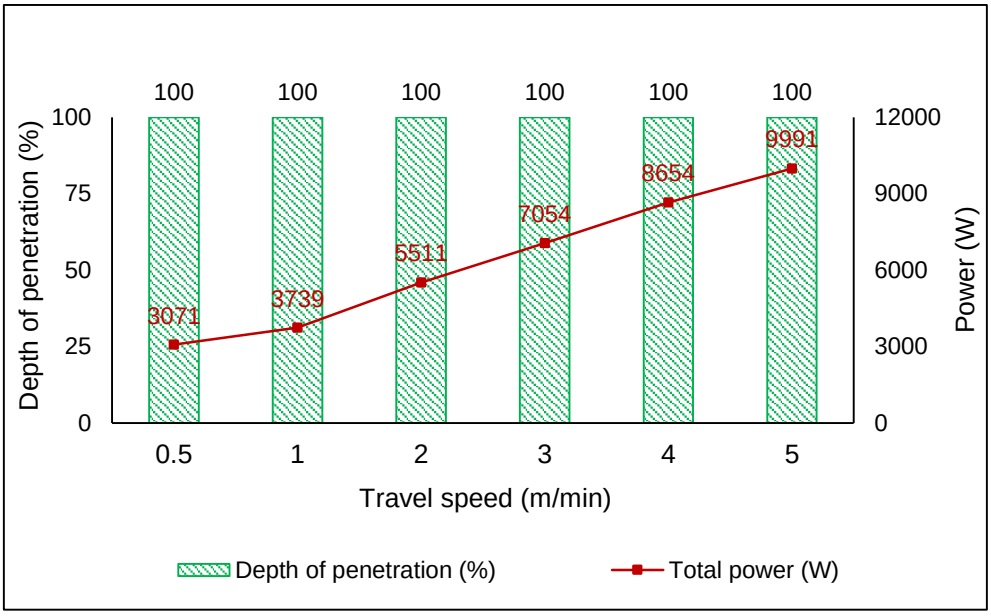

Figure 5-15 Depth of penetration achieved by HLAW process at different parametric conditions – 4 mm thickness

In 8 mm thick plates, pulse mode was used in GMAW process and joints were welded at travels speeds of 0.3 m/min and 0.5 m/min. ALW and HLAW processes were evaluated at travel speeds of 0.5 m/min, 1 m/min and 1.5 m/min. Further increase in travel speed was not tried as the maximum power output of the laser source was reached. Macrographs of the 8 mm thick joints were shown in Figure 5-16.

As there was no groove preparation, complete penetration was not achieved in 8 mm thick joints by GMAW process. However, increase in wire feed speed increases the depth of penetration with an increase in reinforcement and bead width as shown in Figure 5-16, G-17. ALW and HLAW processes produced complete penetration with narrow fusion zone and HAZ. Nevertheless, in HLAW process, underfill was observed with protrusion of excess weld metal on the root side [43]. Achievement of complete penetration in 8 mm thick material without groove preparation can provide significant improvement in productivity.

Process	Macrographs of weld joints – 8 mm thickness		
GMAW - Pulse	WFS = 10.2 m/min TS = 0.3 m/min	WFS = 10.2 m/min TS = 0.5 m/min	WFS = 17 m/min TS = 0.5 m/min
	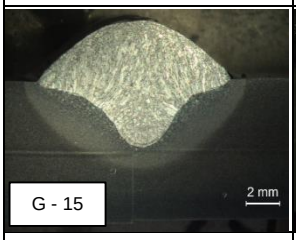	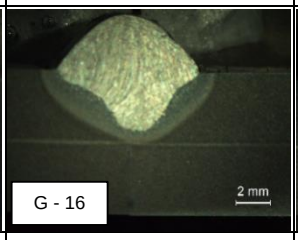	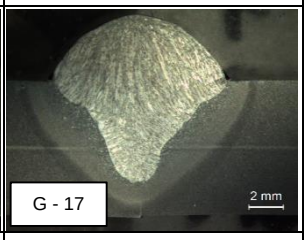
	Depth of fusion = 47%	Depth of fusion = 41%	Depth of fusion = 76%
Autogenous laser welding	P_L = 5100 W, TS = 0.5 m/min	P_L = 6400 W, TS = 1 m/min	P_L = 7600 W, TS = 1.5 m/min
	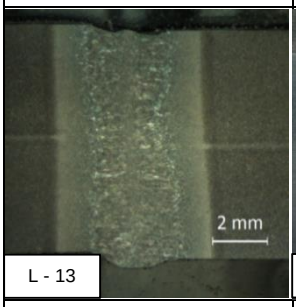	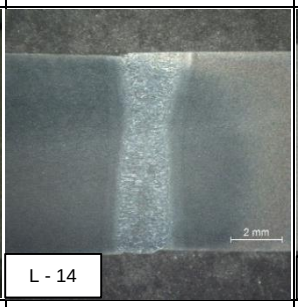	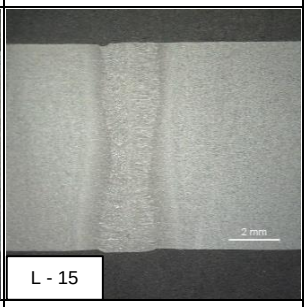
	Depth of fusion = 100%	Depth of fusion = 100%	Depth of fusion = 100%
HLAW – Laser+CMT	P_L = 5100 W, TS = 0.5 m/min, WFS = 2 m/min	P_L = 6400 W, TS = 1 m/min, WFS = 2 m/min	P_L = 7600 W, TS = 1.5 m/min, WFS = 3 m/min
	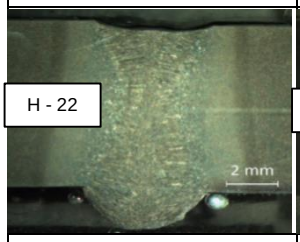	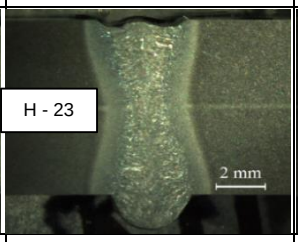	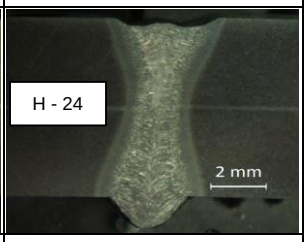
	Depth of fusion = 100%	Depth of fusion = 100%	Depth of fusion = 100%

Figure 5-16 Macrographs of specimen welded by different welding processes – 8 mm thickness

Depth of penetration achieved in 8 mm thick joints by GMAW, ALW and HLAW processes were shown in Figure 5-17, Figure 5-18 and Figure 5-19 respectively.

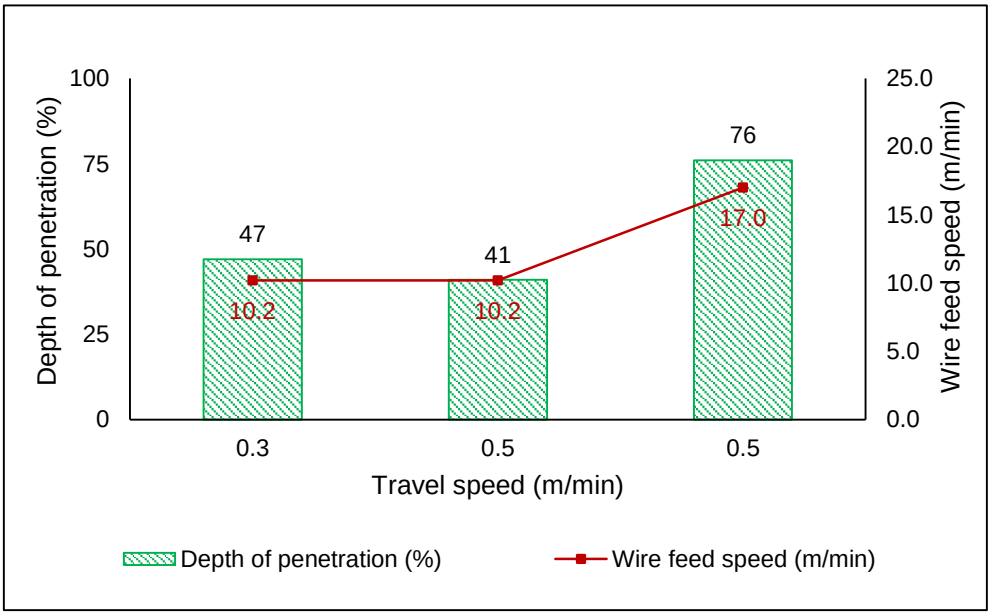

Figure 5-17 Depth of penetration achieved by GMAW process at different parametric conditions – 8 mm thickness

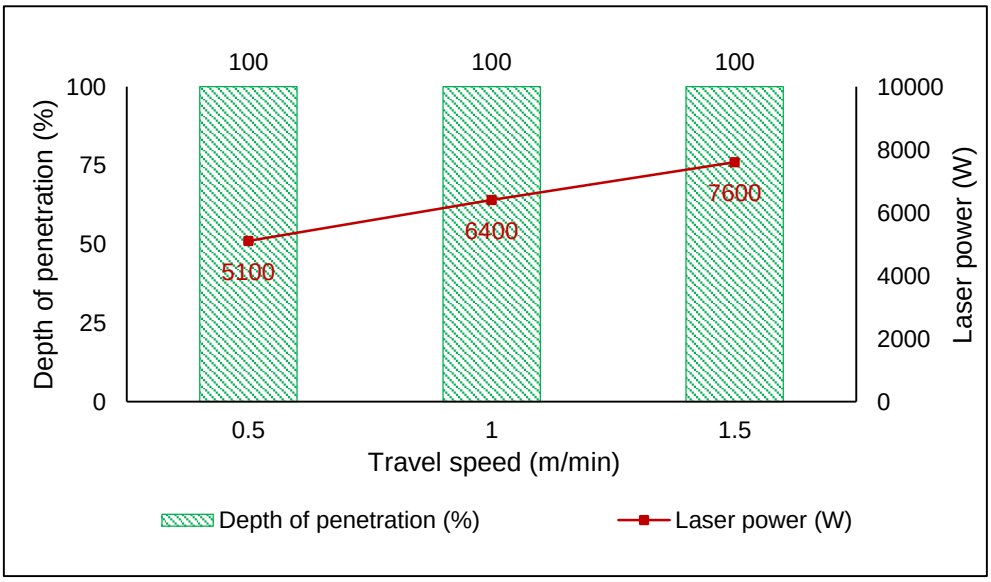

Figure 5-18 Depth of penetration achieved by ALW process at different parametric conditions – 8 mm thickness

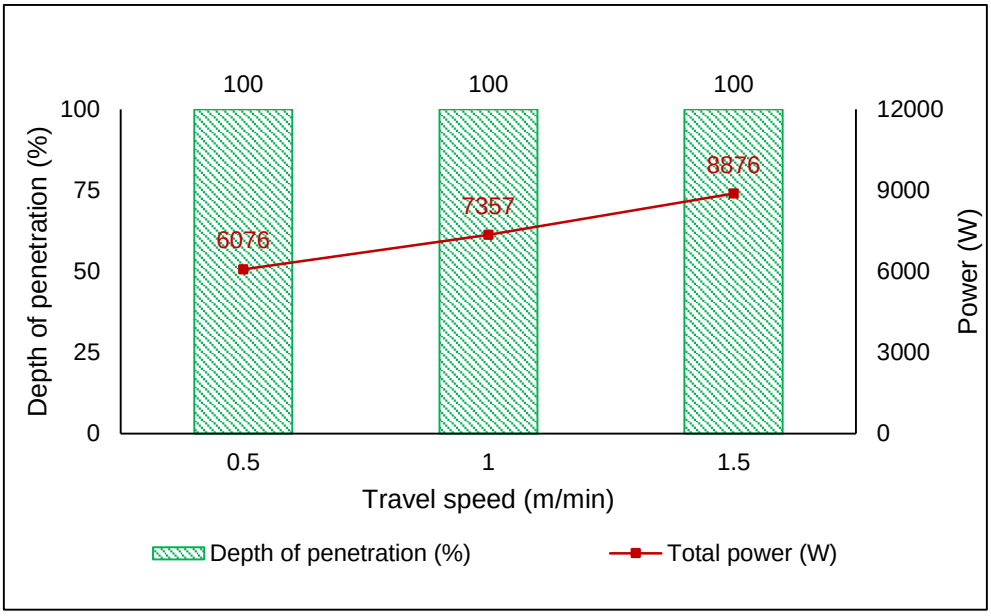

Figure 5-19 Depth of penetration achieved by HLAW process at different parametric conditions – 8 mm thickness

5.3.3 Effects of wire feed speed on weld bead geometry in HLAW process

In HLAW process at constant laser power and travel speed, increase in wire feed speed increases the root reinforcement which can be referred in the macrographs shown in Figure 5-20. Increase in wire feed speed exerts more arc pressure on the molten pool [92]. Because it increases the average current [92] as shown in Figure 5-23. Moreover in complete penetration weld, an increase in arc pressure pushes the molten pool to downwards direction which results in an increase of root reinforcement [92]. Therefore, root humping was observed in 8 mm thick joints. Control of laser energy is very important in achieving the right reinforcement and root profile. At this slow speeds, it is hard to avoid root sagging due to the gravity in down hand position. To avoid this either faster speed [93] or smaller beam size should be used but this was not within the scope of this work. Moreover, an increase in heat input as wire feed speed increases results in increase of fusion area [66] as shown in Figure 5-24. Macrographs of joints welded with different wire feed speeds at constant laser power and travel speed are shown in Figure 5-20.

Thickness = 2 mm			
P_L = 1200 W, TS = 1 m/min, Mode = CMT			
WFS = 2 m/min	WFS = 4 m/min	WFS = 6 m/min	WFS = 8 m/min
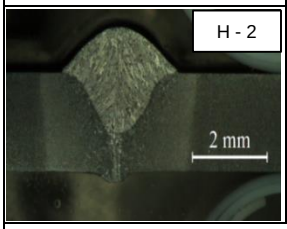	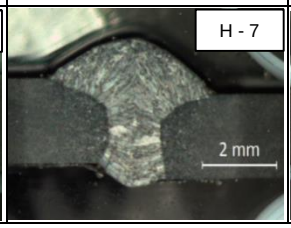	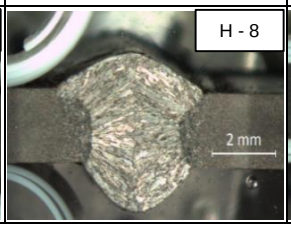	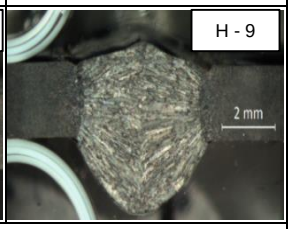
Thickness = 4 mm			
P_L = 2800 W, TS = 1 m/min, Mode = CMT			
WFS = 2 m/min	WFS = 4 m/min	WFS = 6 m/min	
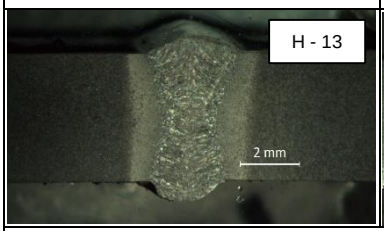	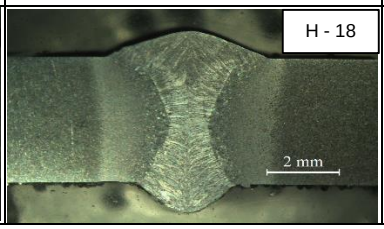	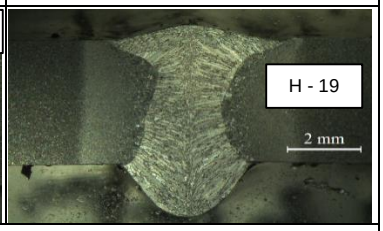	
Thickness = 8 mm			
P_L = 6400 W, TS = 1 m/min, Mode = CMT			
WFS = 2 m/min	WFS = 4 m/min	WFS = 6 m/min	
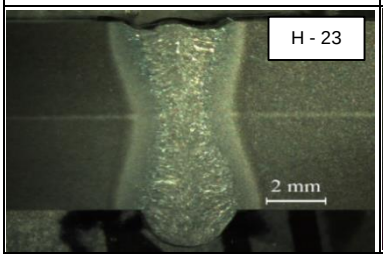	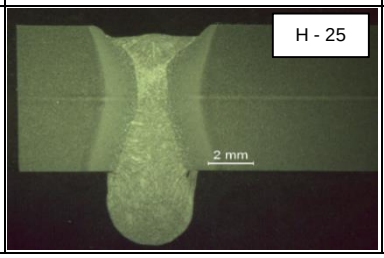	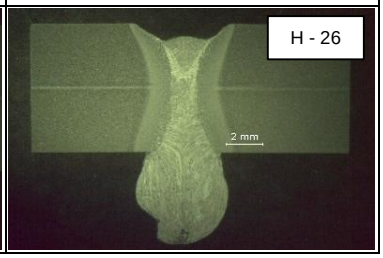	

Figure 5-20 Macrographs of hybrid laser GMAW joints at constant laser power, travel speed and different wire feed speeds

Arc current and voltage waveforms at different wire feed speeds are compared in Figure 5-21 and Figure 5-22 respectively. Increase in wire feed speed increases the average instantaneous current as shown in Figure 5-23.

Arc current waveform at WFS of 2 m/min	Arc current waveform at WFS of 4 m/min
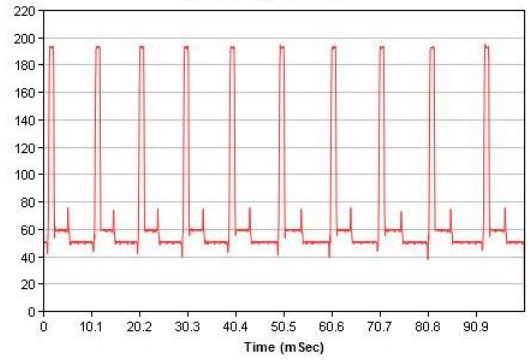	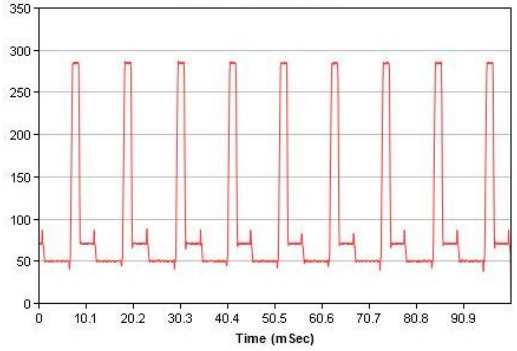

Figure 5-21 Arc current waveform in CMT standard mode at different wire feed speeds

Arc Voltage waveform at WFS of 2 m/min	Arc Voltage waveform at WFS of 4 m/min
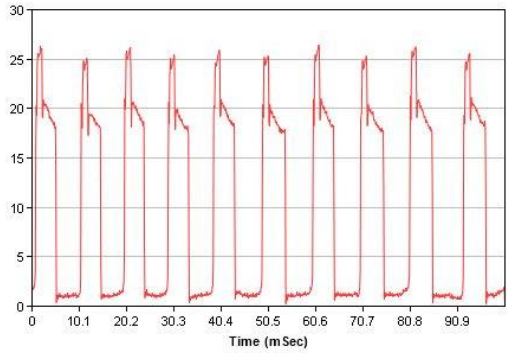	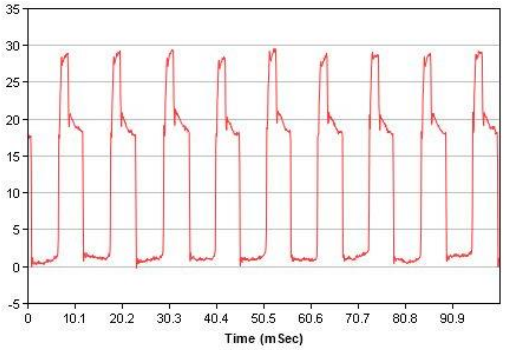

Figure 5-22 Arc Voltage waveform in CMT standard mode at different wire feed speeds

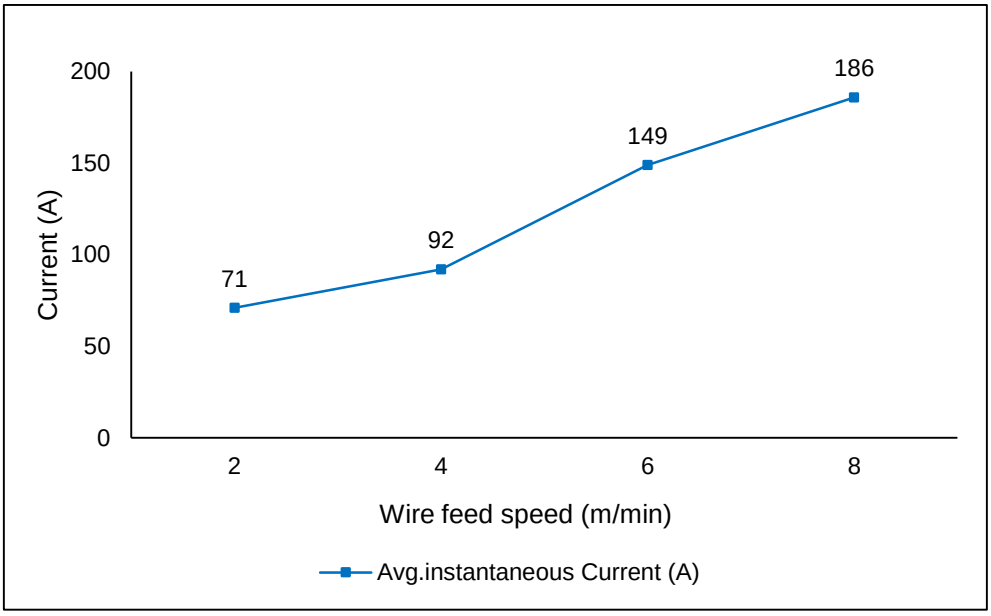

Figure 5-23 Average instantaneous current in CMT standard mode at different wire feed speeds

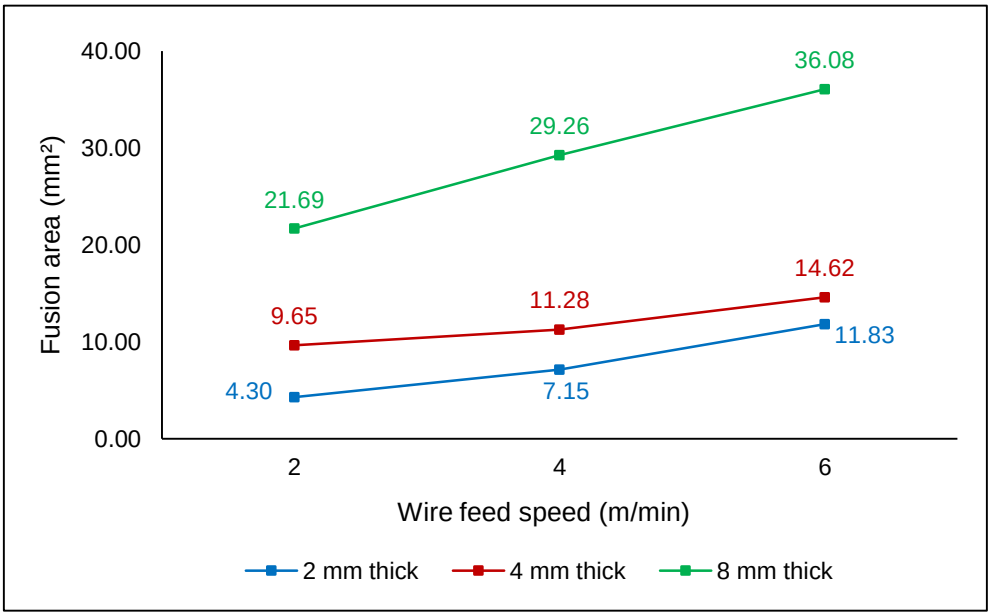

Figure 5-24 Effect of wire feed speed on fusion area at constant travel speed of 1 m/min and different laser power of a) 2 mm thick: P_L = 1200 W, b) 4 mm thick: P_L = 2800 W, c) 8 mm thick: P_L = 6400 W

Increase in wire feed speed produced root humping in 8 mm thick plates. As welding was done in the 1G position, gravitational force plays a crucial role in the metal transfer. Increase in heat input increases the molten pool volume. When the sufficient volume of molten metal is reached then due to the effect of gravity weld metal is drooping into the bottom and eventually solidifies [94]. To overcome this phenomena different welding position or faster travel speed to be used but this could not be tested due to limitation of the laser power. Top and bottom bead appearances of root humping welds and normal welds are compared in Figure 5-25.

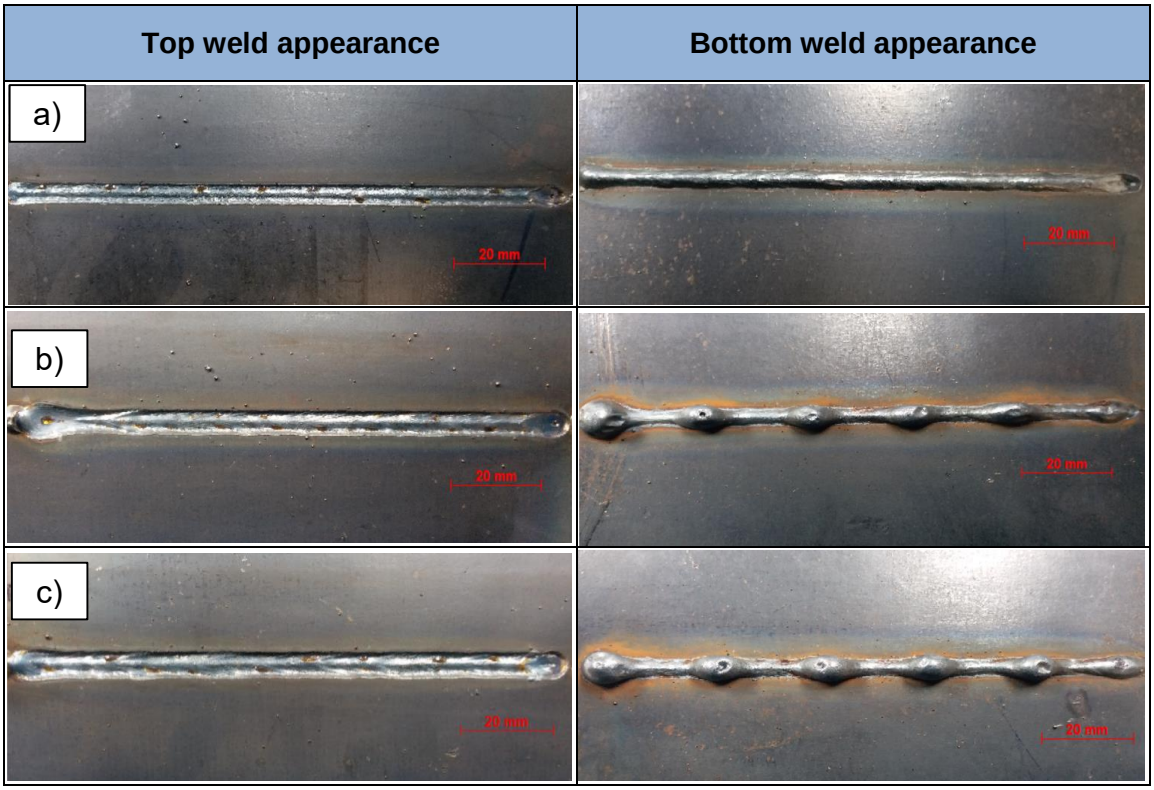

Figure 5-25 Top and bottom weld appearances of the specimen welded at constant P_L = 6400 W, TS = 1 m/min and different wire feed speeds a) WFS = 2 m/min b) WFS = 4 m/min c) WFS = 6 m/min, Mode = CMT, Thickness = 8 mm

Macro section of Valley (Section A-A) and humping (Section B-B) are shown in Figure 5-26. At both valley and humping depth of underfill was found to be almost the same. However, root reinforcement was increased from 1.80 mm to 4.00 mm.

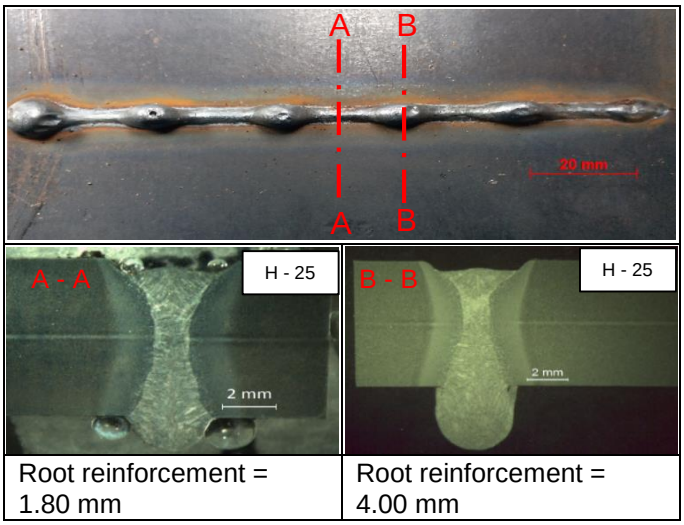

Figure 5-26 Comparison of root reinforcement in valley and root humping welded at P_L = 6400 W, TS = 1 m/min, WFS = 4 m/min

Typically, in all the three thickness of materials, when all other parameters kept constant, wire feed speed shows a direct relation with root reinforcement as presented in Figure 5-27. Similar result was obtained by [92].

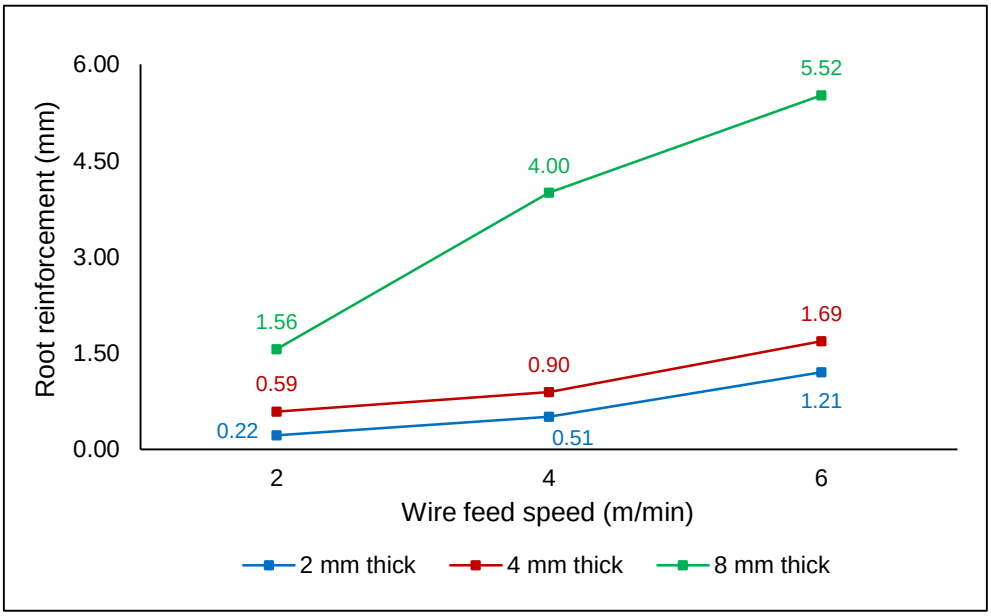

Figure 5-27 Effect of wire feed speed on root reinforcement in HLAW process in different thickness of materials

5.3.4 Comparison of different arc modes in GMAW process

Characteristics of CMT standard and CMT pulse mode were compared with pulse mode at same wire feed speed and travel speed in 4 mm thick plates with respect to weld bead geometry and aesthetic quality.

5.3.4.1 CMT standard mode versus Pulse mode

In the aspect of penetration, pulse mode produced more penetration than CMT mode as shown in Figure 5-28. Comparison of waveforms of both the modes shows that peak current in pulse mode is higher than in CMT as shown in Figure 5-29. At WFS of 8.2 m/min, instantaneous arc power in CMT mode was 3300 W whereas in pulse mode it was 4635 W. Increase in arc power exerts more arc pressure on the molten pool which consequently increases the penetration.

WFS = 8.2 m/min, TS = 0.3 m/min		WFS = 8.2 m/min, TS = 0.5 m/min	
CMT Mode	**Pulse mode**	**CMT mode**	**Pulse mode**
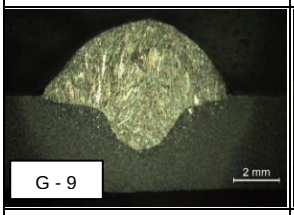	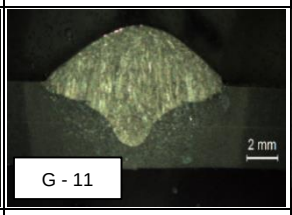	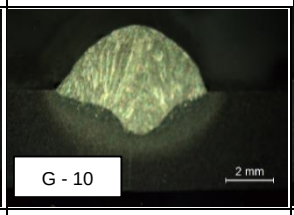	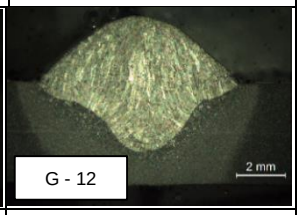
Depth of fusion = 59%	Depth of fusion = 76%	Depth of fusion = 46%	Depth of fusion = 69%

Figure 5-28 Weld bead cross-section at constant WFS and different welding speeds and welding mode of 4 mm thick plates – GMAW

Arc current waveform in CMT standard mode	Arc current waveform in Pulse mode
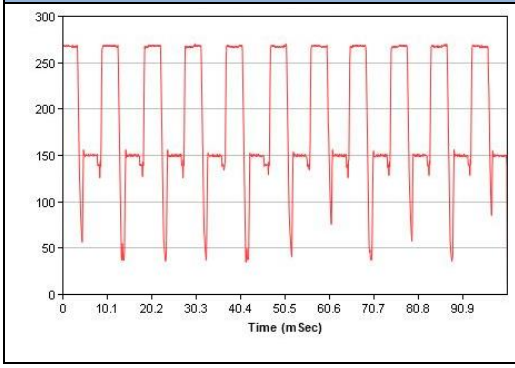	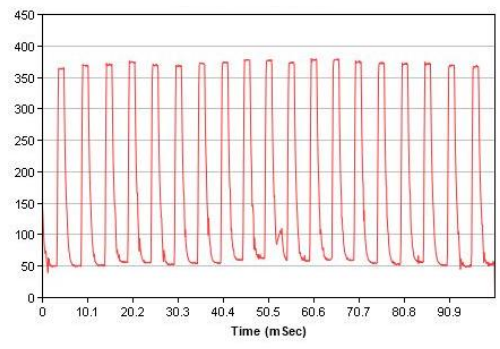

Figure 5-29 Arc current waveform in CMT standard mode and pulse mode at WFS of 8.2 m/min

Arc Voltage waveform in CMT Standard mode	Arc Voltage waveform in Pulse mode
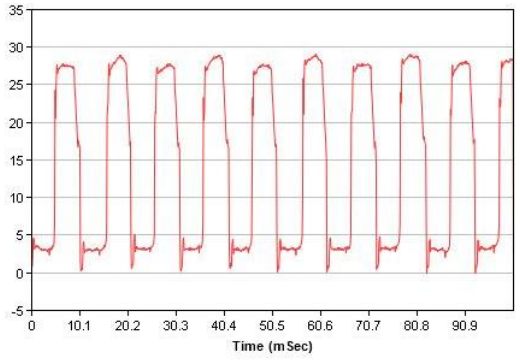	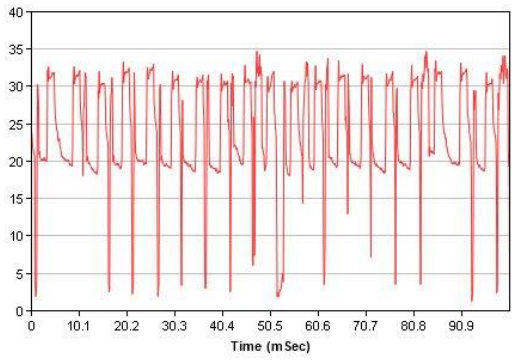

Figure 5-30 Arc current waveform in CMT standard mode and pulse mode at WFS of 8.2 m/min

Increase in travel speed at constant wire feed speed reduced the penetration and fusion zone area in both the modes which is compared in Figure 5-31 and Figure 5-32.

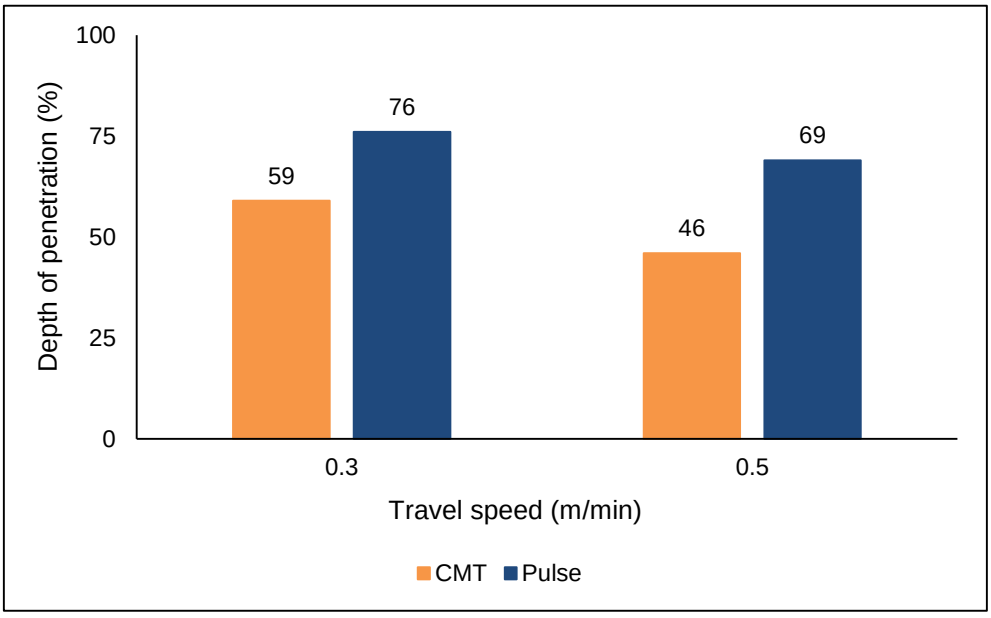

Figure 5-31 Comparison of weld penetration in joints welded at WFS of 8.2 m/min in different travel speeds and arc modes

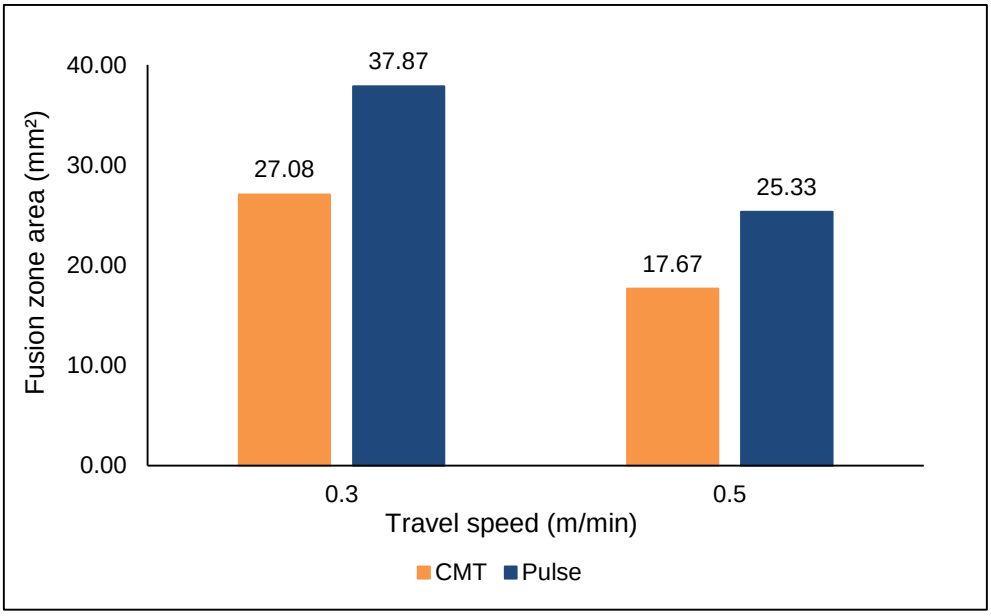

Figure 5-32 Comparison of fusion zone area of joints welded at WFS of 8.2 m/min in different travel speeds and arc modes

Weld beads of CMT and pulse modes were compared in the aspect of aesthetic appearance. Pulse mode produced few spatters as shown in Figure 5-33 whereas no spatters were observed in CMT mode.

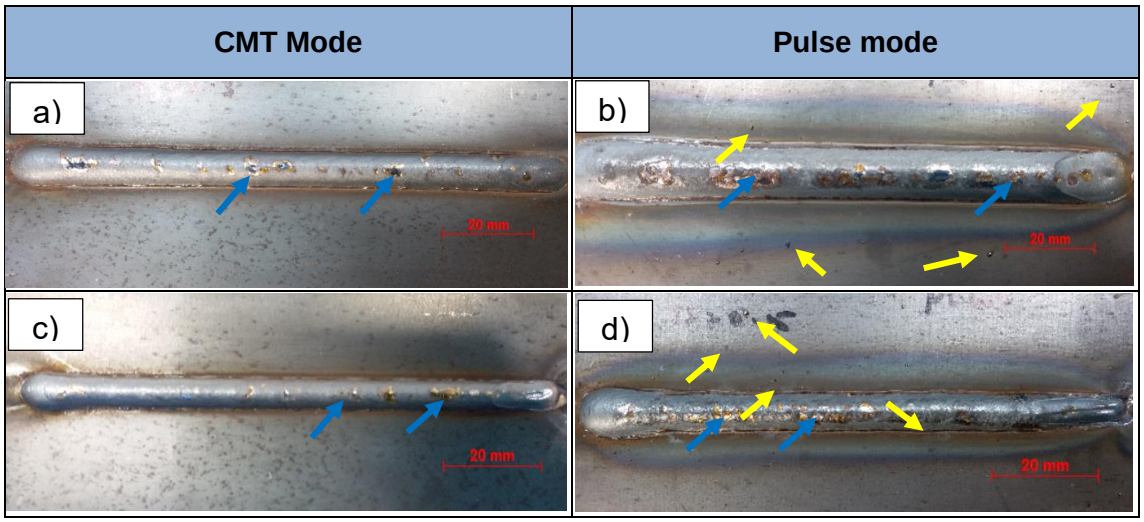

Figure 5-33 Top weld appearances of the specimen welded at WFS = 8.2 m/min in 4 mm thick plate using different welding speeds and arc modes a) TS = 0.3 m/min, Mode = CMT b) TS = 0.3 m/min, Mode = Pulse c) TS = 0.5 m/min, Mode = CMT d) TS = 0.5 m/min, Mode = Pulse

Moreover, pulse mode increases the deposition of silica on the weld bead. Even though pulse mode provided better penetration, the aesthetic quality of the weld was compromised. In Figure 5-33 spatters and glass bead (silica deposition) are marked by yellow and blue arrows respectively.

5.3.4.2 CMT pulse mode versus Pulse mode

At increased wire feed speed and travel speed conditions as per experiments of G-13 and G-14 shown in Table 5-2, CMT pulse mode and pulse mode were studied. Complete penetration was achieved in pulse mode whereas 99% of penetration obtained in CMT pulse mode as shown in Figure 5-34. As mentioned earlier, higher arc pressure in pulse mode produced better penetration profile.

WFS = 13.6 m/min, TS = 0.5 m/min	
CMT Pulse mode	**Pulse mode**
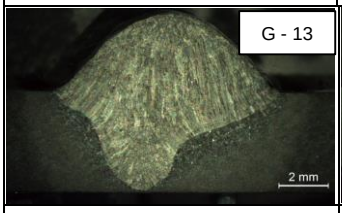	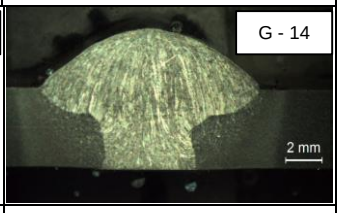
Depth of fusion = 99%	Depth of fusion = 100%

Figure 5-34 Weld bead cross-section at constant WFS of 13.6 m/min, TS of 0.5 m/min and different welding modes in 4 mm thick plate

Arc current and voltage waveforms of both CMT pulse and pulse modes are compared in Figure 5-35 and Figure 5-36 respectively.

Arc current waveform in CMT Pulse mode	Arc current waveform in Pulse mode
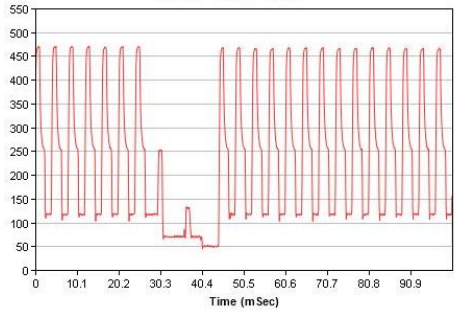	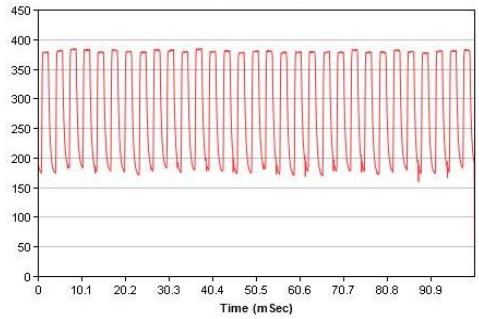

Figure 5-35 Arc current waveform in CMT standard mode and pulse mode at WFS of 13.6 m/min

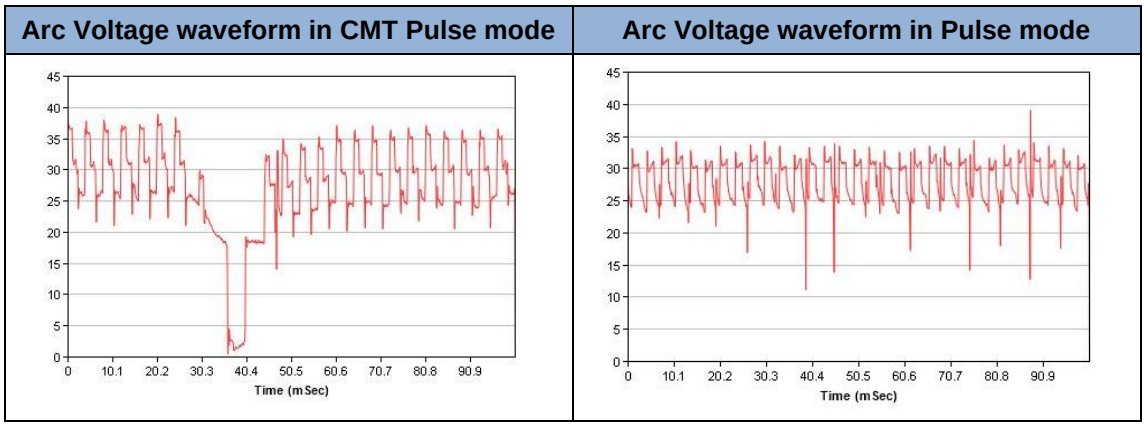

Figure 5-36 Arc voltage waveform in CMT standard mode and pulse mode at WFS of 13.6 m/min

At high wire feed speed, CMT pulse mode produced stable weld whereas uneven weld bead was observed in pulse mode as shown in Figure 5-37. Few spatters and silica deposition were observed in both the modes which have been marked by yellow and blue arrows respectively and bead unevenness was marked by red arrows in Figure 5-37.

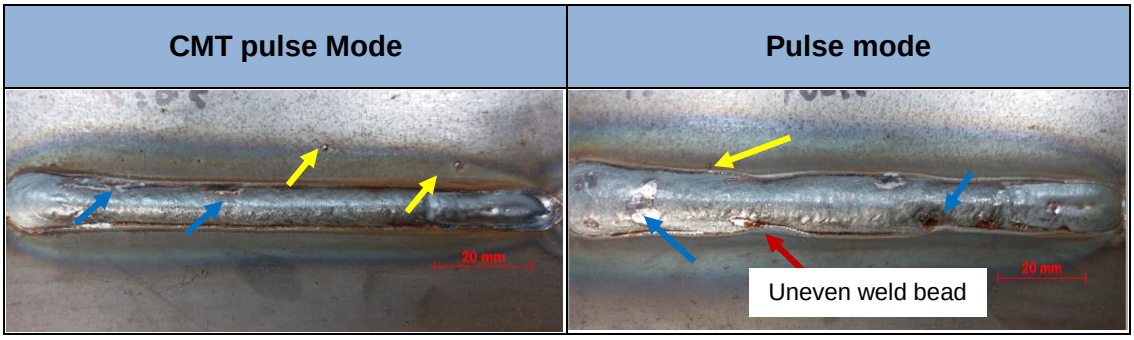

Figure 5-37 Top weld appearances of the specimen welded at WFS = 13.6 m/min, Travel speed of 0.5 m/min and different arc modes

Combination of CMT and pulse cycle in CMT pulse mode eliminates the limitations of both individual modes and provided the benefits of them. This mode comparatively produced better penetration than CMT mode and aesthetically good weld bead than pulse mode. CMT pulse mode delivered more heat input than CMT standard mode and also ensures the smooth droplet transfer.

5.3.5 Comparison of different arc modes in HLAW process

Combination of laser with different arc modes such as CMT standard mode and pulse mode were studied in HLAW process. Critical parameters such as laser power, travel speed were kept constant and at the same wire feed speed, two different modes were selected for welding. Macrographs of joints welded by both the modes are shown in Figure 5-38.

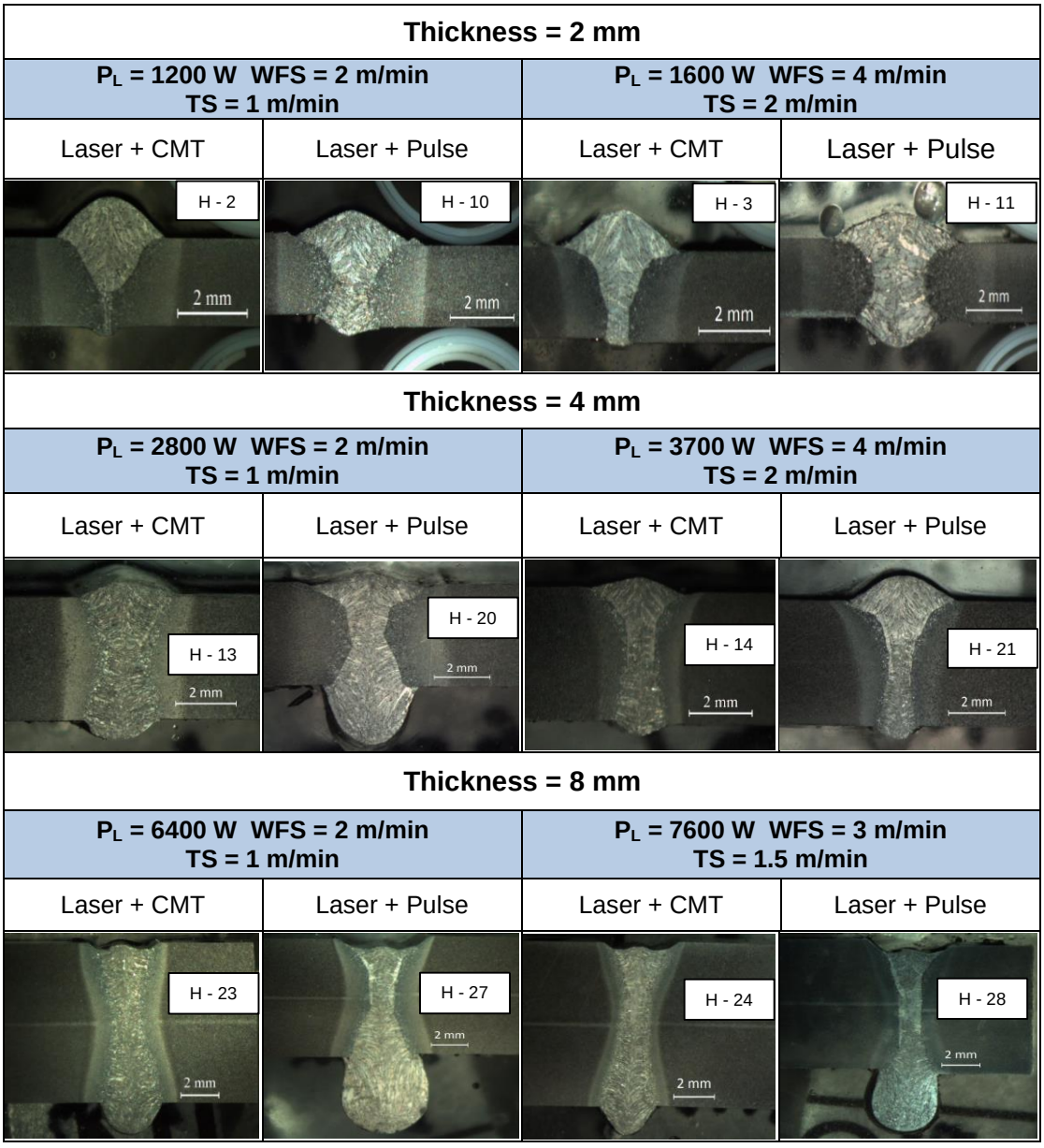

Figure 5-38 Macrographs of joints welded by combination of laser with CMT standard mode and laser with pulse mode

Comparatively with CMT mode, pulse mode produced weld beads with reduced top bead reinforcement and increased root bead reinforcement in all the three thickness of materials as shown in Figure 5-38. Because pulse mode exerts more arc pressure in the molten pool than CMT mode [73].

Uniform weld bead width over the entire length of the weld indicates that both the process conditions are stable in welding of 2 mm thick joints. However, spatters were observed in Laser + Pulse mode as shown in Figure 5-39. Laser + Pulse mode produced better penetration profile than CMT mode which can be referred in Figure 5-38, H-2 and H-10. At same wire feed speed, high voltage in pulse mode increases its instantaneous arc power higher than Laser + CMT mode. As pulse mode is governed by electromagnetic force (Lorentz force), an increase in arc power increases the electromagnetic force which consequently delivers more arc pressure on to the molten pool [95]. This effect results in root humping in 8 mm thick joints welded by laser with pulse mode as shown in Figure 5-38, H-27 and H-28.

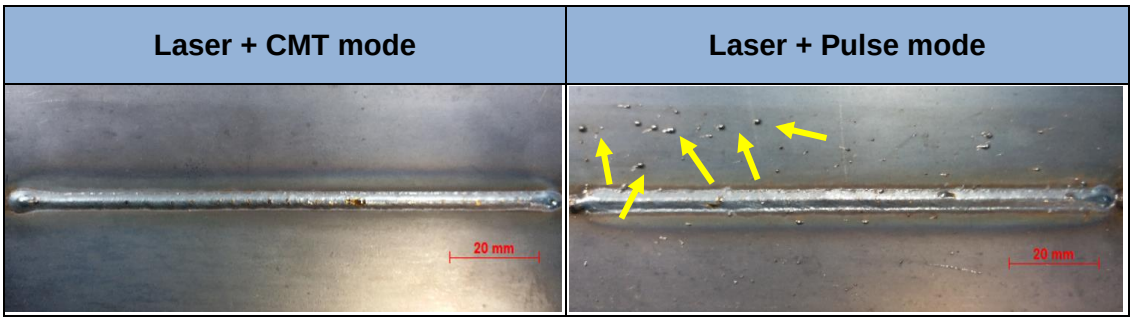

Figure 5-39 Top bead appearances of the specimen welded at P_L = 1200 W, WFS = 2 m/min, TS = 1 m/min and combination of laser with different arc modes

Weld bead profile of top and root reinforcements also differs in both the modes. Laser with CMT produced large semi-hemispherical shape in the top and small reinforcement in the root (Figure 5-40, H-3) whereas laser with pulse produced large semi-hemispherical shape in both top and root reinforcement (Figure 5-40, H-11). Laser + Pulse mode was found to be easier to control both top and root reinforcement. However, it increases the fusion zone area and affects the aesthetic quality of the weld bead.

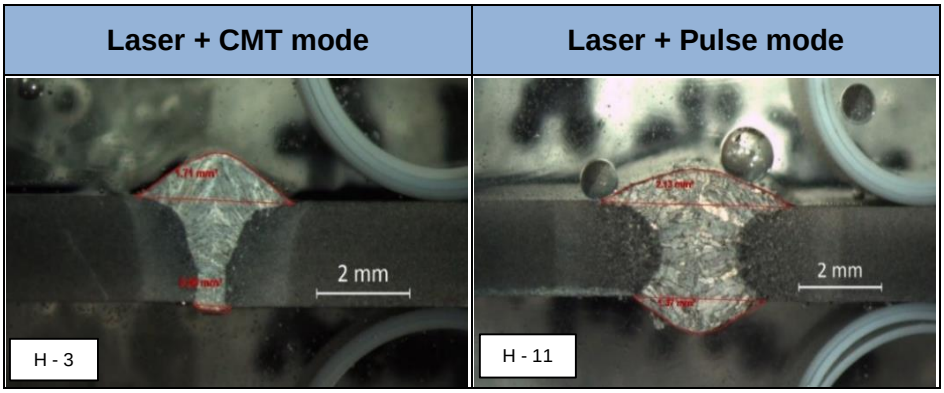

Figure 5-40 Top and root bead reinforcement produced by laser with different arc modes in HLAW process at P_L = 1600 W, TS = 2 m/min, WFS = 4 m/min

5.4 Discussion

5.4.1 Comparative analysis in the aspect of weld penetration

Compared with GMAW process, autogenous laser welding process was found to be advantageous in the context of deep penetration and high welding speed. Complete penetration was achieved with 8 times increase in productivity in case of 2 mm and 4 mm thick materials. Complete penetration with 3 times improvement in productivity was observed in 8 mm thick materials. Figure 5-41 shows that maximum travel speed at which optimal weld bead quality obtained in different welding processes. In 4 mm and 8 mm thick plates, achieving complete penetration in GMAW without groove preparation was difficult whereas ALW process produced complete penetration even at higher welding speed than GMAW process. At macroscopic inspection no porosity and spatters were observed in laser welded joints. As laser welding process produced acceptable welds even at high welding speed shows that quality is not compromised for productivity. However in GMAW process, increased parametric condition exhibited burnthrough in thinner materials and unstable welds in higher thickness materials. Thus, the quality of the weld was greatly compromised for the productivity which is not favourable. Autogenous laser welding process can significantly reduce the consumable cost of the process. Moreover, it eliminates the glass bead defect from the weld joint. On the other hand, unavailability of top bead reinforcement in laser welded joints may affect the mechanical properties

of the welded structure. Convex reinforcement profiles are preferable for the better fatigue life of the welded structure [91].

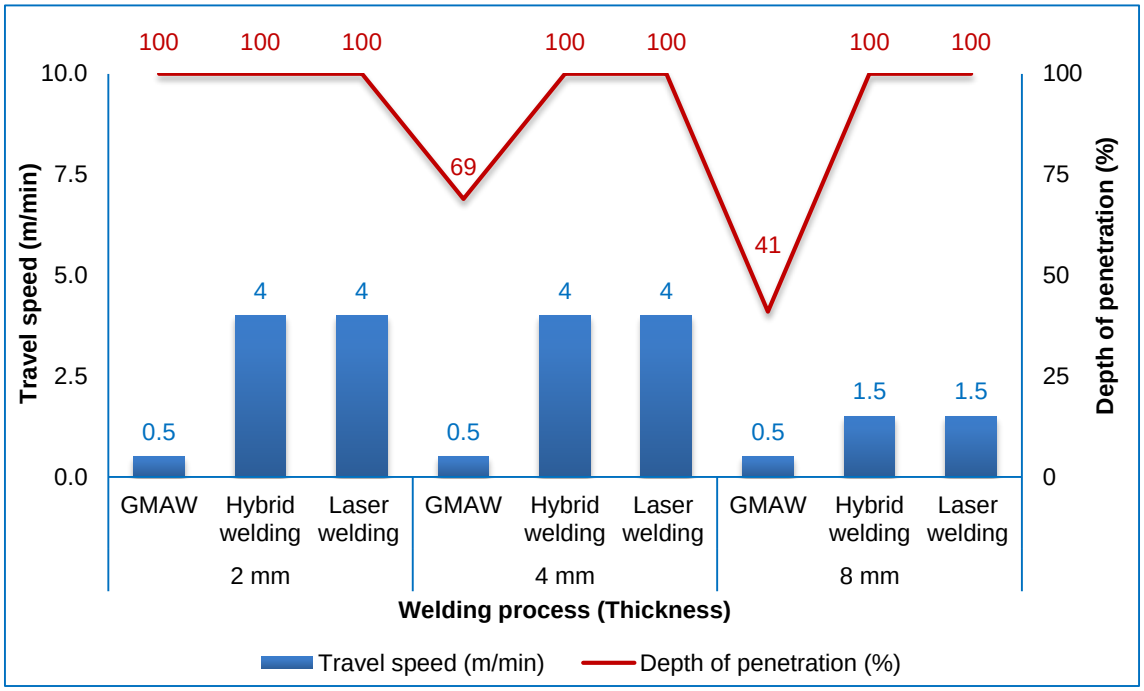

Figure 5-41 Comparison of penetration achievement in different welding processes at different travel speeds

Hybrid laser GMAW process combines the benefits of GMAW and ALW processes, such as superior bead profile and deep penetration respectively. HLAW process produced complete penetration and good bead reinforcement in 2 mm and 4 mm thick materials. However, complete penetration with underfill was observed in 8 mm thick materials. Presence of underfill in 8 mm thick joints indicates that insufficient volume of filler metal was added [43]. Thus the wire feed speed was increased where all other parameters were kept constant. That results in an increase in root humping rather than increasing the top bead deposition as shown in Figure 5-20, H-25 and H-26. Increase in wire feed speed increases the volume of molten metal, due to the effect of gravity, large volume of molten metal flown to the root of the weld [93,94] That causes the formation of root humping. It is more complex to control because it requires the right ratio of laser and arc power to control the reinforcement and root profile. Therefore in down hand position normally high welding speeds are deployed.

Moreover, CMT pulse and pulse modes in GMAW process can be used to improve the penetration. CMT pulse mode offers aesthetically good weld bead with less spatters than pulse mode. This could be an emerging synergic line for the welding of higher thickness materials. Combination of CMT and pulse cycle increases the heat input which consequently increases the weld penetration. However, it increases the fusion zone and HAZ area as well.

5.4.2 Comparative analysis in the aspect of heat input

High power density of ALW and HLAW processes produces deep penetration at very low heat input than GMAW process. Figure 5-42 shows that heat input at which optimal weld bead quality with maximum weld penetration achieved by different welding processes. It indicates that complete weld penetration can be achieved in ALW and HLAW processes even at low heat input. GMAW process provided aesthetically acceptable welds with maximum penetration of 69% and 41% in 4 mm and 8 mm thick plates respectively.

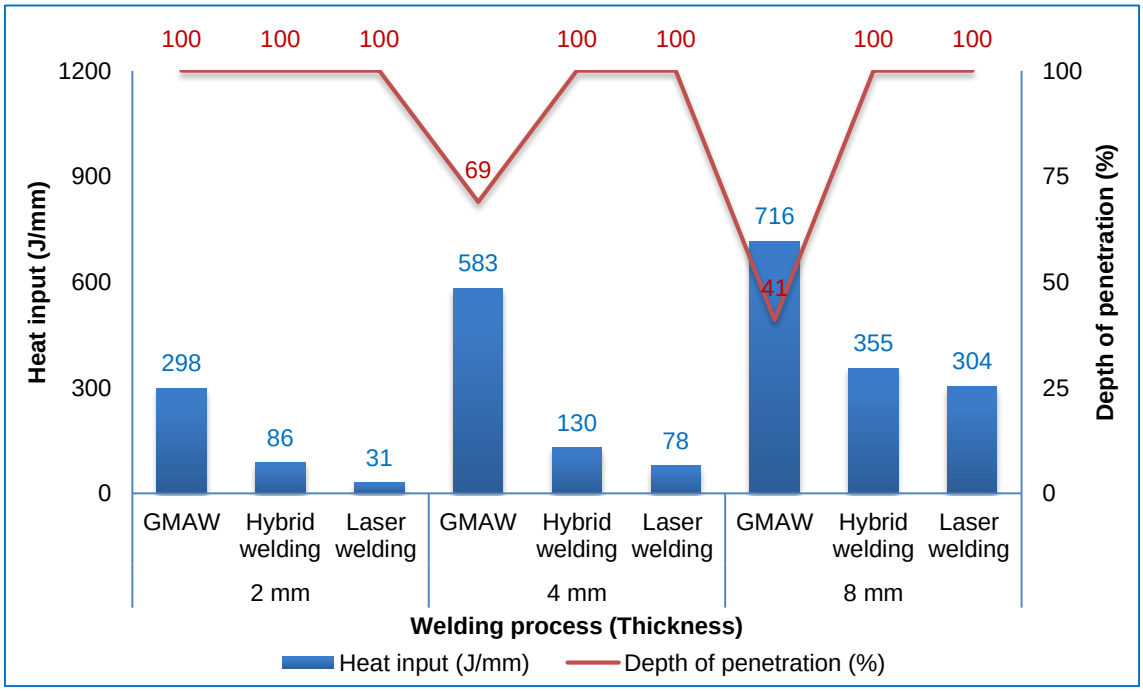

Figure 5-42 Comparison of penetration achievement in different welding processes at different heat inputs

Moreover, the effects of heat input were studied in GMAW and HLAW processes by increasing wire feed speed and by using different arc modes. In both the conditions, it has been observed that heat input is having significant influence on weld bead geometry. Increase in wire feed speed increases the average instantaneous current which in turn increases the heat input. Comparatively with CMT mode, both CMT pulse and pulse modes delivers more arc power at the same wire feed speed. These modes can be used for higher thickness materials for better weld penetration. However, formation spatters and uneven weld bead at high wire feed speed conditions, compromises the aesthetic quality of the weld bead compared to CMT standard mode.

Similarly, a comparative study on laser with CMT standard mode and laser with pulse mode in HLAW process showed that, effects of increased heat input in weld bead geometry. Laser with pulse mode produced a weld with hemispherical shape reinforcement in the top and root whereas laser with CMT produced “wine-cup” like shape weld with less root reinforcement in 2 mm thick material. However, laser with pulse mode produced excess root reinforcement in 8 mm thick materials. Thus, root humping was observed in 8 mm thick joints. Relatively higher heat input causes the melting of larger volume of metal and effects of gravity led to the formation of root humping [94].

5.4.3 Comparative analysis in the aspect of weld bead geometry

Relatively lower heat input in ALW and HLAW process than GMAW process results in a reduction of fusion zone area. Figure 5-43 shows that a comparison of fusion zone area obtained in joints welded by different welding methods. In all three thickness of joints, heat input shows a direct relation with the fusion zone area i.e. increase in heat input increases the fusion zone area. ALW and HLAW processes provided a considerable reduction in the fusion zone area than GMAW process. Moreover, this results in reduction of HAZ width as well.

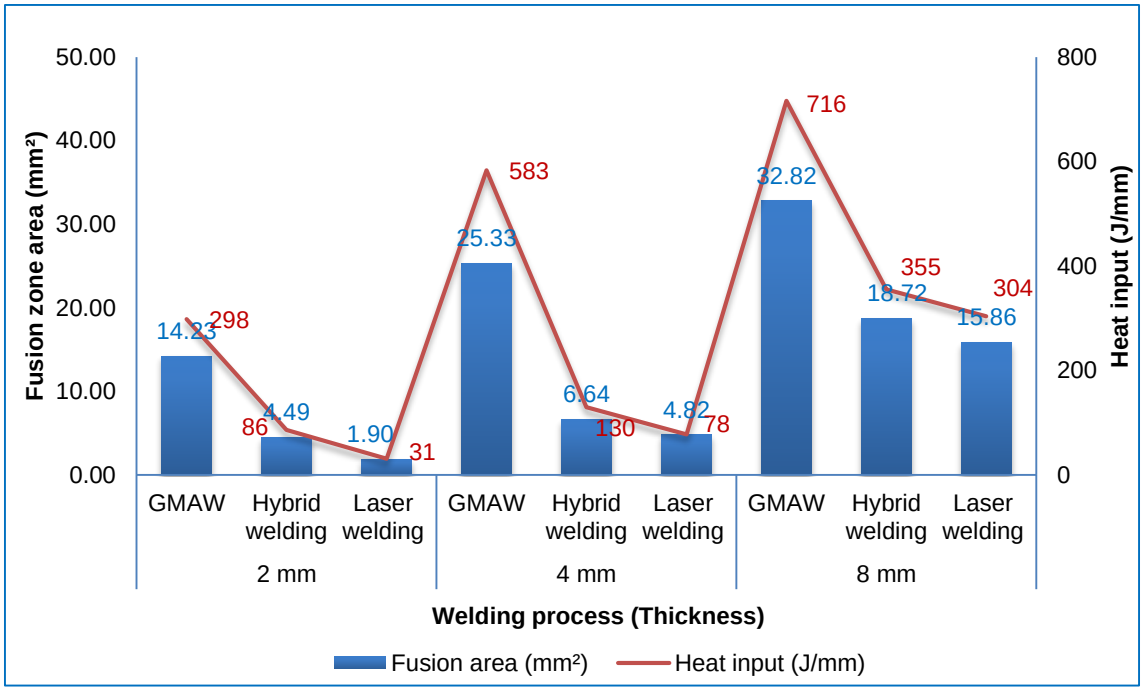

Figure 5-43 Comparison of fusion zone area obtained in different welding processes at different heat inputs

Moreover, with the GMAW process, it was not possible to achieve full penetration beyond certain thickness and it was hard to control the root profile but easy to achieve top bead reinforcement. Moreover, in GMAW process, penetration cannot be independently controlled from the bead reinforcement. On the other hand, ALW process can provide good control in penetration however in higher thickness, it is hard to achieve good top and root beads. Hybridization effect of laser and arc in HLAW process shows possible ways to control penetration and bead profile.

5.4.4 Comparative analysis in the aspect of aesthetic quality

Aesthetic quality of the welded joints was evaluated quantitatively as per the AQI scoring method. The joints welded by the above-mentioned conditions were taken for the study of aesthetic quality. Figure 5-44 shows that aesthetic quality comparison of weld beads. No visual defects were noticed in autogenous laser welded joints. Also, GMAW process produced aesthetically good weld beads in all the three thickness of joints. GMAW-CMT mode does not produce any spatters whereas GMAW-Pulse produced few spatters in welding of higher thickness

plates. Glass bead was identified as a common problem in both GMAW and HLAW processes. However, HLAW process showed a significant reduction in glass bead formation than GMAW process. Few spatters were observed in 4 mm and 8 mm thick joints of HLAW process. In addition to this underfill was also noticed in 8 mm thick joints which consequently increases the AQI score.

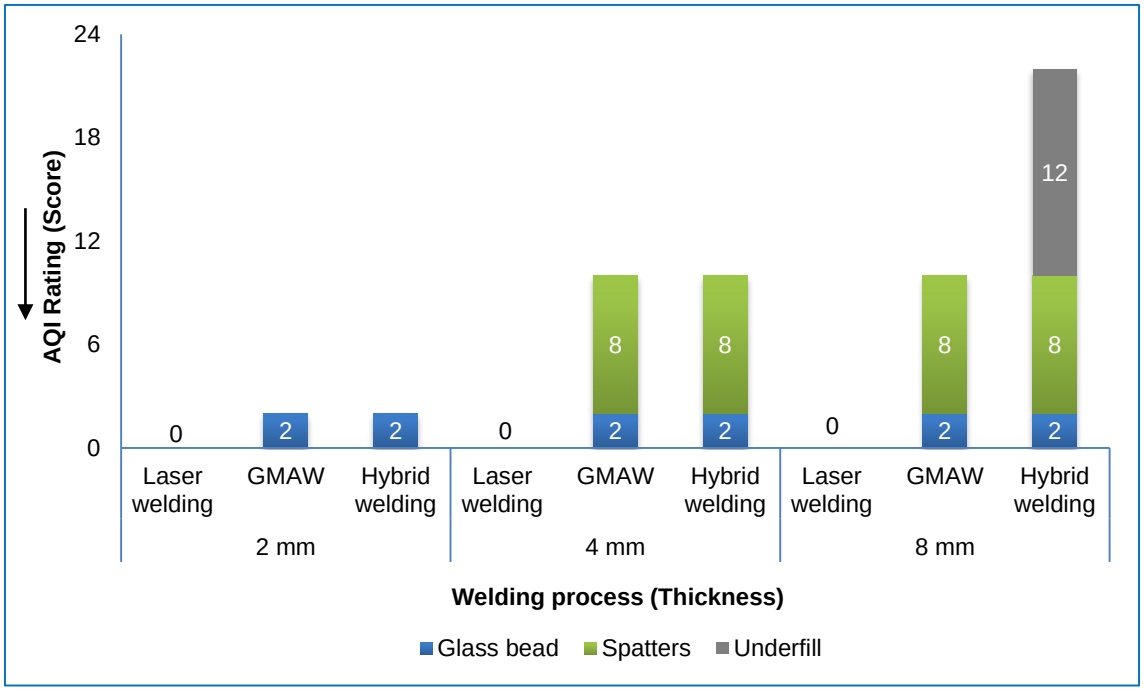

Figure 5-44 Comparison of aesthetic quality of weld beads in different welding processes

To sum up, autogenous laser welding process is capable to produce complete penetration at high welding speed even without groove preparation in higher thickness materials. Compared with GMAW, extremely low heat input of ALW process results in narrow weld bead and HAZ area. Nevertheless, lack of reinforcement and underfill are the critical concerns observed in ALW process. Addition of filler metal in HLAW process can overcome these issues. Moreover, it carries the benefits of both ALW and GMAW processes such as deep penetration at high welding speed and better weld bead profile respectively. Determining the optimized combination of laser and arc parameters are essential to acquire good weld bead quality. In HLAW process, laser with CMT mode was produced aesthetically good weld bead than laser with pulse mode. However,

laser with pulse mode provided more control for optimization of top and root bead reinforcement.

5.5 Conclusions

Through this investigation, different welding processes such as GMAW, autogenous laser welding, and hybrid laser arc welding processes were compared in the aspects of productivity, weld penetration, heat input and weld bead geometry. Based on the experimental results the following are the conclusions arrived.

- ALW and HLAW processes improved the productivity by a factor of 8 times compared to GMAW process in 2 mm and 4 mm thick plates. In 8 mm thick plates, an improvement of productivity by a factor of 3 times was achieved.
- CMT welding mode is suitable for thin structures to acquire complete weld penetration with superior weld bead quality but with limited productivity. Nevertheless, the risk of burnthrough also associated with this conditions. Thus, CMT is very sensitive to variation in material thickness and plate temperature. Moreover, it is difficult to control penetration depth precisely.
- In case of thick structures, achieving complete weld penetration without groove preparation and without compromising the aesthetical quality of the weld bead was found to be not feasible in GMAW process. Moreover, low welding speeds of GMAW process significantly hinders the productivity.
- However, CMT pulse mode exhibited good result in welding of 4 mm thick plates with notable penetration depth and stable weld bead with good aesthetical appearance. Nevertheless, high heat input results in a high amount of reinforcement and fusion zone area which are found to be the limitations of this mode.
- Autogenous laser welding process produced complete weld penetration without any major surface defects even at high welding speed. Without groove preparation, the achievement of complete weld penetration in 8 mm thick plates was found to be a crucial factor in the aspect of productivity.

- Extremely low heat input of ALW process will results in low distortion in thin structures. Moreover, a considerable reduction in the fusion zone and HAZ area was obtained in ALW process. No addition of filler metal led to unavailability of bead reinforcement. This may exhibits an adverse effect on mechanical properties of the welded joints.
- Hybrid laser arc welding process exhibited superior weld bead quality with deep penetration and better bead reinforcement even at high welding speeds. It combines the benefits of both GMAW and ALW processes. Comparatively, laser with pulse mode produced more fusion zone area than laser with CMT mode. Moreover in higher thickness plates, laser with pulse mode produced root humping defect as well.
- Hybrid laser with CMT mode is recommended for deep penetration and better aesthetic quality of weld bead.
- Precise parametric optimization is required in HLAW process to obtain better weld bead geometry with good aesthetic quality.

6 Gap bridging capability of different welding processes

6.1 Introduction

The aim of this chapter is to evaluate the gap bridging capability of autogenous laser welding (ALW) and hybrid laser arc welding (HLAW) processes with respect to weld bead geometry and aesthetic appearance of weld beads. Results of ALW and HLAW processes were compared with the GMAW process. Typically in automobile industries the allowable root gap is a maximum of 1 mm [3]. Hence the welding process must be capable to accomplish the root gap up to 1 mm.

6.2 Experimental procedure

Autogenous laser welding process was evaluated at 0.2 mm and 0.5 mm root gap conditions. As beam diameter of 0.6 mm was used, the root gaps of less than 0.6 mm were examined. GMAW and HLAW processes were assessed at 0.5 mm and 1 mm root gap conditions. In all these experiments, fixed root gap conditions were evaluated. Clamping arrangements were used as shown in Chapter 4 in all three welding processes. The set of welding conditions which were established for complete penetration in each welding processes at zero root gap has been used to weld with fixed root gaps [36]. Root gaps were pre-set by using feeler gauge and plates were tack welded. Experimentation matrix and list of process conditions used are shown in Table 6-1 and Table 6-2 respectively.

Table 6-1 Experimentation matrix for gap bridgeability analysis

#	Thickness (mm)	Root gap (mm)	Process
1	2, 4 and 8	0.2	ALW
2		0.5	ALW
3			GMAW
4			HLAW
5		1	GMAW
6			HLAW

Table 6-2 Set of welding conditions used for evaluation of gap bridgeability

Parameters/ Process	Autogenous laser welding			Gas metal arc welding			Hybrid laser GMAW		
Thickness	2 mm	4 mm	8 mm	2 mm	4 mm	8 mm	2 mm	4 mm	8 mm
Laser power (W)	1200	5200	6400	-			1200	2800	6400
Beam spot size (mm)	0.6			-			0.6		
Focal position (mm)	0			-			0		
Travel speed (m/min)	1	4	1	0.3			1		
Shielding gas composition	-			80% Ar + 20% CO_2			80% Ar + 20% CO_2		
Gas flow rate (l/min)	-			20			20		
Filler wire diameter (mm)	-			1			1		
Wire feed speed (m/min)	-			5.6	8.2	10.2	2		
Process separation (mm)	-			-			2 to 3		
Process orientation	-			-			Laser leading		
Average current (A)	-			139	187	201	68		
Average voltage (V)	-			11.8	14.8	24.7	8.9		
Arc mode	-			CMT	CMT	Pulse	CMT		
CTWD (mm)	-			11 mm			13.5 mm		

6.3 Results

6.3.1 Aesthetic quality evaluation

Aesthetic quality of the weld joints was evaluated quantitatively as per the AQI scoring method. Each weld defects have been rated and AQI score was compared among different welding methods. Weld bead appearance of 2 mm thick samples which were welded at various root gap conditions are shown in

Figure 6-1. In 2 mm thick sheets, autogenous laser welding produced weld with underfill at 0.2 mm root gap level whereas at 0.5 mm root gap, almost laser passed through the gap and did not produce acceptable weld bead. On the other hand, GMAW and HLAW processes were produced aesthetically good weld beads at both 0.5 mm and 1 mm root gap conditions. Width of the weld beads were found to be uniform over the entire length which implies that both the processes are steady even at root gap conditions.

Process	Root gap	Top weld appearance	Bottom weld appearance
ALW	0.2 mm	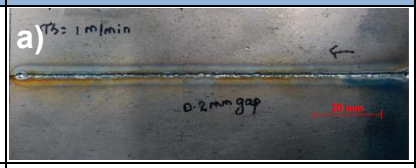	
	0.5 mm	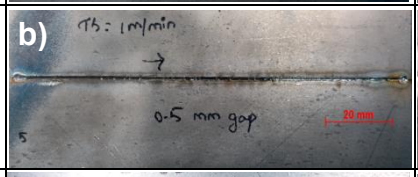	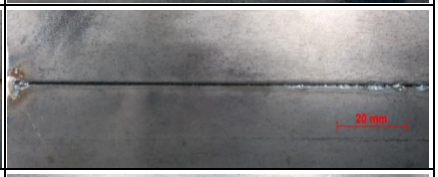
GMAW	0.5 mm		
	1 mm	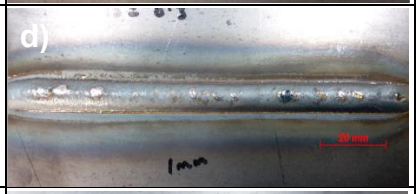	
HLAW	0.5 mm		
	1 mm		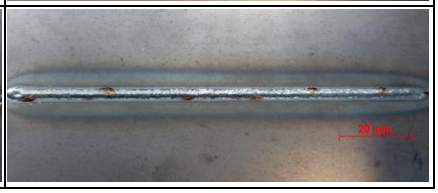

Figure 6-1 Top and bottom bead appearances of the specimen welded by three different processes under various root gaps – 2 mm thickness

Figure 6-2, Figure 6-3 and Figure 6-4 shows that AQI score rating of 2 mm, 4 mm and 8 mm thick joints produced at different welding conditions respectively. Addition of filler metal enhances the gap bridgeability of both GMAW and HLAW processes. In both of these processes, top bead reinforcement tends to decrease as the gap increases from 0.5 mm to 1 mm. This is due to the fact that the joint area increases with root gap. Presence of glass bead was found to be the visual defect in GMAW welded joints. As CMT mode was used in the welding of 2 mm and 4 mm thick joints, spatters were not observed. Nevertheless, it was observed in 8 mm thick joints as pulse mode was employed. In HLAW process, the glass bead witnessed was less than with GMAW process as low wire feed speed was used. In addition to the glass bead, spatters were also observed in 4 mm and 8 mm thick joints. Moreover, depth of underfill was found to be increased with the root gap in 8 mm thick HLAW welded joints. At zero root gap condition, no defects were noticed in the ALW process. However, an increase in root gap led to the formation of underfill. At 0.5 mm root gap condition in 2 mm thick joint, the presence of incomplete weld increases the AQI score. Also, significant underfill was observed at 0.5 mm root gap condition in 4 mm and 8 mm thick joints.

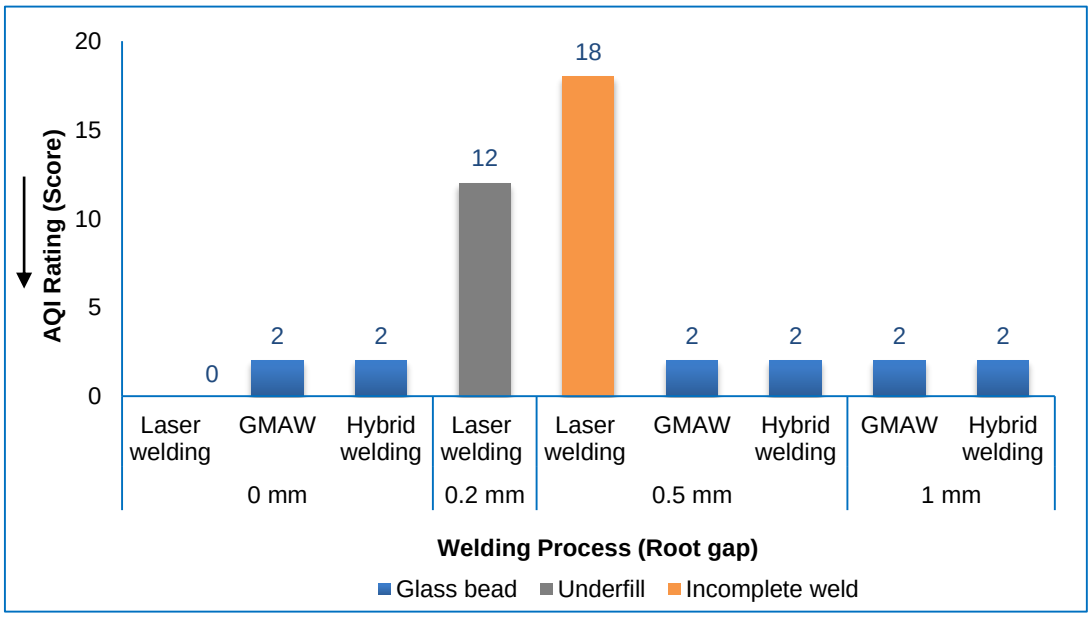

Figure 6-2 Effect of root gap on aesthetic quality of weld bead – 2 mm thickness

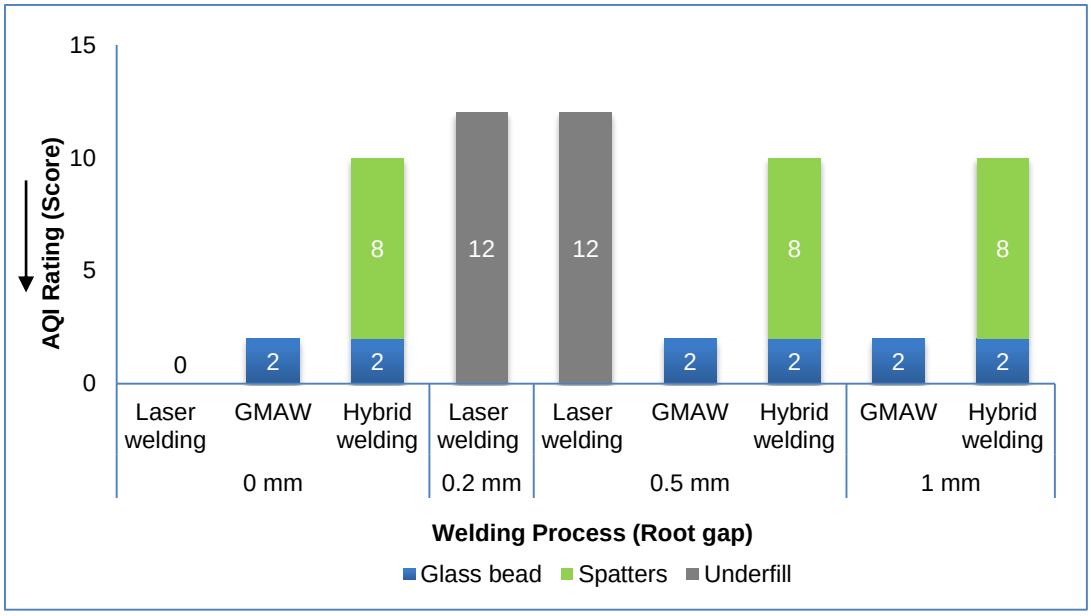

Figure 6-3 Effect of root gap on aesthetic quality of weld bead – 4 mm thickness

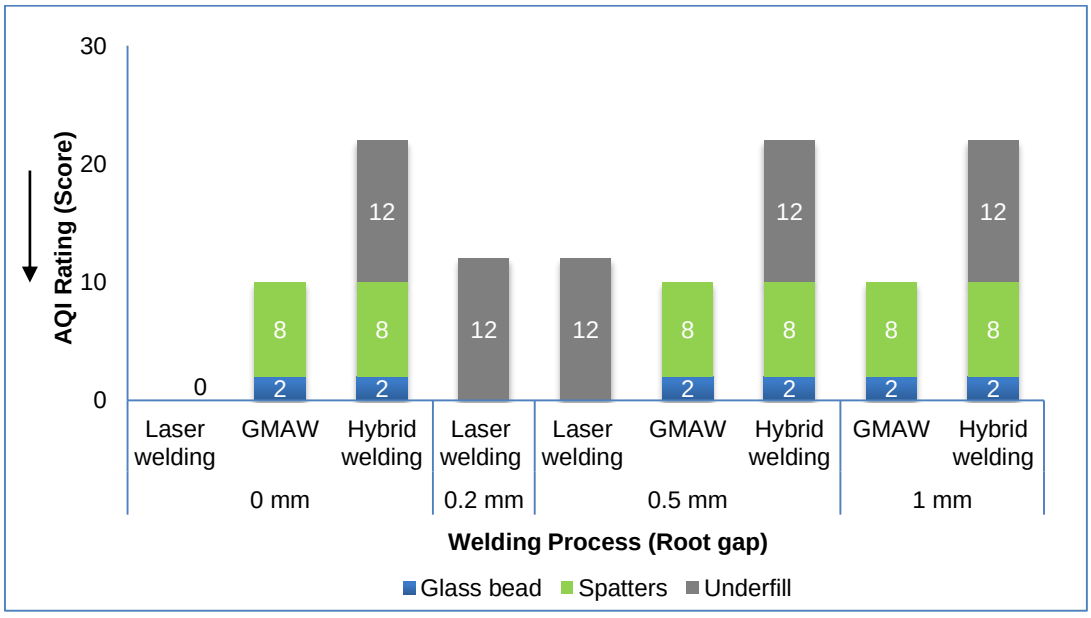

Figure 6-4 Effect of root gap on aesthetic quality of weld bead – 8 mm thickness

6.3.2 Macroscopic evaluation

Macroscopic evaluation of 2 mm, 4 mm and 8 mm joints welded at various root gap conditions are shown in Figure 6-5, Figure 6-6 and Figure 6-7 respectively. Cross-sections of joints welded by ALW process at 0.2 mm root gap condition are shown in Figure 6-8.

Process/ Root gap	0 mm gap	0.5 mm gap	1 mm gap
Gas metal arc welding		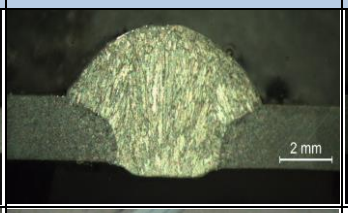	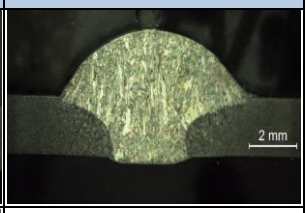
Autogenous laser welding	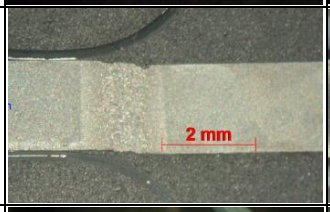	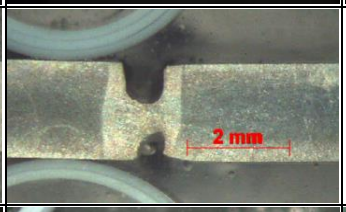	-
Hybrid laser GMAW	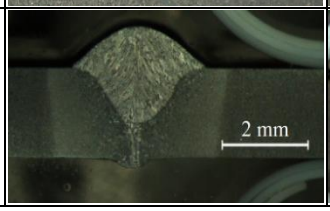	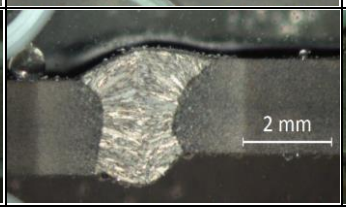	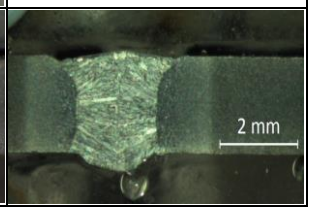

Figure 6-5 Weld cross-sections of different welding processes at different root gap conditions - 2 mm thickness

Process/ Root gap	0 mm gap	0.5 mm gap	1 mm gap
Gas metal arc welding	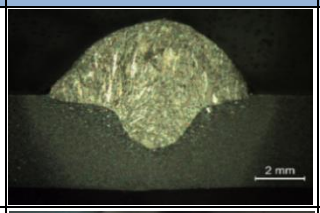	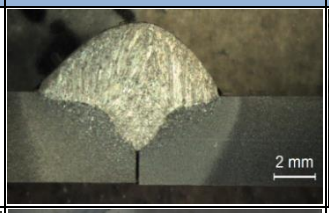	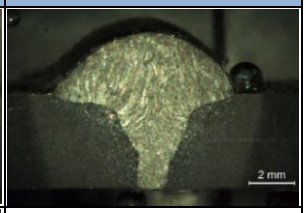
Autogenous laser welding	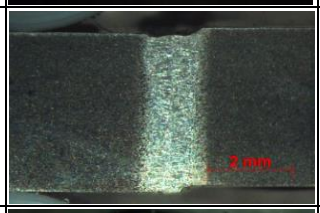	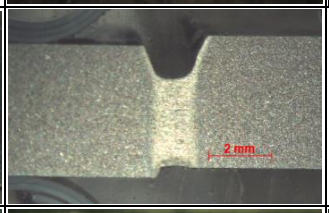	-
Hybrid laser GMAW	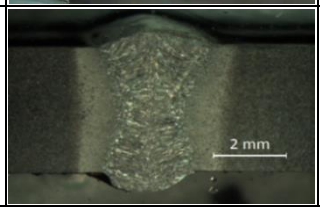	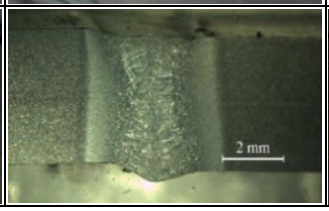	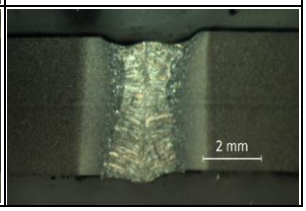

Figure 6-6 Weld cross-sections of different welding processes at different root gap conditions – 4 mm thickness

Process/ Root gap	0 mm gap	0.5 mm gap	1 mm gap
Gas metal arc welding	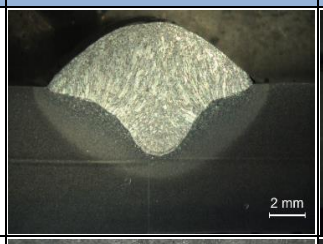	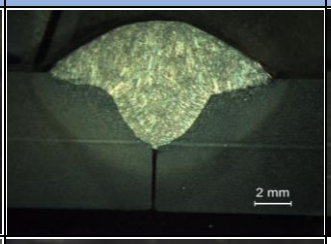	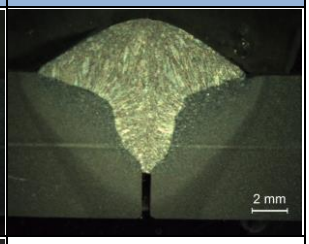
Autogenous laser welding	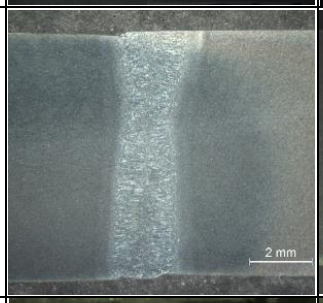	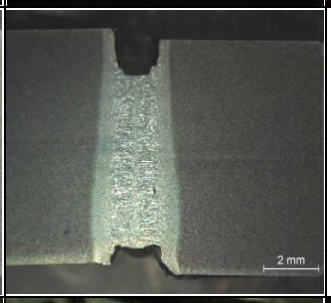	-
Hybrid laser GMAW	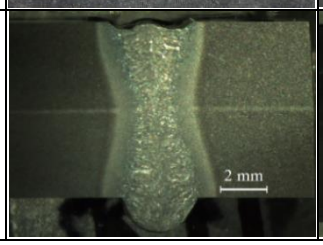	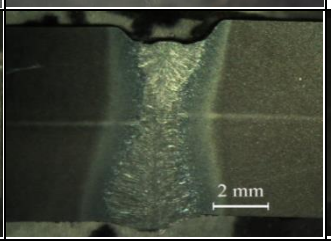	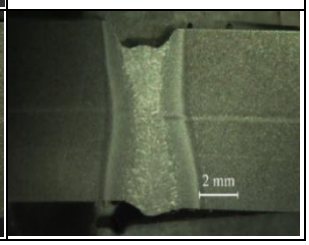

Figure 6-7 Weld cross-sections of different welding processes at different root gap conditions – 8 mm thickness

Description	Thickness = 2 mm	Thickness = 4 mm	Thickness = 8 mm
Autogenous laser welding at 0.2 mm root gap	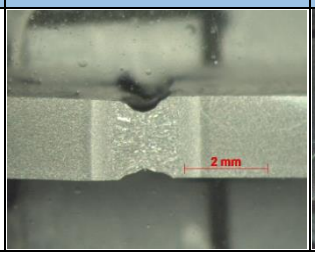	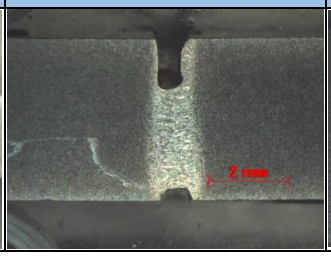	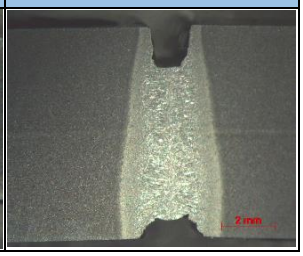

Figure 6-8 Autogenous laser welded joints at 0.2 mm root gap in 2 mm, 4 mm and 8 mm thickness

In ALW joints formation of underfill, incomplete weld and root concavity were found to be the major concerns whilst welding with root gaps. The depth of underfill increases with root gap. The decrease in amount of metal available for melting and increase in joint area as root gap increases causes the formation of underfill. This trend of the result was observed in all the three thickness of materials as shown in Figure 6-9. In 2 mm and 8 mm thick materials, experiments

were carried out at travel speed of 1 m/min whereas, in 4 mm thick joints, high speed of 4 m/min was used. Both low and high travel speed circumstances exhibited similar weld imperfections whilst welding with root gap.

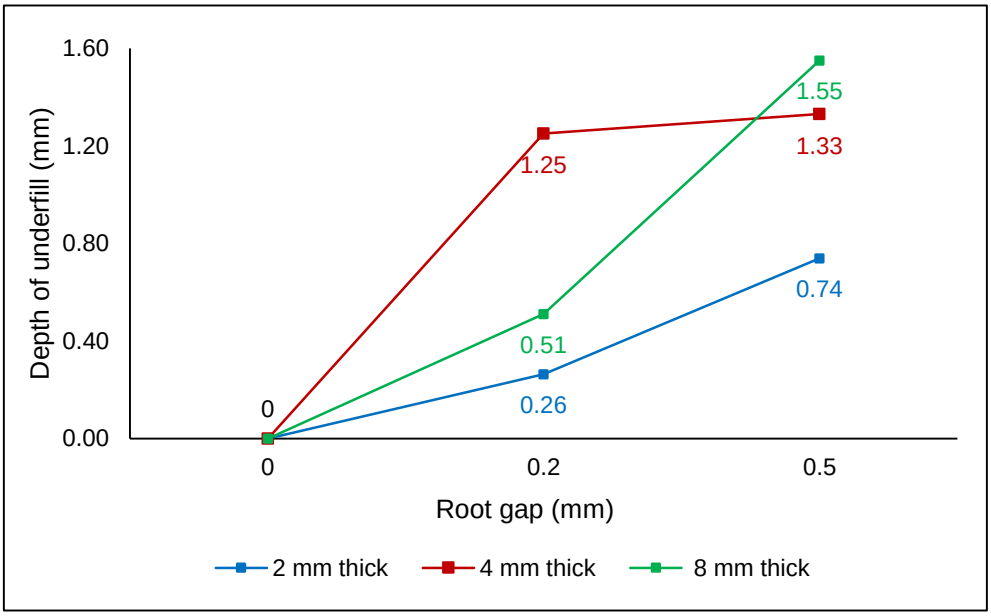

Figure 6-9 Influence of root gap on underfill in ALW process

Addition of filler metal in GMAW process makes this process less sensitive to root gap. On the one hand, as complete penetration was achieved in 2 mm thick materials, no significant difference was noticed on weld bead geometry when the presence of root gap. However, a marginal decrease in top bead reinforcement was observed as shown in Figure 6-10. On the other hand, as partial penetration was achieved in 4 mm and 8 mm thick materials, an increase in root gap increases the depth of penetration. Presence of root gap allows the molten metal to flow deeper before solidification. Root gap of 1 mm showed an increase of penetration by 69% and 45% compared with zero root gap condition in 4 mm and 8 mm thick materials respectively which are represented in Figure 6-11. Nevertheless, in 4 mm thick material, inconsistent penetration was noticed at 1 mm root gap and the range of penetration varied from 89% to 100%.

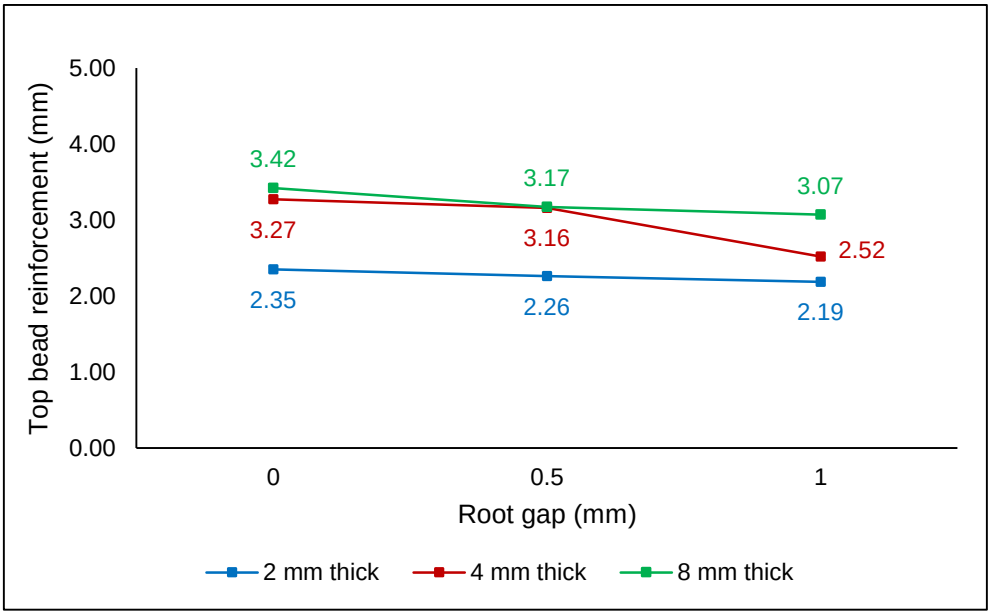

Figure 6-10 Influence of root gap on top bead reinforcement in GMAW process

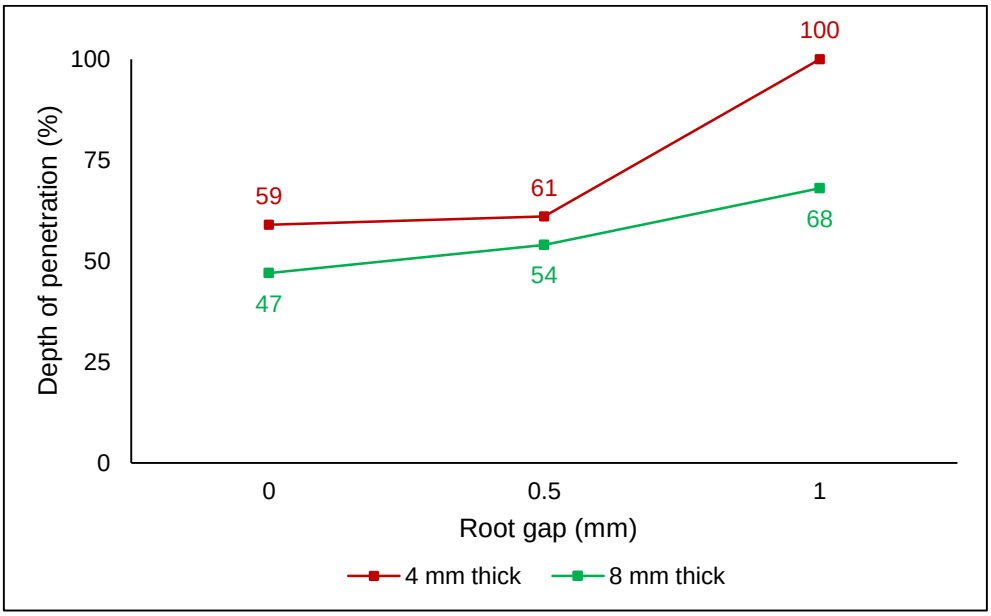

Figure 6-11 Influence of root gap on depth of penetration in GMAW process

Synergic effects of laser and arc penetration in HLAW process provided better gap bridgeability with complete penetration in all the three thickness of materials even at both 0.5 mm and 1 mm root gap conditions. The presence of a gap has an adverse effect on bead reinforcement [36]. This effects can be understood from Figure 6-12. Increase in root gap reduces the reinforcement and leads to the formation of undercut. Further increase in root gap causes the formation of

minor underfill. Moreover, the reduction in excess of penetration was also witnessed. These results are similar to [73] where the weld bead geometry was analysed in linearly varying root gap condition in HLAW process.

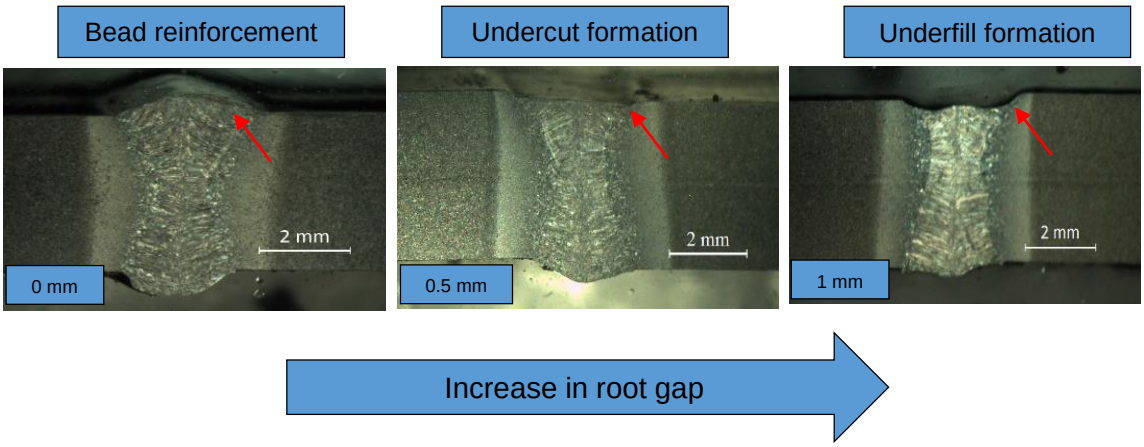

Figure 6-12 Influence of root gap on top bead reinforcement in HLAW process

As it can be seen in Figure 6-13, the depth of underfill increases with root gap in 8 mm thick joints. Even at zero root gap condition, no top bead reinforcement was obtained. Thus the underfill depth tends to be increased with root gap where the excess penetration tends to be decreased which can be referred in Figure 6-14.

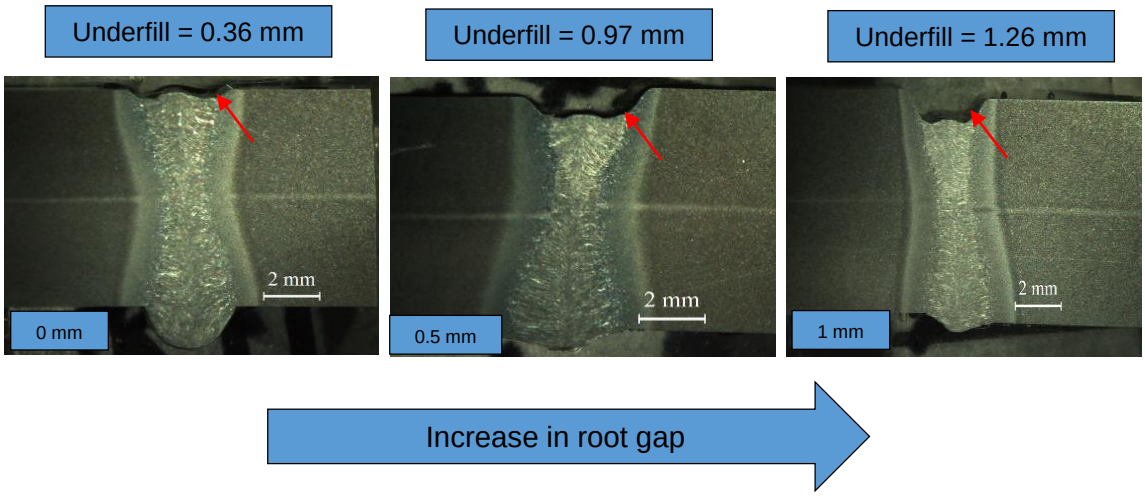

Figure 6-13 Influence of root gap on underfill formation in HLAW process – 8 mm thickness

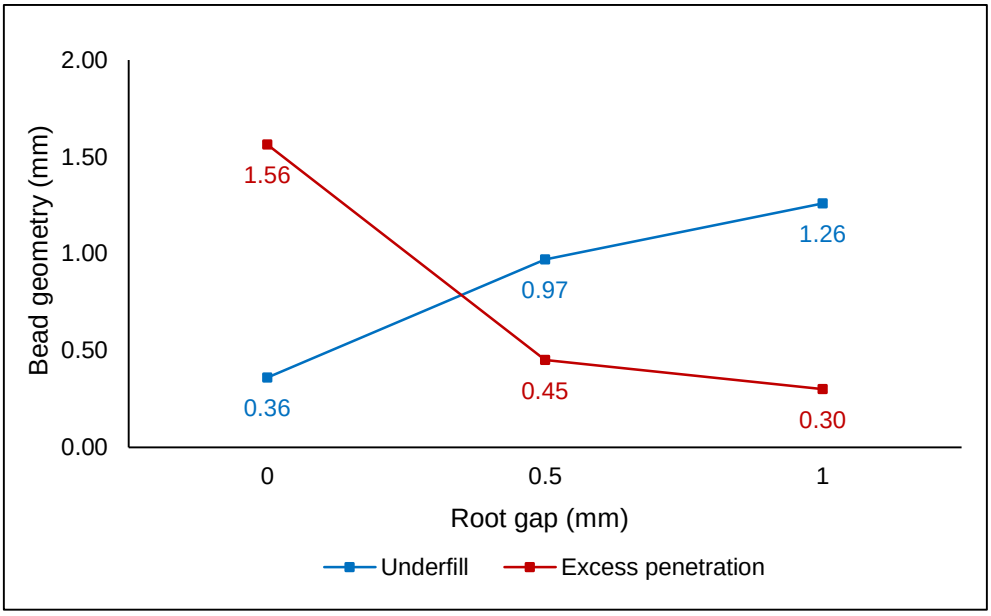

Figure 6-14 Influence of root gap on underfill and excess penetration in HLAW process – 8 mm thickness

6.4 Discussion

6.4.1 Effects of root gap on aesthetic quality

In the aspect of AQI score, comparatively GMAW process produced weld beads with less AQI score in all the experimented conditions. Similar AQI score of all the three thickness of joints at zero root gap as well as different root gap conditions clearly shows that existence of root gap does not have much effect on aesthetic quality of the weld in GMAW and HLAW processes. In ALW process at zero root gap condition, no visual defect was observed. Nevertheless, the presence of root gap led to the formation of underfill and incomplete weld which consequently increased the AQI score. HLAW process produced aesthetically acceptable welds even at 1 mm of root gap. In 2 mm thick sheet as shown in Figure 6-2, other than glass bead, no other defect was observed. However in 4 mm and 8 mm thick joints, in addition to glass bead, few spatters were also observed. As top bead reinforcement was not obtained in 8 mm thick joints even at zero root gap condition, depth of underfill was found to be increased with root gap which increases the AQI score as shown in Figure 6-4. Silica deposition

(Glass bead) was observed in all the root gap conditions of GMAW and HLAW weld beads. As low wire feed speed was used in HLAW process, significant reduction in silica deposition was noticed when compared to the GMAW process. Therefore, HLAW process can significantly reduce the rework of glass bead removal.

6.4.2 Comparison of gap bridging capability

It is apparent from the results that GMAW and HLAW processes are superior to autogenous laser welding process in the aspect of gap bridgeability. At root gap conditions, ALW process produced welds with high AQI score and critical defects such as underfill and incomplete weld. Addition of filler metal in GMAW and HLAW process enhances the gap bridging capability of these processes. Better gap bridgeability with complete penetration was found to be advantageous of HLAW process. Underfill was the main issue in welding of higher thickness material by HLAW process. Therefore, WFS and TS would be the key factors which needs to be optimized according to the range of root gaps in order to obtain better weld quality in HLAW process [36].

To sum up, compared with ALW process, HLAW process has shown a positive sign to satisfy the needs of an automotive industries in the aspect of gap bridgeability without much compromise on weld quality. Nevertheless, advanced methods such as laser twin-beam [96,97] and oscillation of laser beam [98] could increase the fit-up tolerance of autogenous laser welding process. However, these processes increase the complexity and it was beyond the scope of this project.

6.5 Conclusions

In this investigation, the gap bridging capability of autogenous laser welding and hybrid laser GMAW processes were evaluated and results were compared with the GMAW process. The following are the main conclusions derived,

- It is possible to produce acceptable welds with a root gap of 1 mm by HLAW process whereas ALW process could not produce acceptable welds in the experimented conditions. Precise combination of laser power and arc power is required to avoid underfill and control of root reinforcement in 8 mm thick joints.
- Aesthetic quality of the weld joints was not greatly compromised in both GMAW and HLAW processes even at root gap conditions. It is evident by the similar AQI score of both zero root gap and different root gap welds.
- Underfill, incomplete weld and root concavity are the critical defects observed in the ALW process whilst welding with root gaps and consequently it also affects the aesthetic quality of the weld beads.
- Existence of root gap increases the depth of penetration in welding of higher thickness materials in the GMAW process.
- The hybridization effect of laser and arc in HLAW process provided complete penetration and control of weld bead geometry with better gap bridgeability.

7 Propensity of welding methods on weldment distortion

7.1 Introduction

Welding induced distortion results in dimensional variation [76], reduction of load carrying capacity [75] and poor aesthetic quality [74] of the welded structure. In two-wheeler frame, the above-mentioned deviations create a huge impact on overall vehicle level quality and performance. Welding methods play a vital role in the weldment distortion. Hence this chapter aims to study the distortion propensity of different welding methods.

7.2 Experimental Methodology

7.2.1 Distortion measurement locations

Distortion measurement locations i.e. grid points were marked in the tack welded samples. Layout of the distortion measurement points are shown in Figure 7-1. Experimental methodology was adopted from [79]. Out of plane distortion was studied by measuring the surface height in each grid point. Measurements were taken before and after welding. Only static distortion measurements were carried out [79]. In all the trials, welded components were allowed to cool down for 10 minutes before unclamping. Based on the observations the following interpretations were made.

- Distortion index
- Peak distortion
- Surface deflection

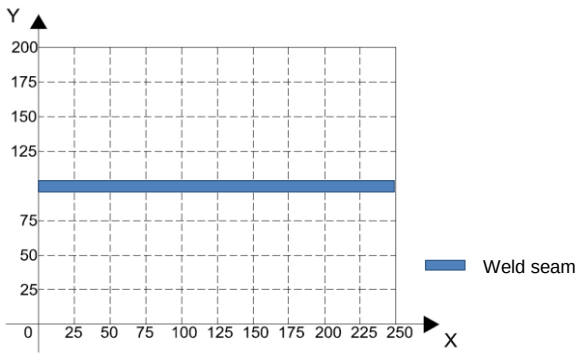

Figure 7-1 Layout for distortion measurement

The reference plate of each thickness presumably distortion-free was kept at the beginning and dial indicators were positioned over that and set to zero. The specimen with marked grid points was positioned with respect to the reference plate. Then the position of dial indicators were adjusted to the grid points. After that dial indicators were moved over the sample and surface height was measured in each grid point.

7.2.2 Experimentation matrix

Experiments were carried out in all three welding processes at the same welding speed of 0.5 m/min. In addition to that ALW and HLAW processes were performed at high welding speed of 4 m/min. Experimentation matrix is shown in Table 7-1. The used experimental parameters for 2 mm and 4 mm thick plates are described in Table 7-2 and Table 7-3 respectively. These parameters were chosen as it produced optimal weld quality during the evaluation of weld bead geometry. However, the input power was marginally optimized to ensure the consistent depth of penetration.

Table 7-1 Experimentation matrix for distortion analysis

#	Thickness (mm)	Travel speed (m/min)	Welding process
1	2	0.5	GMAW
2		0.5 and 4	ALW
3		0.5 and 4	HLAW
4	4	0.5	GMAW
5		0.5 and 4	ALW
6		0.5 and 4	HLAW

Table 7-2 Critical welding parameters used in different welding processes – 2 mm thick sheet

Process	WFS (m/min)	TS (m/min)	P_L (W)	Average current (A)	Average voltage (V)	CTWD (mm)	Arc mode
GMAW	6.2	0.5	-	156	12.1	11	CMT
ALW	-		1150	-	-	-	-
HLAW	2		1150	68	8.9	13.5	CMT
ALW	-	4	2550	-	-	-	-
HLAW	8		2450	185	14.4	13.5	CMT

Table 7-3 Critical welding parameters used in different welding processes – 4 mm thick plate

Process	WFS (m/min)	TS (m/min)	P_L (W)	Average current (A)	Average voltage (V)	CTWD (mm)	Arc mode
GMAW	9.2	0.5	-	183	23.8	11	Pulse
ALW	-		2150	-	-	-	-
HLAW	2		2150	68	8.9	13.5	CMT
ALW	-	4	5600	-	-	-	-
HLAW	8		5300	185	14.4	13.5	CMT

7.3 Results

7.3.1 Macroscopic evaluation

Complete penetration was achieved in 2 mm thick joints by all the welding conditions as shown in Figure 7-2. In 4 mm thick joint, partial penetration (80% in the thickness) was achieved in GMAW process with heat input of 592 J/mm at a travel speed of 0.5 m/min. Further increase in heat input results in formation of non-uniform weld bead. However, complete penetration was achieved in ALW and HLAW processes. Macrographs of 4 mm thick joints are shown in Figure 7-3.

GMAW (0.5 m/min)	ALW (0.5 m/min)	HLAW (0.5 m/min)
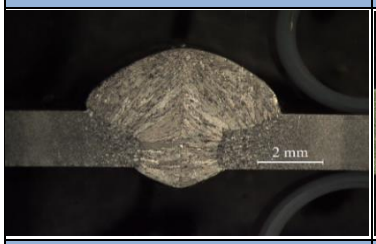	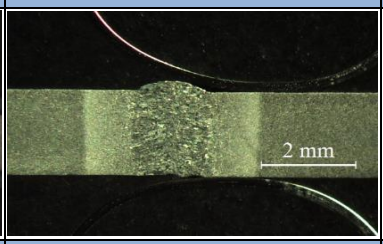	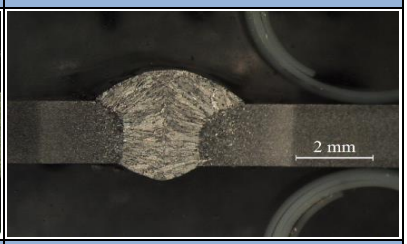
ALW (4 m/min)	**HLAW (4 m/min)**	**-**
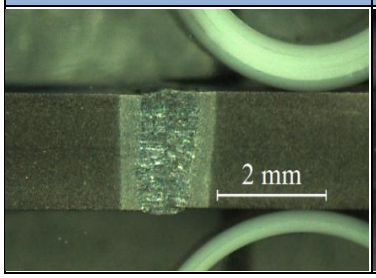	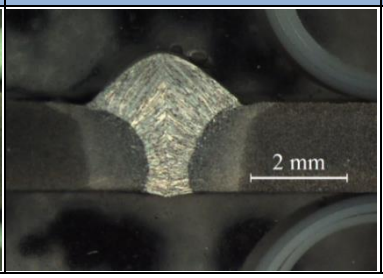	-

Figure 7-2 Macrographs of specimen welded by different welding processes at different travel speeds – 2 mm thickness

GMAW (0.5 m/min)	ALW (0.5 m/min)	HLAW (0.5 m/min)
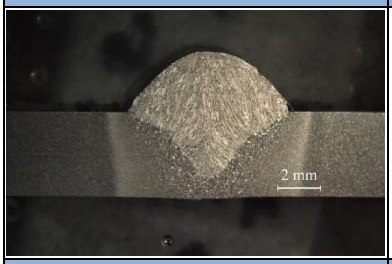	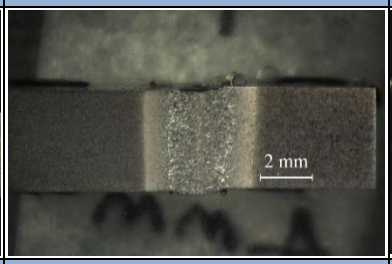	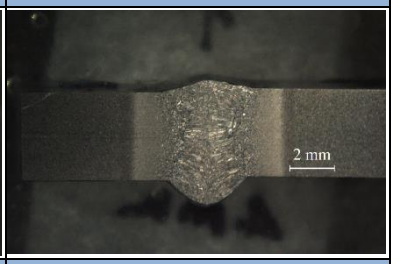
ALW (4 m/min)	**HLAW (4 m/min)**	**-**
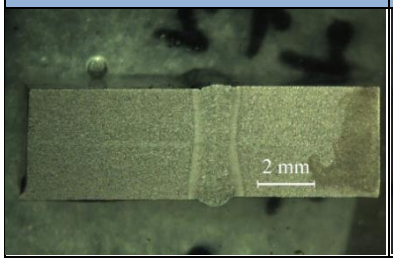	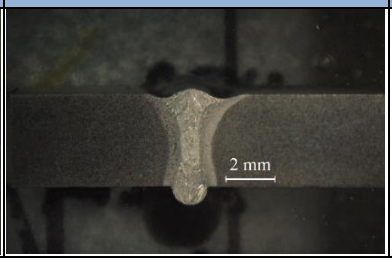	-

Figure 7-3 Macrographs of specimen welded by different welding processes at different travel speeds – 4 mm thickness

Deformation of 2 mm thick samples welded by different welding processes at different travel speeds are compared in Figure 7-4. GMAW process produced maximum deflection whereas minimal deflection was observed in autogenous laser welding process at high welding speed of 4 m/min.

GMAW (0.5 m/min)	ALW (0.5 m/min)	HLAW (0.5 m/min)
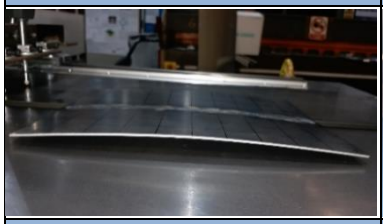	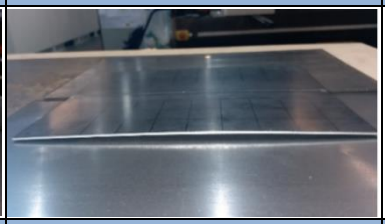	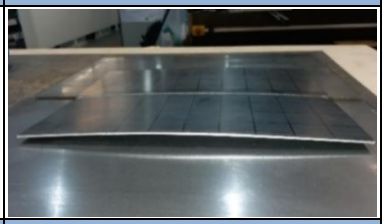
ALW (4 m/min)	**HLAW (4 m/min)**	
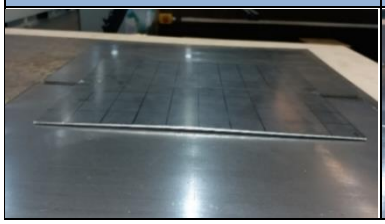	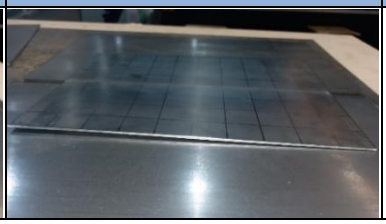	

Figure 7-4 Samples welded by different welding processes at different travel speeds – 2 mm thickness

7.3.2 Distortion measurement

Distortion index was calculated by taking an average of distortion values across the plate whereas the maximum distortion was tracked as a peak distortion [79]. The distortion index and peak distortion values obtained in all three welding processes are compared in Figure 7-5 to Figure 7-8. In all the cases, GMAW induced much higher distortion than HLAW and ALW processes.

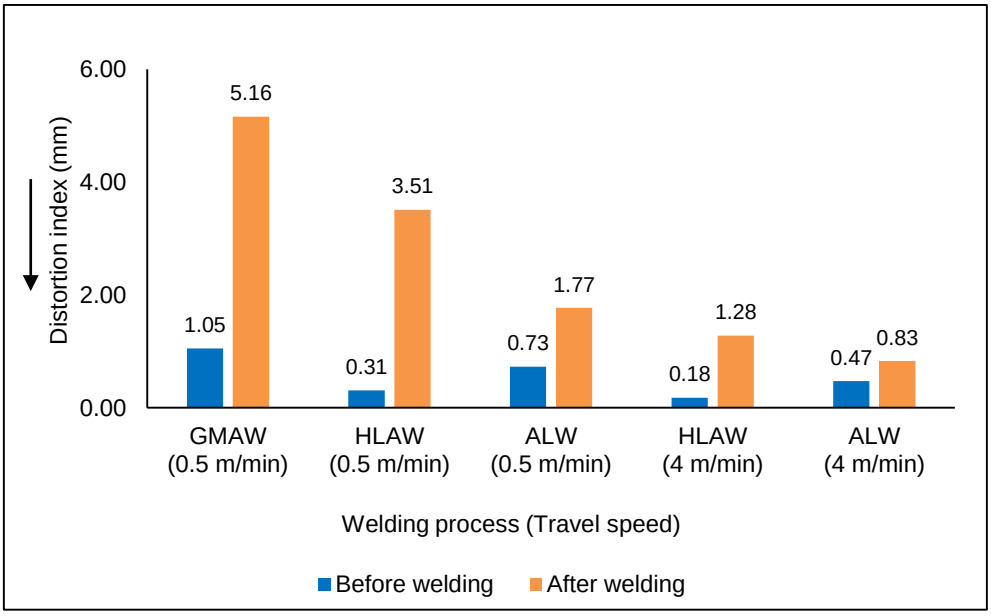

Figure 7-5 Comparison of distortion indices of different welding process conditions – 2 mm thickness

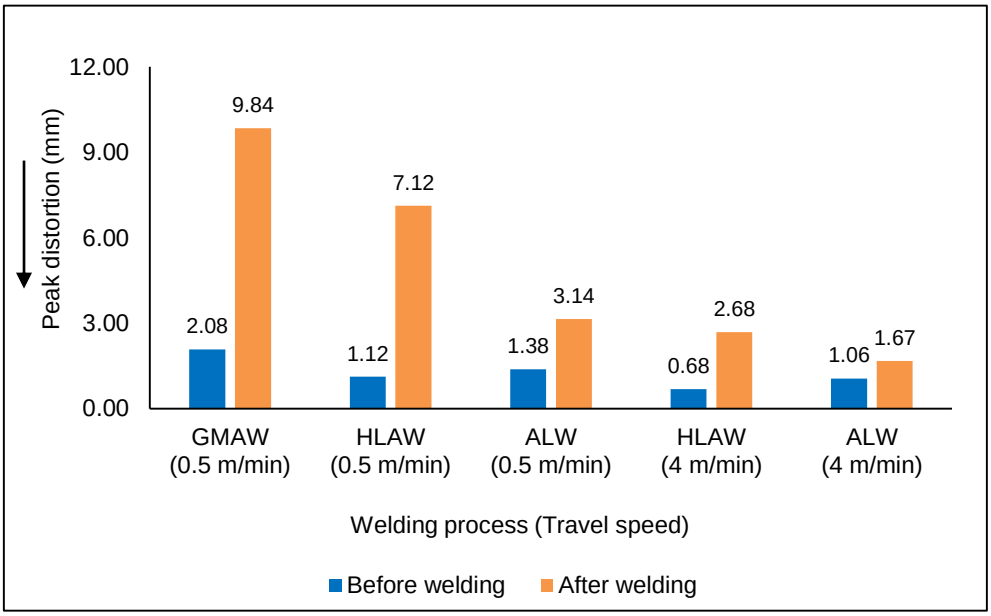

Figure 7-6 Comparison of peak distortion of different welding process conditions – 2 mm thickness

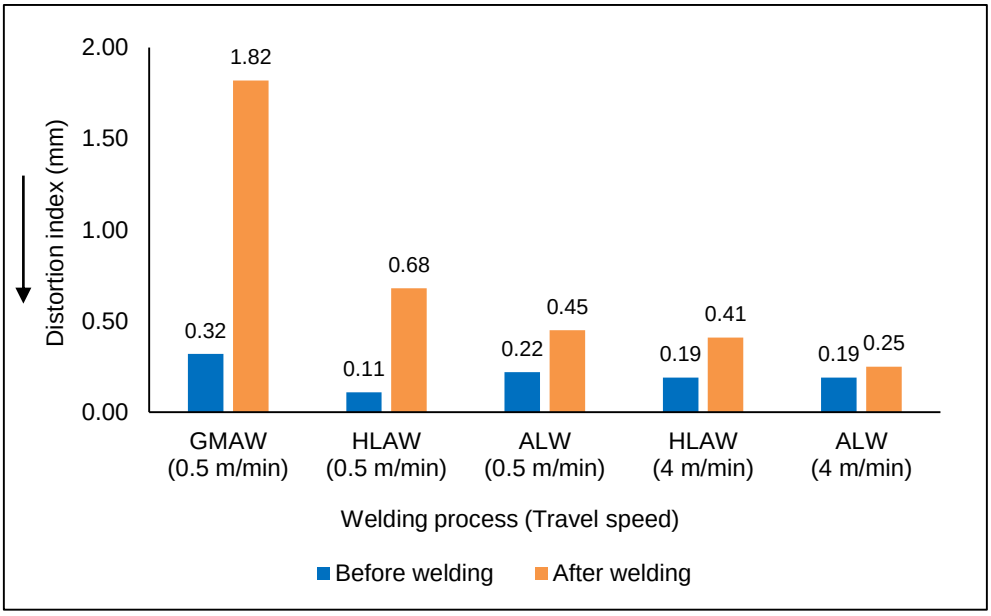

Figure 7-7 Comparison of distortion indices of different welding process conditions – 4 mm thickness

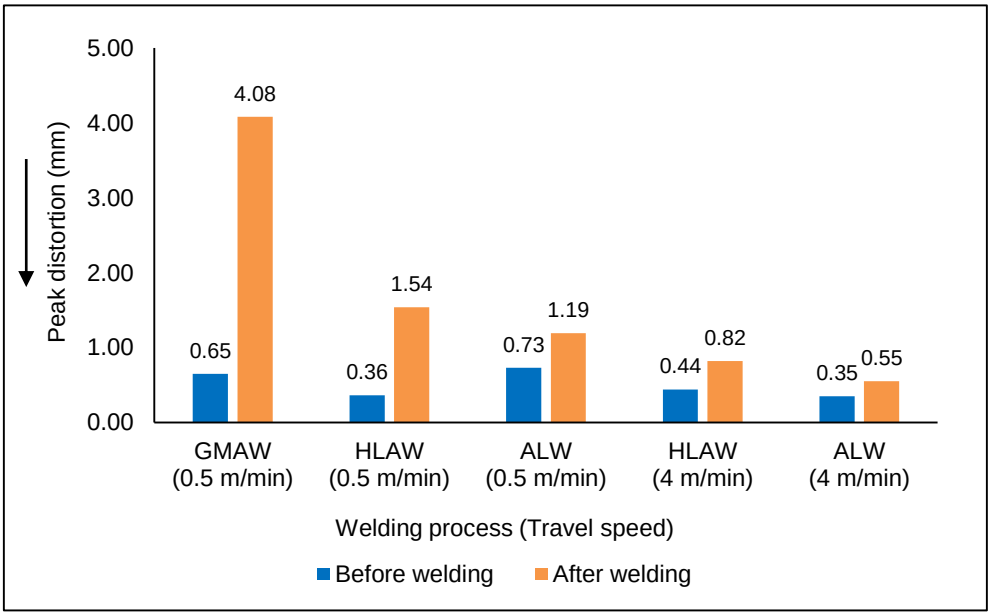

Figure 7-8 Comparison of peak distortion of different welding process conditions – 4 mm thickness

Average of distortion values over the length of the plate was plotted as a surface deflection [79] for 2 mm and 4 mm thick samples which are shown in Figure 7-9 and Figure 7-10 respectively. The maximum deflection was observed in GMAW process whereas ALW process at high welding speed produced the least

deflection in both the thickness of samples. Significant reduction in surface deflection was observed in ALW and HLAW processes at high welding speed conditions compared to GMAW process.

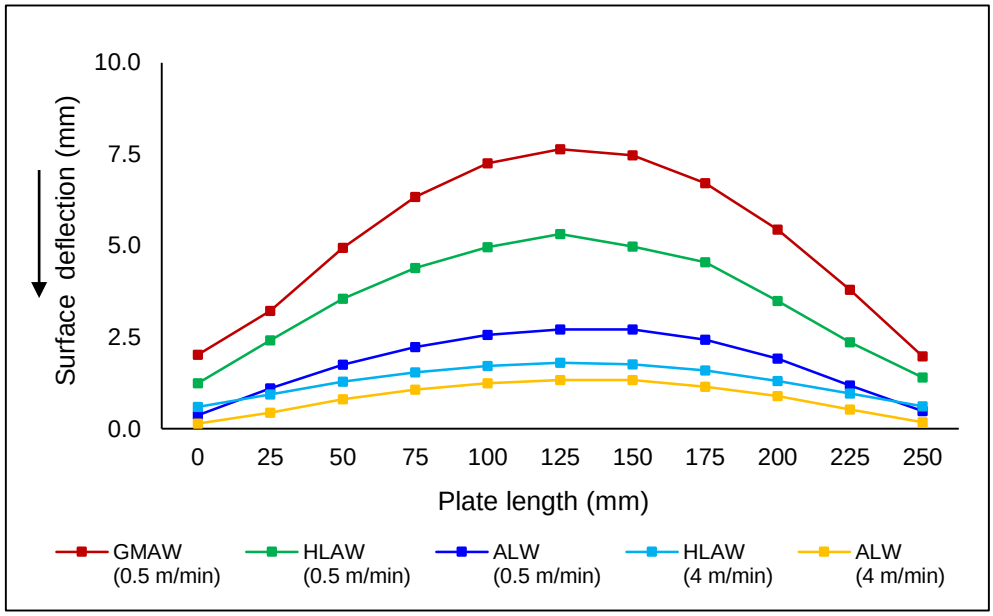

Figure 7-9 Comparison of surface deflection produced by different welding processes at different welding speeds – 2 mm thickness

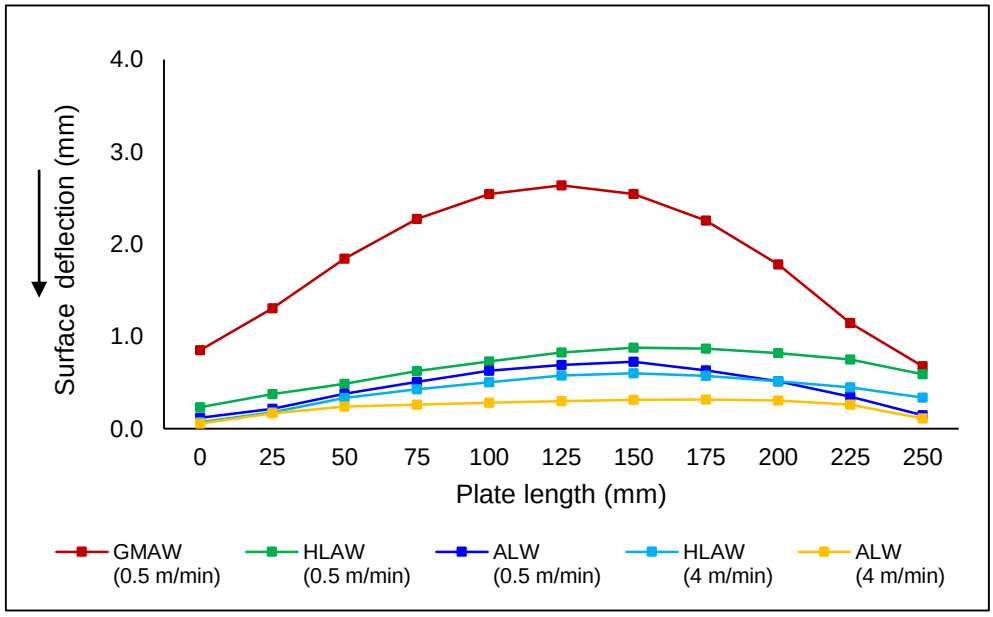

Figure 7-10 Comparison of surface deflection produced by different welding processes at different welding speeds – 4 mm thickness

7.4 Discussion

7.4.1 Heat input in different welding methods

Comparatively with GMAW process, ALW and HLAW processes provided complete penetration at the same welding speed of 0.5 m/min in both 2 mm and 4 mm thick joints even at lower heat input. However, a significant reduction in heat input was observed at a high welding speed of 4 m/min. Heat input comparison of different welding conditions for both 2 mm and 4 mm thick joints are shown in Figure 7-11 and Figure 7-12 respectively.

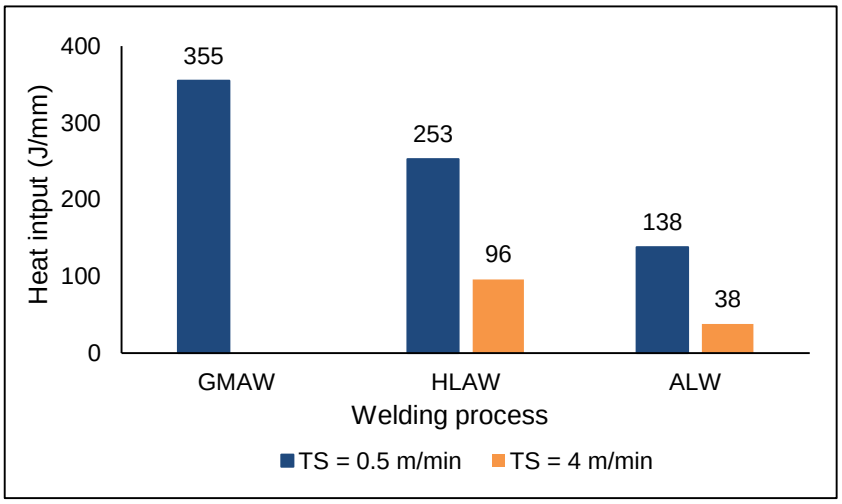

Figure 7-11 Heat input used in different welding processes – 2 mm thickness

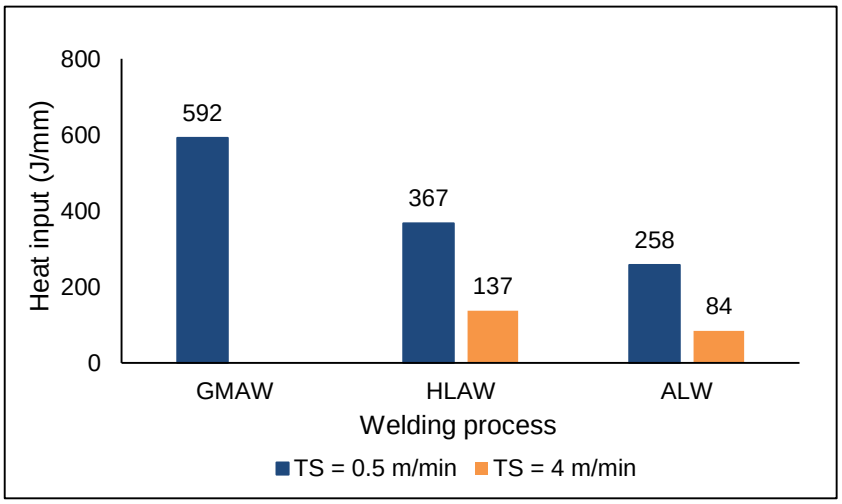

Figure 7-12 Heat input used in different welding processes – 4 mm thickness

7.4.2 Comparison of heat input and distortion

Heat input and fusion zone area are the key parameters which have a huge impact on weldment distortion [79]. Comparative study of these two parameters among different welding processes were carried out to understand the effect of these processes on distortion. Heat input exhibits a direct relation with distortion and fusion zone area [29]. In 2 mm thick samples, comparatively with GMAW process, 73% and 89% of reduced heat input were used to acquire complete penetration in HLAW and ALW processes respectively. Reduction in heat input results in a decrease in the fusion zone area and distortion. In 2 mm thick samples, 75% and 84% of reduced distortion index and 72% and 88% of reduced fusion zone area was observed in HLAW and ALW processes respectively than GMAW process. The detailed comparison of heat input, distortion index and fusion zone area are given in Table 7-4.

Table 7-4 Comparison of heat input with distortion index and fusion zone area produced by different welding processes – 2 mm thickness

Process (Travel speed)	Heat input (J/mm)	% of Heat input reduction with respect to GMAW	Measured fusion zone area (mm^2)	Distortion index (mm)	% of reduction in distortion index with respect to GMAW
GMAW (0.5 m/min)	355	-	16.95	5.16	-
HLAW (0.5 m/min)	253	29	7.76	3.51	32
ALW (0.5 m/min)	138	61	3.47	1.77	66
HLAW (4 m/min)	96	73	4.80	1.28	75
ALW (4 m/min)	38	89	2.10	0.83	84

In 4 mm thick samples, GMAW process with a heat input of 592 J/mm produced penetration depth of 80% in the thickness with fusion zone area of 26.06 mm^2. ALW and HLAW processes produced complete penetration with less fusion area and low distortion. At high speed of 4 m/min, 77% and 86% of reduction in distortion index were observed in HLAW and ALW processes respectively. Similarly, 79% and 82% of reduced fusion zone area were observed in HLAW

and ALW processes respectively. Comparison of heat input, distortion index and fusion zone area for 4 mm thick samples are shown in Table 7-5.

Table 7-5 Comparison of heat input with distortion index and fusion zone area produced by different welding processes – 4 mm thickness

Process (Travel speed)	Heat input (J/mm)	% of Heat input reduction with respect to GMAW	Measured fusion zone area (mm^2)	Distortion index (mm)	% of reduction in distortion index with respect to GMAW
GMAW (0.5 m/min)	592	-	26.06	1.82	-
HLAW (0.5 m/min)	367	38	14.95	0.68	63
ALW (0.5 m/min)	258	56	9.52	0.45	75
HLAW (4 m/min)	137	77	5.56	0.41	77
ALW (4 m/min)	84	86	4.65	0.25	86

Distortion index and fusion zone area are plotted against the heat input and different welding processes are marked with respect to the heat input used. Results were obtained in HLAW and ALW processes at high welding speed conditions are compared with GMAW process. Heat input shows a near-linear relation with distortion index and fusion zone area in both 2 mm and 4 mm thick samples which can be referred in Figure 7-13 to Figure 7-16.

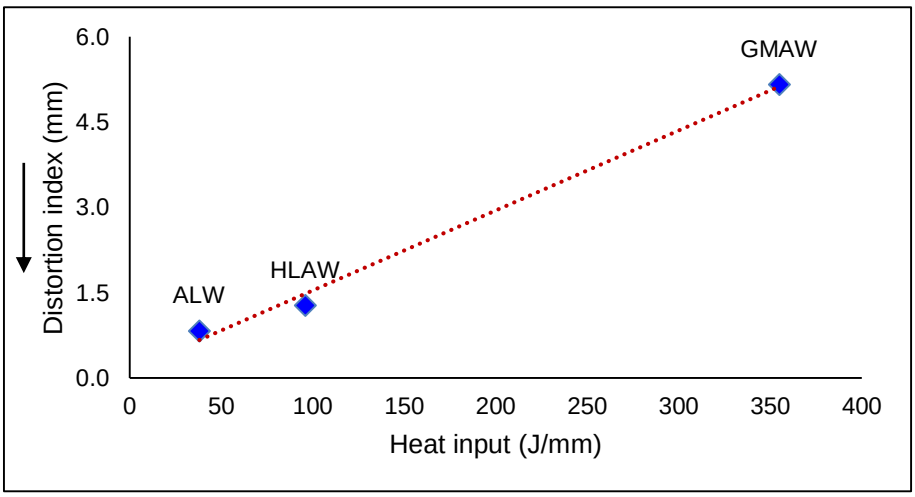

Figure 7-13 Variation of distortion index with heat input – 2 mm thickness

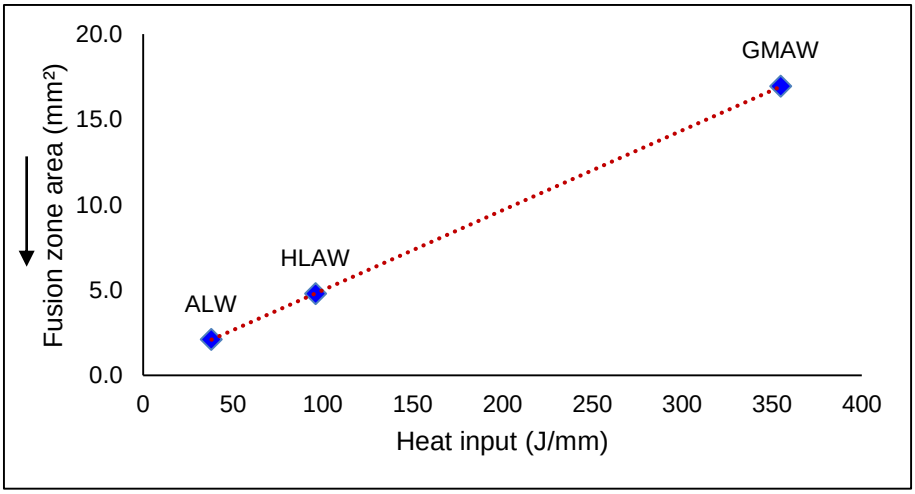

Figure 7-14 Variation of fusion zone area with heat input – 2 mm thickness

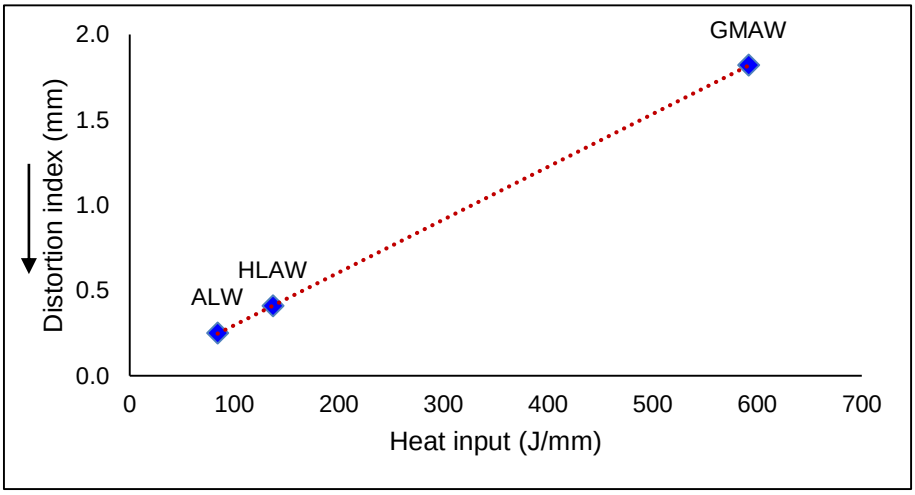

Figure 7-15 Variation of distortion index with heat input – 4 mm thickness

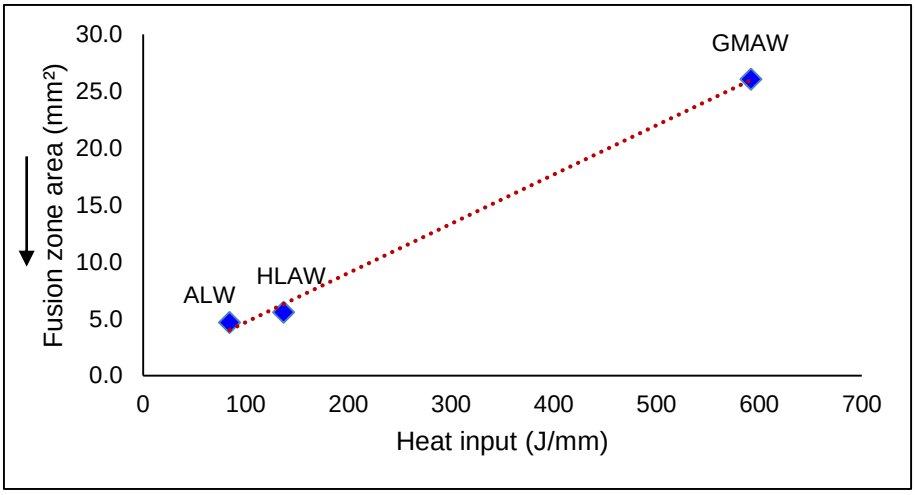

Figure 7-16 Variation of fusion zone area with heat input – 4 mm thickness

High power density of laser welding processes produced complete penetration with less distortion in both 2 mm and 4 mm thick plates than GMAW process. This is due to much higher energy is needed for penetration in GMAW process than laser which consequently increases the distortion index as it is proportional to heat input. Figure 7-13 and Figure 7-15 shows a near linear trend which proves that distortion is process independent but only depends on the ratio of heat input per depth. GMAW needs to melt more metal to penetrate the same thickness than laser hence higher ratio of the melt area to depth and greater the distortion.

7.5 Conclusions

- From the evaluation of three welding processes, it can be inferred that laser welding processes produced least distortion whereas GMAW exhibited larger distortion. ~75% and ~85% less distortion was observed in HLAW and ALW processes respectively than GMAW process.
- Heat input exhibited a near-linear relation with distortion index and fusion zone area. High power density of ALW and HLAW processes provided complete penetration with less distortion even at ~70% to 80% less heat input than GMAW process.
- Both autogenous laser and hybrid laser arc welding processes can benefit the automotive industries as these processes were produced significantly less distortion than existing GMAW process.
- Despite the complexity of hybrid laser arc welding process, it was found to be more beneficial in terms of low distortion, complete penetration and better weld bead geometry.
- This considerable reduction in distortion will greatly reduce the quantum of rework process on the welded structure and expected to improve functional performance of the frame. In addition, it will provide benefits in the reduction of production lead time and manufacturing cost.

8 Mechanical properties of weldment

8.1 Introduction

This chapter covers the evaluation of metallurgical and mechanical properties of welded joints which includes microhardness and tensile strength. Both the parameters were evaluated on the specimen welded by all three welding processes such as GMAW, ALW and HLAW. The samples welded for distortion study has been taken for analysis of microhardness and tensile strength test.

8.2 Experimental procedure

The experimentation matrix for both microhardness and tensile strength test is shown in Table 8-1.

Table 8-1 Experimentation matrix for microhardness test and tensile test

#	Thickness (mm)	Travel speed (m/min)	Welding process	Penetration
1	2	0.5	GMAW	Complete
2		0.5 and 4	ALW	Complete
3		0.5 and 4	HLAW	Complete
4	4	0.5	GMAW	Partial
5		0.5 and 4	ALW	Complete
6		0.5 and 4	HLAW	Complete

8.2.1 Microhardness test

Microindentation hardness measurement was done as per ASTM E384-17 standard. The testing conditions are detailed in Table 8-2. The process was carried out at room temperature. Hardness has been measured in the middle of the fusion zone in complete penetration joints and in case of partial penetration joints, it was measured in the middle to the overall depth of penetration.

Table 8-2 Parametric conditions for microindentation hardness test

Description / Process	ALW	GMAW	HLAW
Testing machine	Zwick Roell $HV_{0.2}$ – HV_{10}	Zwick Roell $HV_{0.2}$ – HV_{10}	Zwick Roell $HV_{0.2}$ – HV_{10}
Load (kg)	0.3	0.3	0.3
Dwell time (sec)	15	15	15
Interval distance (mm)	0.15	0.20	0.20

8.2.2 Tensile strength test

Tensile properties of the weldment were investigated as per ASTM E8/E8M-16a standard. The tests were carried out at room temperature with crosshead speed of 0.5 mm/min. Figure 8-1 shows the dimensional specification of tensile specimen. The test specimen surface was spray painted to create random speckles on the surface which are shown in Figure 8-2. DIC system was used to measure the distribution of strain on the specimen. Three samples were tested in each experimental conditions as shown in Table 8-1.

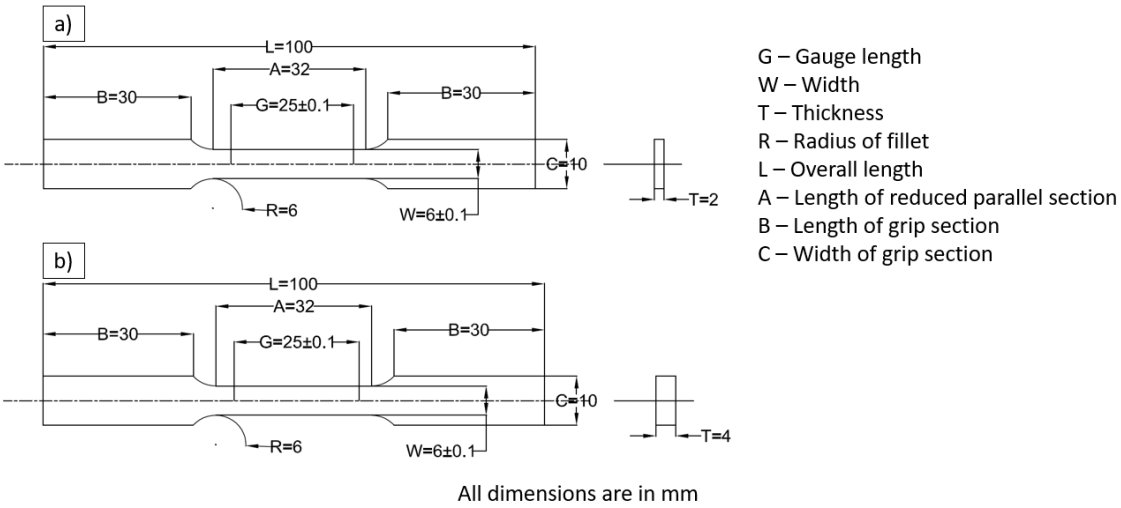

Figure 8-1 Tensile Specimen dimensions a) 2 mm thick specimen b) 4 mm thick specimen

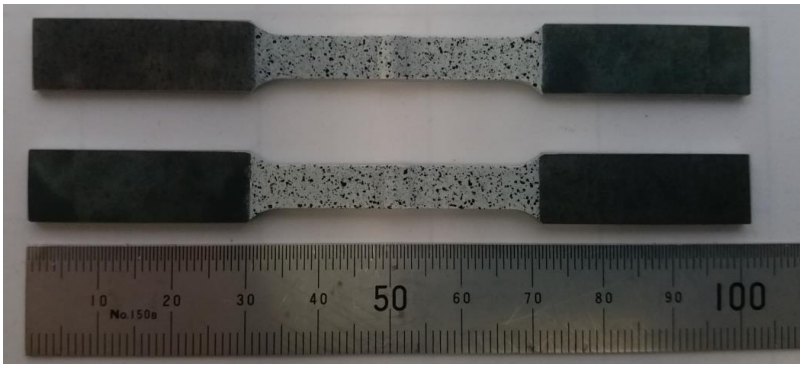

Figure 8-2 Spray painted specimen for tensile test

In order to replicate the actual condition of application, samples were tested with weld beads on the surface. Therefore the influence of bead geometry and weld imperfections on strength of the weld can be evaluated. Cross sectional area of the gauge length was used for the stress calculation.

8.3 Results

8.3.1 Microhardness measurement

The hardness distribution of ALW, HLAW and GMAW joints welded in both low and high welding speed conditions are compared. At the same welding speed of 0.5 m/min, comparatively with GMAW, both ALW and HLAW joints exhibited marginal increase in average hardness of fusion zone. For instance, in 2 mm thick joints at same welding speed of 0.5 m/min, the average hardness in fusion zone of GMAW, HLAW and ALW processes are 192 $HV_{0.3}$, 203 $HV_{0.3}$ and 210 $HV_{0.3}$ respectively. Nevertheless, at high welding speed of 4 m/min, HLAW and ALW processes produced high hardness in fusion zone than GMAW which are 224 $HV_{0.3}$ and 298 $HV_{0.3}$ respectively. The average hardness achieved in HAZ of joints welded by all three processes are higher than the hardness of base material. Comparatively, ALW process produced joints with higher hardness than HLAW and GMAW processes.

Macrographs with marked hardness measurement location with corresponding hardness distribution profile and the range of hardness in different zones of the weldment are given in the following Figures.

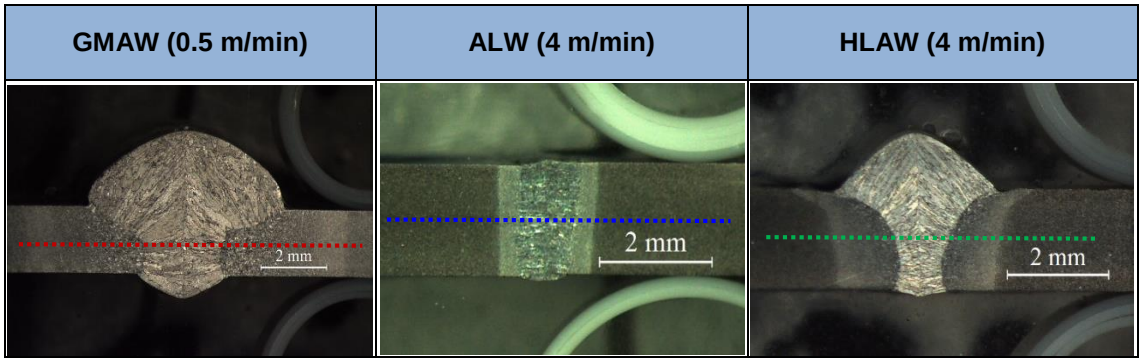

Figure 8-3 Macrographs of weld joints and marked hardness measurement location in 2 mm thick joints – Process (Travel speed)

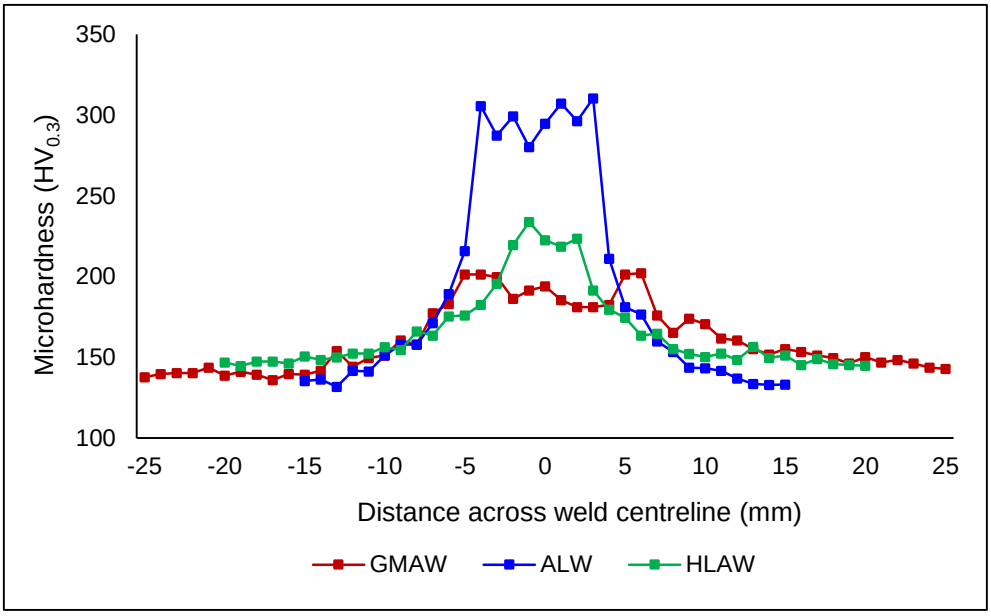

Figure 8-4 Microhardness profiles achieved with different welding processes at welding speed of 0.5 m/min-CMT (355 J/mm), 4 m/min-HLAW (96 J/mm), 4 m/min - ALW (38 J/mm) – 2 mm thick joints

Table 8-3 Range of hardness achieved by different welding methods in 2 mm thick joints - Process (Travel speed)

Zone	GMAW (0.5 m/min)	ALW (4 m/min)	HLAW (4 m/min)
BM	136 to 153 $HV_{0.3}$	132 to 160 $HV_{0.3}$	145 to 157 $HV_{0.3}$
HAZ	155 to 183 $HV_{0.3}$	171 to 216 $HV_{0.3}$	164 to 196 $HV_{0.3}$
FZ	181 to 202 $HV_{0.3}$	280 to 310 $HV_{0.3}$	219 to 234 $HV_{0.3}$

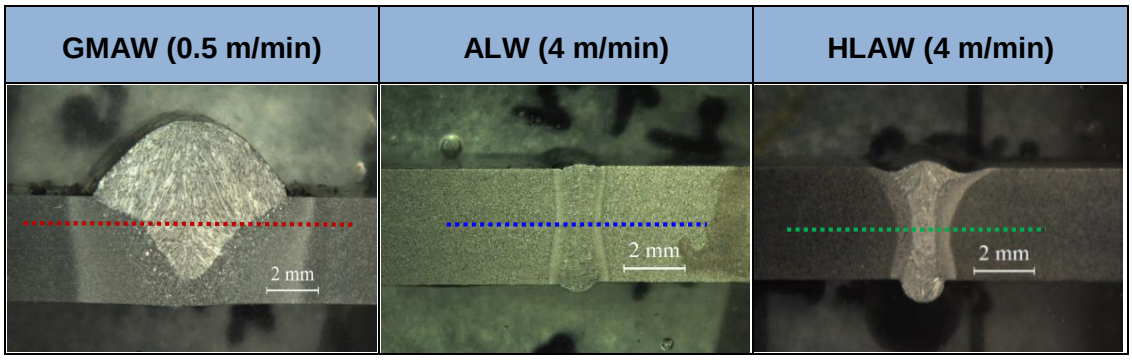

Figure 8-5 Macrographs of weld joints and marked hardness measurement location in 4 mm thick joints – Process (Travel speed)

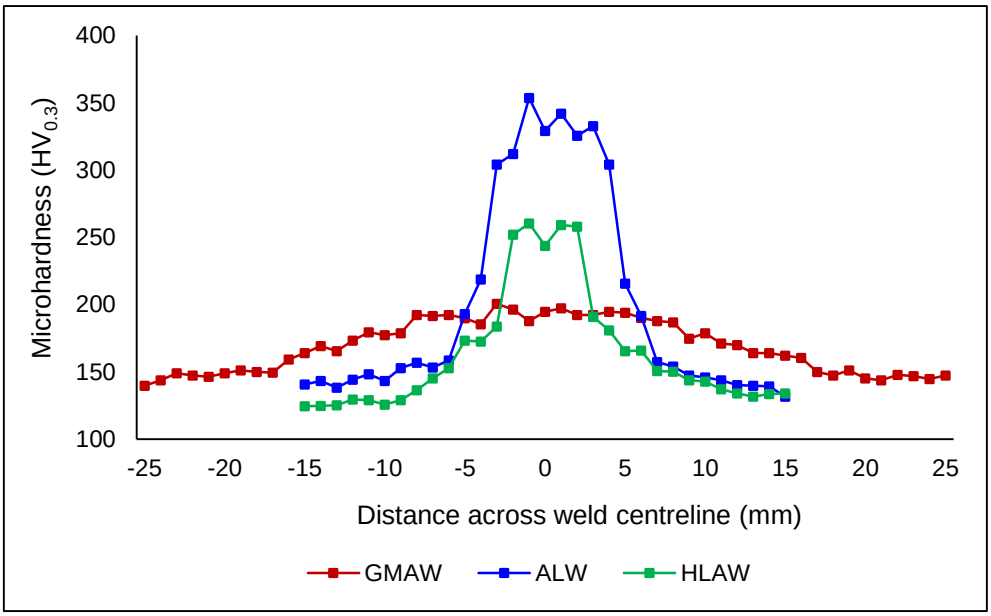

Figure 8-6 Microhardness profiles achieved with different welding processes at welding speed of 0.5 m/min-GMAW (592 J/mm), 4 m/min-HLAW (137 J/mm) 4 m/min-ALW (84 J/mm) – 4 mm thick joints

Table 8-4 Range of hardness achieved by different welding methods in 4 mm thick joints - Process (Travel speed)

Zone	GMAW (0.5 m/min)	ALW (4 m/min)	HLAW (4 m/min)
BM	140 to 151 $HV_{0.3}$	132 to 159 $HV_{0.3}$	125 to 153 $HV_{0.3}$
HAZ	159 to 180 $HV_{0.3}$	192 to 219 $HV_{0.3}$	165 to 191 $HV_{0.3}$
FZ	180 to 201 $HV_{0.3}$	304 to 354 $HV_{0.3}$	244 to 260 $HV_{0.3}$

Moreover the comparison of fusion zone and HAZ width obtained in different welding conditions are shown in Figure 8-7 and Figure 8-8 respectively. Microstructure of base material, heat affected zone and fusion zone were observed in microscope. Number of indents on each zone such as base material, fusion zone and heat affected zone were counted which was converted into width of HAZ and fusion zone. Even at same welding speed of 0.5 m/min, both ALW and HLAW processes exhibited reduction in fusion zone and HAZ width than GMAW. However, significant reduction was achieved at high welding speed of 4 m/min. HAZ width was measured on both sides of the fusion zone as HAZ_1 and HAZ_2 width.

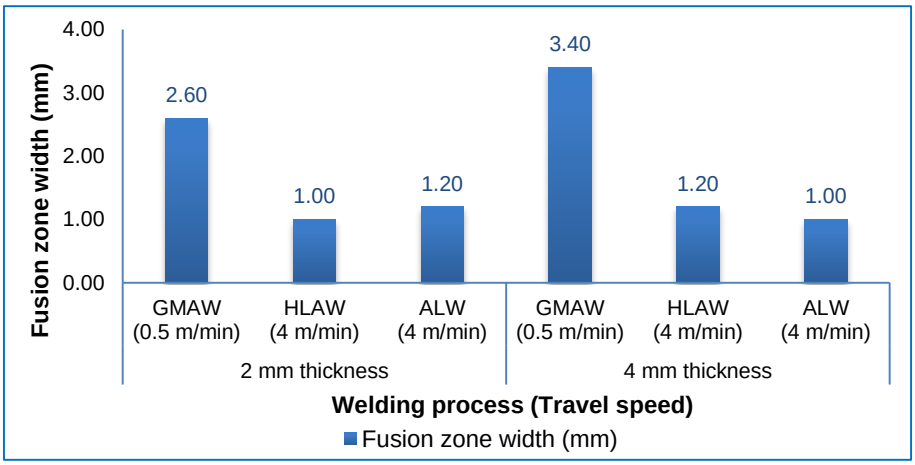

Figure 8-7 Fusion zone width produced by different welding processes in 2 mm and 4 mm thick samples

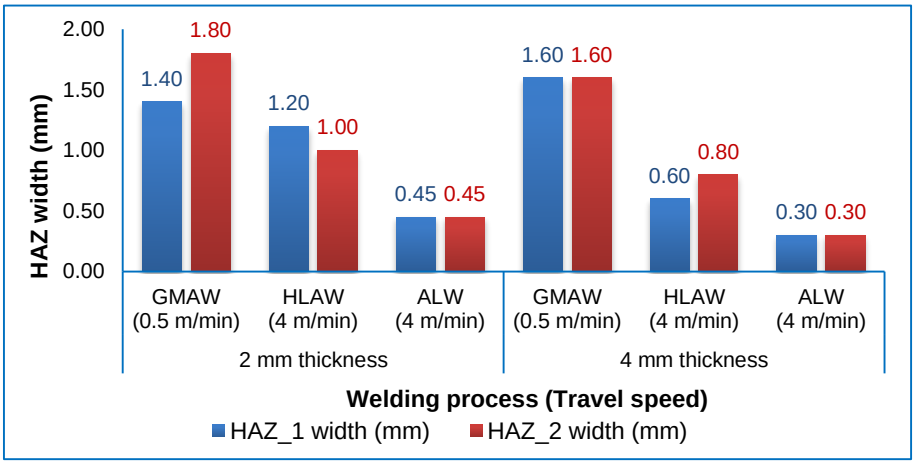

Figure 8-8 HAZ width produced by different welding processes in 2 mm and 4 mm thick samples

8.3.2 Tensile strength

In tensile strength test, the base material encountered fracture in all three process' samples as shown in Figure 8-9. However the tensile strength achieved by the welded sample was found to be lower than the tensile strength of the base material. The necking phenomena was observed in all the samples which indicates that fracture mode was ductile [30]. The tensile strength achieved by samples welded by all three processes are plotted in Figure 8-10.

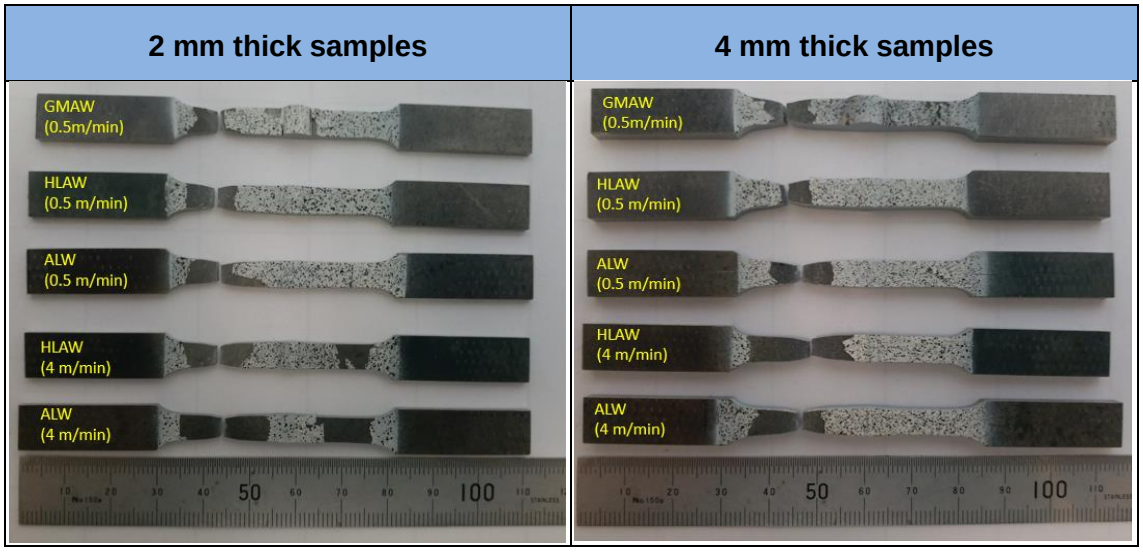

Figure 8-9 Photograph of 2 mm and 4 mm thick tensile samples welded at different conditions – Welding process (Travel speed)

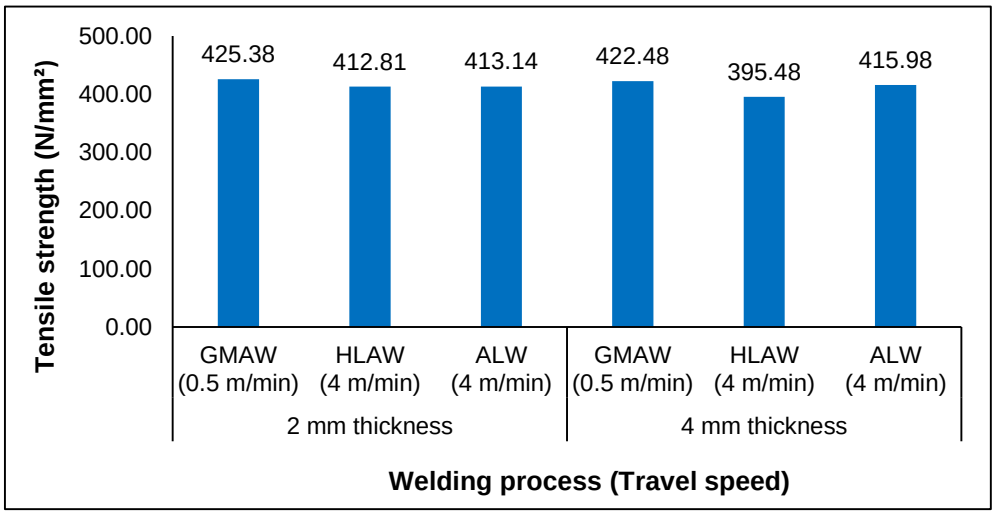

Figure 8-10 Tensile strength of samples welded by three different processes

8.4 Discussion

8.4.1 Effects of welding methods on hardness

Extremely low heat input and high cooling rate of ALW process, increases the hardness higher than GMAW whereas HLAW produced hardness in the intermediate range of both the other two processes. Comparison of fusion zone and HAZ hardness in 2 mm and 4 mm thick joints are detailed in Table 8-5 and Table 8-6 respectively. In 2 mm thick samples, ALW and HLAW processes produced 55% and 17% higher hardness than GMAW process respectively. Similarly, in 4 mm thick samples ALW and HLAW processes produced 69% and 33% higher hardness in fusion zone than GMAW process respectively.

Moreover, at welding speed of 4 m/min, the maximum hardness achieved by ALW in fusion zone of 2 mm and 4 mm thick samples are 310 $HV_{0.3}$ and 354 $HV_{0.3}$ which are substantially higher than GMAW. This higher hardness is one of the key factor which restricting the application of very high welding speed in laser welding process as excessive hardness is undesirable [28] to the performance of the welded structure. Addition of arc energy in HLAW process, increases the heat input higher than ALW process which consequently reduces the hardness. Therefore, HLAW process found to be more beneficial as it is improving productivity with marginal increase in hardness.

Table 8-5 Comparison of fusion zone and HAZ hardness produced by different welding processes – 2 mm thickness

Process (Travel speed)	Heat input (J/mm)	Average hardness in FZ ($HV_{0.3}$)	% of increase in average hardness in FZ with respect to GMAW	Average hardness in HAZ ($HV_{0.3}$)	% of increase in average hardness in HAZ with respect to GMAW
GMAW (0.5 m/min)	355	192	-	160	-
HLAW (4 m/min)	96	224	17	176	10
ALW (4 m/min)	38	298	55	191	19

Table 8-6 Comparison of fusion zone and HAZ hardness produced by different welding processes – 4 mm thickness

Process (Travel speed)	Heat input (J/mm)	Average hardness in FZ ($HV_{0.3}$)	% of increase in average hardness in FZ with respect to GMAW	Average hardness in HAZ ($HV_{0.3}$)	% of increase in average hardness in HAZ with respect to GMAW
GMAW (0.5 m/min)	592	192	-	170	-
HLAW (4 m/min)	137	255	33	176	4
ALW (4 m/min)	84	325	69	205	21

Low heat input of ALW and HLAW processes significantly reduced the fusion zone and HAZ width than GMAW process in both 2 mm and 4 mm thick joints which are detailed in Table 8-7. This consequently results in less metallurgical damage to the parent material.

Table 8-7 Comparison of fusion zone and HAZ width produced by different welding processes

Thickness	Process (Travel speed)	Fusion zone width (mm)	% of reduction in FZ width with respect to GMAW	Average HAZ width (mm)	% of reduction in average HAZ width with respect to GMAW
2 mm	GMAW (0.5 m/min)	2.60	-	1.60	-
	HLAW (4 m/min)	1.00	62	1.10	31
	ALW (4 m/min)	1.20	54	0.45	72
4 mm	GMAW (0.5 m/min)	3.40	-	1.60	-
	HLAW (4 m/min)	1.20	65	0.70	56
	ALW (4 m/min)	1.00	71	0.30	81

In 2 mm thick samples, comparatively with GMAW, both ALW and HLAW processes produced 54% and 62% reduction in fusion zone width at welding speed of 4 m/min. Similarly in 4 mm thick samples, 71% and 65% reduction in

fusion zone width was obtained at welding speed of 4 m/min in ALW and HLAW processes respectively. Also the average reduction in HAZ width of 72% and 31% in 2 mm thick joints and 81% and 56% in 4 mm thick joints were observed in ALW and HLAW processes respectively than GMAW process.

8.4.2 Effects of welding methods on tensile strength

As from the hardness measurement results of all three processes, high hardness in weld region than base materials indicates that weld regions are stronger than base material. Consequently, fracture occurred in base material of all the samples during tensile test. DIC system supports for visualization of relative displacement in sample and thereby enabling the identification of fracture zone [99]. Contour plot of strain distribution in the samples at same load condition are showed that strain on the weld metal is negligible in all three welding processes. A comparison of strain distribution in samples welded at different process conditions is shown in Figure 8-11. Compared with the weld region of HLAW and ALW samples, GMAW weld exhibited much lower strain which can be inferred from Figure 8-11 a) and d). Larger cross sectional area of the GMAW weld led to lower strain.

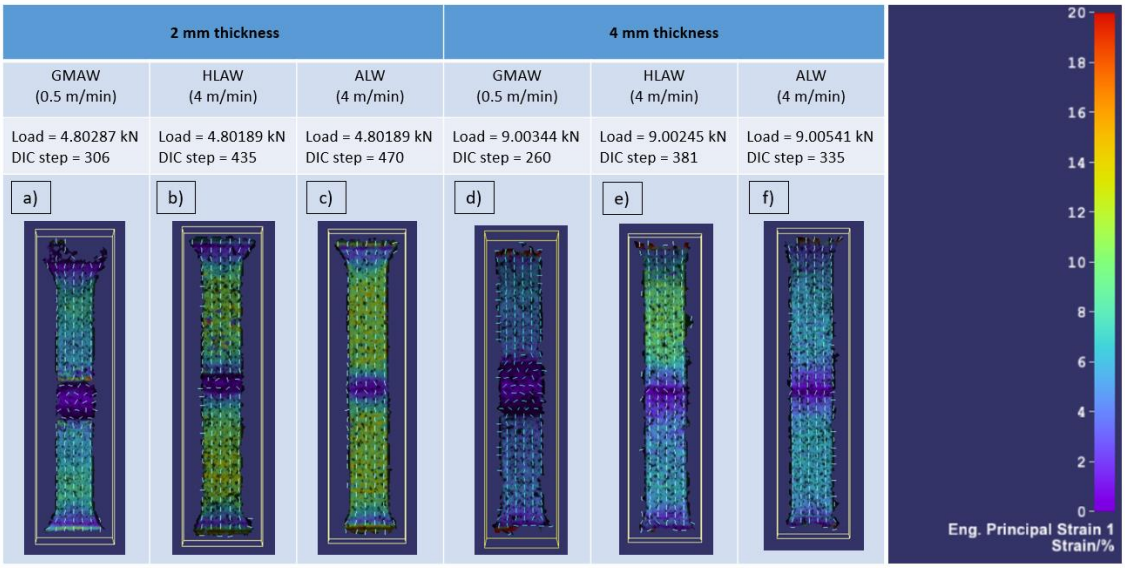

Figure 8-11 Visual observation of strain by DIC in the samples welded at different conditions

In hybrid laser welded 2 mm thick sample, the comparison of strain distribution at various load conditions till fracture are shown in Figure 8-12. As the load increases, the strain on the base material and HAZ increases. However, fracture zone was located in the base material due to significant increase in strain. In all load conditions, no increase in strain was observed on the fusion zone which can be referred in Figure 8-12 a) to k). Due to higher hardness in the fusion zone and HAZ than base material, strain was localized to the base material [43]. As shown in Figure 8-12, j) fracture occurred at the load of 3.8 kN whereas paint peel-off was observed during necking phase which causes loss of some tracking points (Figure 8-12, g).

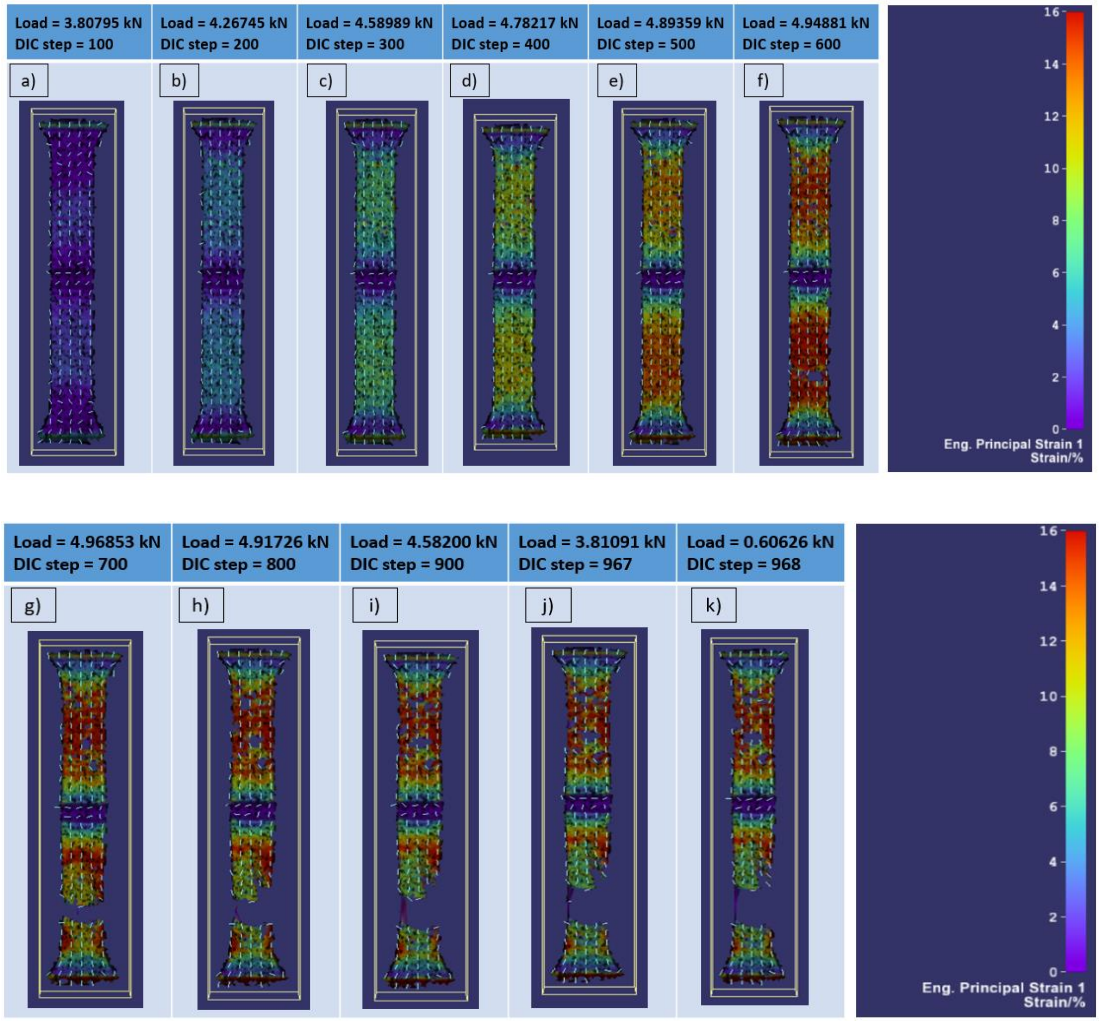

Figure 8-12 Comparison of strain distribution at different load conditions in 2 mm thick sample welded by HLAW process at welding speed of 4 m/min

As all the samples were fractured at the base material, almost similar strain distribution was observed in all other samples as well. The comparative strain distribution study of these samples are given in Appendix A1.

8.5 Conclusions

- The microhardness in ALW joints was found to be higher than GMAW and HLAW joints. In ALW joints, average fusion zone hardness was increased by 55% and 69% than GMAW in 2 mm and 4 mm thick joints respectively.
- At high welding speed of 4 m/min ALW and HLAW processes increases the maximum hardness in the fusion zone by 76% and 29% respectively than GMAW process in 4 mm thick materials.
- Productivity was improved by a factor of 8 times by HLAW process with 17% (2 mm thickness) and 33% (4 mm thickness) increase in average fusion zone hardness than GMAW whereas 55% (2 mm thickness) and 69% (4 mm thickness) increase in hardness was observed in ALW process.
- Comparatively with GMAW process, HLAW process improves the productivity with marginal increase in average fusion zone hardness whereas significant increase in hardness was observed in ALW process.
- Low heat input of ALW and HLAW processes provided considerable reduction in fusion zone and heat affected zone width.
- The weld region of all three processes have not experienced fracture and the increase in strain on the fusion zone was negligible. Moreover, the larger the weld bead area the lower the strain on the weld.

9 Critical discussion

GMAW process produced welds with better bead reinforcement and good aesthetic quality. However, limited depth of penetration and low welding speed significantly hinders the quality and productivity. Moreover, high heat input produced more fusion zone and HAZ area and also causes for larger distortion. It was difficult to achieve complete penetration in higher thickness materials with control of bead geometry in GMAW. Therefore in GMAW process, penetration and bead geometry cannot be controlled independently. On the other hand, high power density of autogenous laser welding process produced welds with complete penetration even at low heat input. This also resulted in less fusion zone and HAZ area. Complete penetration at high welding speed in thin structures and full penetration without groove preparation in higher thickness materials leads to significant improvement in productivity. However a narrow heat source of ALW restricts the fit-up tolerance for the parts. In addition, lack of weld reinforcement and high hardness in the weld region were also found to be the critical limitations of ALW process. The synergy of laser and arc in HLAW process enables deep penetration with better weld bead geometry. Operating window for welding speed of HLAW is comparable to ALW and significantly higher than GMAW. Addition of filler wire improves the gap bridgeability and supports to alter the properties of the fusion zone. Because, HLAW joints produced hardness intermediate to that of GMAW and ALW processes. However, HLAW Process is more complex than the individual processes as numerous process parameters are involved. Therefore, precise optimization of parameters is required to obtain better weld quality. All three processes produced stronger weld region with higher hardness than base material. Hence failure occurred in the base material during tensile test. In both low and high travel speed conditions, failure was observed in base material of both ALW and HLAW welded samples. Almost no increase in strain was witnessed on the weld metal. Subjective comparison of all three welding processes are shown in Table 9-1 as per the experimental results. Hybrid laser arc welding process can be considered as the future welding in the automobile sector.

Table 9-1 Subjective comparison of three welding processes

Process	Productivity	Heat input	Bead geometry	Gap bridging	Distortion	Mechanical properties	Aesthetic quality
GMAW	Low	High	Good	Good	High	Good	Good
ALW	High	Low	Poor	Poor	Low	Good	Medium
HLAW	High	Low	Good	Good	Low	Good	Good

Good Fair Poor

10 Conclusions and Future work

10.1 Conclusions

The main conclusions are,

- Hybrid laser arc welding process is capable to fulfil the specified quality requirements of the two-wheeler frame in the aspect of productivity, weld bead geometry, gap bridgeability, distortion and mechanical properties.
- Comparatively with GMAW process, both ALW and HLAW processes improved the productivity by a factor of 8 times in 2 mm and 4 mm thick materials whereas 3 times improved productivity was achieved in 8 mm thick materials with complete penetration.
- High power density of ALW and HLAW processes produced complete penetration even at ~70% to 80% less heat input than GMAW process.
- Hybrid laser arc welding process exhibited a comparable gap bridging behaviour to GMAW process without compromising an aesthetic quality of the weld bead. HLAW process produced acceptable welds even at 1 mm of root gap.
- Compared with GMAW process, ~ 75% and ~ 85% less distortion was observed in HLAW and ALW processes respectively in both 2 mm and 4 mm thick materials.
- HLAW process significantly improved the productivity with marginal increase in hardness of the weld region compared with GMAW process whereas considerable increase in hardness was observed in ALW process.
- HLAW and ALW processes produced stronger weld region with higher hardness than base material hence fracture occurred in the base material.
- HLAW process is easier to control aesthetic quality of the weld through optimization of parameters for better bead geometry. Laser with CMT produced aesthetically good weld beads. Lack of filler in ALW process makes it difficult to control the reinforcement without underfill.

Thus hybrid laser arc welding process can be recommended for automotive structural application. The key benefits are significant improvement in productivity with enhancement of quality improvements including deep penetration, low distortion, better mechanical properties and good gap bridgeability. However, more complexity [41] and high investment [33] are the two main drawbacks of hybrid laser arc welding process.

10.2 Recommendations for future work

Fundamental evaluation of laser welding processes for application in two-wheeler frame was carried out in this project. There is a scope for further research for this application. Following are the recommendations for future work.

- Studying the application of hybrid laser arc welding process on weld quality in T-joint and lap joint configurations.
- Microstructural investigation of hybrid laser arc welded joints and correlation study with mechanical properties of the weldment.
- Studying the effects of HLAW process parameters on critical weld defects.
- Detailed investigation on HLAW process in higher thickness material to attain the suitable combination of laser and arc parameters to obtain better weld geometry.
- Studying the process monitoring systems to control weld quality on hybrid laser arc welding process.

References

1. The Society of Indian Automobile Manufactureres (SIAM). Performance of Indian Automobile industries. 2019. Available at: http://www.siamindia.com/ (Accessed: 17 August 2019)

2. Staufer H. A look at laser hybrid welding in the automotive industry. The fabricator. 2016. Available at: https://www.thefabricator.com/article/laserwelding/a-look-at-laser-hybrid-welding-in-the-automotive-industry (Accessed: 17 August 2019)

3. TVS Motor Company Ltd. (TVSM). Internal documents/standards. 2019.

4. TVS Motor Company Ltd. (TVSM). Available at: https://www.tvsapache.com/rr310/#craftedforagility (Accessed: 17 August 2019)

5. Rege S., Khatri C., Nandedkar M., Wagh N. Design and analysis of frame for electric motorcycle. International Journal of Innovative Research in Science, Engineering and Technology. 2017; 6(10): 19500–19507. Available at: DOI:10.15680/IJIRSET.2017.0610039

6. Hiremath S., Kumar N., Nagareddy.G., Rathod L. Modal analysis of two wheeler chassis. International Journal of Engineering Sciences & Research Technology. 2016; 5(7): 68–73. Available at: DOI:10.5281/zenodo.56899

7. T. Kondaiah and D.Pavan Kumar. Shape and material optimization of a two wheeler front suspension frame for pipe type and rectangular cross sections. International Journal of Emerging Trends in Engineering Research. 2016; 4(6): 41–49. Available at: http://www.warse.org/IJETER/static/pdf/file/ijeter01462016.pdf

8. Kim S., Jin K., Sung W., Nam S. Effect of lack of penetration on the fatigue strength of high strength steel butt weld. KSME Journal. 1994; 8(2): 191–197. Available at: DOI:10.1007/BF02953268

9. Sun J., Liu X., Tong Y., Deng D. A comparative study on welding temperature fields, residual stress distributions and deformations induced by laser beam welding and CO2 gas arc welding. Materials and Design. Elsevier Ltd; 2014; 63: 519–530. Available at: DOI:10.1016/j.matdes.2014.06.057

10. Nguyen TC., Weckman DC., Johnson DA., Kerr HW. High speed fusion weld bead defects. Science and Technology of Welding and Joining. 2006; 11(6): 618–633. Available at: DOI:10.1179/174329306x128464

11. Sun Q., Di H-S., Li J-C., Wu B-Q., Misra RDK. A comparative study of the microstructure and properties of 800 MPa microalloyed C-Mn steel welded joints by laser and gas metal arc welding. Materials Science and Engineering A. Elsevier; 2016; 669: 150–158. Available at: DOI:10.1016/j.msea.2016.05.079

12. Wu C-W., Pearn WL., Kotz S. An overview of theory and practice on process capability indices for quality assurance. International Journal of Production Economics. 2009; 117(2): 338–359. Available at: DOI:10.1016/j.ijpe.2008.11.008

13. Moskvitin G V., Polyakov AN., Birger EM. Application of laser welding methods in industrial production. Welding International. 2013; 27(7): 572–580. Available at: DOI:10.1080/09507116.2012.715953

14. S T Riches. Industrial lasers and applications in automotive welding. Lasers in the Automotive Industry. 1998; (October 1998): 1–12. Available at: https://www.twi-global.com/technical-knowledge/published-papers/industrial-lasers-and-applications-in-automotive-welding

15. Jacques L., Ouafi A El. Experimental investigation of laser welding process in butt-joint configurations. World Journal of Engineering and Technology. 2017; 05(01): 77–89. Available at: DOI:10.4236/wjet.2017.51007

16. Suder WJ. Study of fundamental parameters in hybrid laser welding. PhD

thesis. Cranfield University; 2011.

17. Kou S. Welding metallurgy. 2nd edn. New Jersey: John Wiley & Sons, Inc.; 2003. 4 p.

18. Quintino L., Liskevich O., Vilarinho L., Scotti A. Heat input in full penetration welds in gas metal arc welding (GMAW). International Journal of Advanced Manufacturing Technology. 2013; 68(9–12): 2833–2840. Available at: DOI:10.1007/s00170-013-4862-8

19. Welding fundamentals and processes. ASM Handbook. Voluma 6A. Ohio: ASM International; 2011.

20. Němeček S., Mužík T., Míšek M. Differences between laser and arc welding of HSS Steels. Physics Procedia. 2012; 39: 67 – 74. Available at: DOI:10.1016/j.phpro.2012.10.015

21. Sukrongpang P. Laser welding to improve the productivity of thin structural steels. MSc thesis. Cranfield Uiversity; 2016.

22. Mazmudar CP., Patel K. Effect of laser welding process parameters on mechanical properties of stainless steel-316. International Journal of Advance Engineering and Research Development (IJAERD). 2014; 1(05): 1–11. Available at: DOI:10.21090/ijaerd.010593

23. Sa´nchez-Amaya JM., Delgado T., Damborenea JJ De., Lopez V., Botana FJ. Laser welding of AA 5083 samples by high power diode laser. Science and Technology of Welding and Joining. 2009; 14(1): 78–86. Available at: DOI:10.1179/136217108X347629

24. Ayoola WA., Suder WJ., Williams SW. Parameters controlling weld bead profile in conduction laser welding. Journal of Materials Processing Technology. 2017; 249(August 2016): 522–530. Available at: DOI:10.1016/j.jmatprotec.2017.06.026

25. Svenungsson J., Choquet I., Kaplan AFH. Laser welding process - A review of keyhole welding modelling. Physics Procedia. Elsevier B.V.; 2015; 78:

182–191. Available at: DOI:10.1016/j.phpro.2015.11.042

26. Guo W. Laser welding of high strength steels. PhD thesis. The University of Manchester; 2015.

27. E.M.Stanciu., Păvălache AC., G.M.Dumitru., O.G.Dontu., D.Besnea., I.M.Vasile. Mechanism of keyhole formation in laser welding. The Romanian Review Precision Mechanics, Optics & Mechatronics. 2010; 20(38): 171–176. Available at: https://www.researchgate.net/publication/268412313_Mechanism_of_keyhole_formation_in_laser_welding

28. Sokolov M., Salminen A., Kuznetsov M., Tsibulskiy I. Laser welding and weld hardness analysis of thick section S355 structural steel. Materials and Design. Elsevier Ltd; 2011; 32(10): 5127–5131. Available at: DOI:10.1016/j.matdes.2011.05.053

29. Colegrove P., C. Ikeagu., Thistlethwaite A., Williams S., Nagy T., Suder W., et al. Welding process impact on residual stress and distortion. Science and Technology of Welding and Joining. 2009; 14(8): 717–725. Available at: DOI:10.1179/136217109X406938

30. Oyyaravelu R., Kuppan P., Arivazhagan N. Comparative study on metallurgical and mechanical properties of laser and laser-arc-hybrid welding of HSLA steel. Materials Today: Proceedings. 2018. Available at: DOI:10.1016/j.matpr.2018.02.253

31. Oyyaravelu R., Kuppan P., Arivazhagan N. Metallurgical and mechanical properties of laser welded high strength low alloy steel. Journal of Advanced Research. 2016; 7(3): 463–472. Available at: DOI:10.1016/j.jare.2016.03.005

32. Katayama S., Kawahito Y., Mizutani M. Elucidation of laser welding phenomena and factors affecting weld penetration and welding defects. Physics Procedia. 2010; 5: 9–17. Available at:

DOI:10.1016/j.phpro.2010.08.024

33. Casalino G., Dal Maso U., Angelastro A., Campanelli SL. Hybrid laser welding: A review. DAAAM International Scientific Book 2010. Vienna, Austria: DAAAM International; 2010. pp. 413–430. Available at: DOI:10.2507/daaam.scibook.2010.38

34. Ono M., Shinbo Y., Yoshitake A., Ohmura M. Welding properties of thin steel sheets by laser-arc hybrid welding: laser focused arc welding. First International Symposium on High-Power Laser Macroprocessing. 2003; 4831(March 2003): 369. Available at: DOI:10.1117/12.497756

35. Sun Z., Kuo M. Bridging the joint gap with wire feed laser welding. Journal of Materials Processing Technology. 1999; 87(1–3): 213–222. Available at: DOI:10.1016/S0924-0136(98)00346-X

36. Shi G., Hilton P. A comparison of the gap bridging capability of CO2 laser and hybrid CO2 laser MAG welding on 8mm thickness C-Mn steel plate. 58th Annual Assembly and International Conference of International Institute of Welding. Prague, Czech Republic; 2005. pp. 1–10. Available at: http://www.twi.co.uk/technical-knowledge/published-papers/a-comparison-of-the-gap-bridging-capability-of-co2-laser-and-hybrid-co2-laser-mag-welding-on-8mm-thickness-c-mn-steel-plate-july/

37. Lappalainen E., Purtonen T., Salminen A. Effect of arc parameters in high brightness hybrid laser arc welding of low alloyed steel. International Congress on Applications of Lasers & Electro-Optics. 2011; 599: 599–605. Available at: DOI:10.2351/1.5062298

38. Kah P., Salminen A., Martikainen J. The influence of parameters on penetration, speed and bridging in laser hybrid welding. Mechanika. 2011; 17(3): 324–333. Available at: DOI:10.5755/j01.mech.17.3.511

39. Cai C., Feng J., Li L., Chen Y. Influence of laser on the droplet behavior in short-circuiting, globular, and spray modes of hybrid fiber laser-MIG

welding. Optics and Laser Technology. 2016; 83: 108–118. Available at: DOI:10.1016/j.optlastec.2016.03.029

40. Nilsson K., Heimbs S., Engström H., Kaplan AFH. Parameter influence in CO2-laser/MIG hybrid welding. 2003; IIW Doc. I(July 2003): 1–11. Available at: http://svelas.nu/papers/30917085035.pdf

41. Eriksson I., Powell J., Kaplan A. Guidelines in the choice of parameters for hybrid laser arc welding with fiber lasers. Physics Procedia. 2013; 41: 119–127. Available at: DOI:10.1016/j.phpro.2013.03.059

42. Acherjee B. Hybrid laser arc welding: State-of-art review. Optics and Laser Technology. Elsevier Ltd; 2018; 99: 60–71. Available at: DOI:10.1016/j.optlastec.2017.09.038

43. Munro C., Nolting AE., Cao XJ., Wanjara P. Hybrid laser-arc welding of HSLA-65 steel plate: microstructural and mechanical property evaluation of butt welds. Materials Science Forum. 2012; 706–709(March 2015): 2992–2997. Available at: DOI:10.4028/www.scientific.net/msf.706-709.2992

44. Ribic B., Palmer TA., DebRoy T. Problems and issues in laser-arc hybrid welding. International Materials Reviews. 2009; 54(4): 223–244. Available at: DOI:10.1179/174328009x411163

45. William MS., Jyotirmoy M. Laser material processing. 4th Editio. Springer London Dordrecht Heidelberg New York; 137 p. Available at: DOI:10.1007/978-1-84996-062-5

46. Kaplan AFH. Fresnel absorption of 1 μm- and 10 μm-laser beams at the keyhole wall during laser beam welding: Comparison between smooth and wavy surfaces. Applied Surface Science. Elsevier B.V.; 2012; 258(8): 3354–3363. Available at: DOI:10.1016/j.apsusc.2011.08.086

47. Liu L., Chen M. Interactions between laser and arc plasma during laser-arc hybrid welding of magnesium alloy. Optics and Lasers in Engineering.

2011. pp. 1224–1231. Available at: DOI:10.1016/j.optlaseng.2011.04.012

48. Selvi S., Vishvaksenan A., Rajasekar E. Cold metal transfer (CMT) technology - An overview. Defence Technology. Elsevier Ltd; 2018; 14(1): 28–44. Available at: DOI:10.1016/j.dt.2017.08.002

49. Prakasham G., Krishna LSR., Kumar AS. A review on the effect of various process parameters in cold metal transfer (CMT) GMAW welding. International Journal of Engineering Research. 2016; 5(Special 2): 432–435. Available at: DOI:10.17950/ijer/v5i2/030

50. Imoudu NE. The characteristic of cold metal transfer (CMT) and its application for cladding. Master's thesis. The arctic university of norway; 2017. Available at: https://hdl.handle.net/10037/12968

51. Chen M., Zhang D., Wu C. Current waveform effects on CMT welding of mild steel. Journal of Materials Processing Technology. Elsevier B.V.; 2017; 243: 395–404. Available at: DOI:10.1016/j.jmatprotec.2017.01.004

52. Stanciu EM., Pascu A., Gheorghiu I. CMT Welding of Low Carbon Steel Thin Sheets. IOP Conference Series: Materials Science and Engineering. 2017. Available at: DOI:10.1088/1757-899X/209/1/012051

53. Madsen K. Tracking welding productivity. Available at: https://weldingproductivity.com/article/tracking-welding-productivity/ (Accessed: 18 August 2019)

54. Nykänen T., Li X., Björk T., Marquis G. A parametric fracture mechanics study of welded joints with toe cracks and lack of penetration. Engineering Fracture Mechanics. 2005; 72(10): 1580–1609. Available at: DOI:10.1016/j.engfracmech.2004.11.004

55. Nguyen TC., Weckman DC., Johnson DA. Predicting onset of high speed gas metal arc weld bead defects using dimensional analysis techniques. Science and Technology of Welding and Joining. 2007; 12(7): 634–648. Available at: DOI:10.1179/174329307x236797

56. dos Santos Paes LE., Pereira M., Weingaertner WL., Scotti A., Souza T. Comparison of methods to correlate input parameters with depth of penetration in Laser welding. International Journal of Advanced Manufacturing Technology. T; 2019; 101(5–8): 1157–1169. Available at: DOI:10.1007/s00170-018-3018-2

57. Sathiya P., Abdul Jaleel MY., Katherasan D., Shanmugarajan B. Optimization of laser butt welding parameters with multiple performance characteristics. Optics and Laser Technology. Elsevier; 2011; 43(3): 660–673. Available at: DOI:10.1016/j.optlastec.2010.09.007

58. Deshmukh AR., Venkatachalam G., Divekar H., Saraf MR. Effect of weld penetration on fatigue life. Procedia Engineering. 2014; 97: 783–789. Available at: DOI:10.1016/j.proeng.2014.12.277

59. Quintino L., Costa A., Miranda R., Yapp D., Kumar V., Kong CJ. Welding with high power fiber lasers - A preliminary study. Materials and Design. 2007; 28(4): 1231–1237. Available at: DOI:10.1016/j.matdes.2006.01.009

60. Zhang M., Wang X., Zhu G., Chen C., Hou J., Zhang S., et al. Effect of laser welding process parameters on microstructure and mechanical properties on butt joint of new hot-rolled nano-scale precipitation-strengthened steel. Acta Metallurgica Sinica (English Letters). 2014; 27(3): 521–529. Available at: DOI:10.1007/s40195-014-0081-z

61. Benyounis KY., Olabi AG., Hashmi MSJ. Effect of laser welding parameters on the heat input and weld-bead profile. Journal of Materials Processing Technology. 2005; 164–165: 978–985. Available at: DOI:10.1016/j.jmatprotec.2005.02.060

62. Suder WJ., Williams S. Power factor model for selection of welding parameters in CW laser welding. Optics and Laser Technology. 2014; 56: 223–229. Available at: DOI:10.1016/j.optlastec.2013.08.016

63. Suder WJ., Williams SW. Investigation of the effects of basic laser material

interaction parameters in laser welding. Journal of Laser Applications. 2012; 24(3): 032009. Available at: DOI:10.2351/1.4728136

64. Kim YC., Hirohata M., Murakami M., Inose K. Effects of heat input ratio of laser–arc hybrid welding on welding distortion and residual stress. Welding International. Taylor & Francis; 2015. pp. 245–253. Available at: DOI:10.1080/09507116.2014.921039

65. Shi S. Laser and hybrid laser MAG welding of thick section. International Forum on Welding Technologies in Energy Engineering. 2005; (September): 21–23. Available at: https://www.twi-global.com/technical-knowledge/published-papers/laser-and-hybrid-laser-mag-welding-of-thick-section-c-mn-steel-september-2005

66. Wang XN., Zhang SH., Zhou J., Zhang M., Chen CJ., Misra RDK. Effect of heat input on microstructure and properties of hybrid fiber laser-arc weld joints of the 800 MPa hot-rolled Nb-Ti-Mo microalloyed steels. Optics and Lasers in Engineering. Elsevier; 2017; 91(November 2016): 86–96. Available at: DOI:10.1016/j.optlaseng.2016.11.010

67. Bunaziv I., Frostevarg J., Akselsen OM., Kaplan AFH. The penetration efficiency of thick plate laser-arc hybrid welding. International Journal of Advanced Manufacturing Technology. 2018; 97(5–8): 2907–2919. Available at: DOI:10.1007/s00170-018-2103-x

68. Fellman A., Salminen A. Study of the phenomena of fiber laser-MAG hybrid welding. International Congress on Applications of Lasers & Electro-Optics. 2007; 1604: 871–880. Available at: DOI:10.2351/1.5061017

69. C.Roepke., S.Liu., S.Kelly., R.Martukanitz. Hybrid laser arc welding process evaluation on DH36 and EH36 steel. Welding Journal. 2010; 89(July): 140–150. Available at: http://files.aws.org/wj/supplement/wj0710-140.pdf

70. Liu S., Liu F., Zhang H., Shi Y. Analysis of droplet transfer mode and

forming process of weld bead in CO 2 laserMAG hybrid welding process. Optics and Laser Technology. Elsevier; 2012; 44(4): 1019–1025. Available at: DOI:10.1016/j.optlastec.2011.10.016

71. Kong F., Liu W., Ma J., Levert E., Kovacevic R. Feasibility study of laser welding assisted by filler wire for narrow-gap butt-jointed plates of high-strength steel. Welding in the World. 2013; 57(5): 693–699. Available at: DOI:10.1007/s40194-013-0068-9

72. Möller F., Kügler H., Kötschau S., Geier A., Goecke SF. Gap bridging ability in laser GMA hybrid welding of thin 22MnB5 sheets. Physics Procedia. Elsevier B.V.; 2014; 56(C): 620–629. Available at: DOI:10.1016/j.phpro.2014.08.052

73. Lamas J., Frostevarg J., Kaplan AFH. Gap bridging for two modes of laser arc hybrid welding. Journal of Materials Processing Tech. Elsevier B.V.; 2015; 224: 73–79. Available at: DOI:10.1016/j.jmatprotec.2015.04.022

74. Rao PY., Rajesh Kumar S., Mohanty BS., Arunkumar N. Distortion control in thin low carbon steel plates using stiffeners and sequential welding. International Journal of Scientific and Research Publications. 2015; 5(8): 1–9. Available at: http://www.ijsrp.org/research-paper-0815.php?rp=P444402

75. Yang YP., Dull R., Castner H., Huang TD., Fanguy D. Material strength effect on weld shrinkage and distortion. Welding Journal. 2014; 93(11): 421s-430s. Available at: https://www.researchgate.net/publication/281006634_Material_Strength_Effect_on_Weld_Shrinkage_and_Distortion

76. Chavan MHK., Shelake MGD., Kadam DMS. Effect of heat input and speed of welding on distortion in MIG welding. International Journal of Industrial Engineering. 2012; 3(12): 42–50. Available at: https://www.semanticscholar.org/paper/EFFECT-OF-HEAT-INPUT-AND-SPEED-OF-WELDING-ON-IN-MIG-Chavan-

Shelake/8a33133f97f9df15f7c253ffc4b48dd51ed31e9f

77. Gangwar AS., Srivastava A., Gupta N., Rajan R. Experimental study of distortion in butt welds of mild steel plates and EN-31 plates having different thickness and weld cross sections. IOSR Journal of Mechanical and Civil Engineering. 2017; 14(03): 51–80. Available at: DOI:10.9790/1684-1403045180

78. Nasir NSM., Razab MKAA., Mamat S., Ahmad MI. Review on welding residual stress. ARPN Journal of Engineering and Applied Sciences. 2016; 11(9): 6166–6175. Available at: https://www.researchgate.net/publication/303788758_Review_on_Welding_Residual_Stress

79. Ikeagu CR. Evaluating the effect of different welding processes on the distortion of 4mm thick DH36 ship panels. MSc thesis. Cranfield University; 2011.

80. Kazanas P. Evaluation of heating methods for distortion reduction of 4 mm S355 ship plates. MSc thesis. Cranfield University; 2008.

81. Suder W., Ganguly S., Williams S., Paradowska AM., Colegrove P. Comparison of joining efficiency and residual stresses in laser and laser hybrid welding. Science and Technology of Welding and Joining. 2011; 16(3): 244–248. Available at: DOI:10.1179/1362171810Y.0000000020

82. Anbarasan N., Oyyaravelu R., Kuppan P. Effect of GMAW process parameters on the influence of bead geometry and HAZ area on ASTM A516 grade 70 Low alloy Pressure vessel steel. International Journal of TechnoChem Research. 2015; 01(01): 1–10. Available at: www.technochemsai.com

83. Melo LGTC de., Cardoso FI., Mendes CE., Ferreira RAS., Barros PS., Rolim TL. Welded joints' heat affected zone's extension prediction by switching welding parameters. Materials Research. 2017; 20(suppl 2):

651–656. Available at: DOI:10.1590/1980-5373-mr-2016-1019

84. Winarto W., Oktadinata H., Siradj ES. Microstructure and hardness properties of butt and fillet GMAW welded joints on HY80 high strength steel plate. In: Hari Prasetyo, Nurul Hidayati ES and TW (ed.) AIP Conference Proceedings. Surakarta, Indonesia; 2018. pp. 060020–060021 to 060020–060027. Available at: DOI:10.1063/1.5046656

85. Dong H., Hao X., Deng D. Effect of welding heat input on microstructure and mechanical properties of HSLA steel joint. Metallography, Microstructure, and Analysis. 2014; 3(2): 138–146. Available at: DOI:10.1007/s13632-014-0130-z

86. Santillan Esquivel A., Nayak SS., Xia MS., Zhou Y. Microstructure, hardness and tensile properties of fusion zone in laser welding of advanced high strength steels. Canadian Metallurgical Quarterly. 2012; 51(3): 328–335. Available at: DOI:10.1179/1879139512Y.0000000002

87. Y. Tobe and f.v. lawrence J. Effect of inadequate joint penetration on fatigue resistance of high-strength structural steel welds. Welding Research Supplement. 1977; (September): 259s-266s. Available at: https://app.aws.org/wj/supplement/WJ_1977_09_s259.pdf

88. Joseph A., Harwig D., Farson DF., Richardson R. Measurement and calculation of arc power and heat transfer efficiency in pulsed gas metal arc welding. Science and Technology of Welding and Joining. 2003; 8(6): 400–406. Available at: DOI:10.1179/136217103225005642

89. Talaş Ş. The assessment of carbon equivalent formulas in predicting the properties of steel weld metals. Materials and Design. 2010; 31(5): 2649–2653. Available at: DOI:10.1016/j.matdes.2009.11.066

90. Tong H., Ueyama T., Harada S., Ushio M. Quality and productivity improvement in aluminium alloy thin sheet welding using alternating current pulsed metal inert gas welding system. Science and Technology of Welding

and Joining. 2004; 6(4): 203–208. Available at: DOI:10.1179/136217101101538776

91. Churiaque C., Chludzinski M., Porrua-Lara M., Dominguez-Abecia A., Abad-Fraga F., Sánchez-Amaya J. Laser hybrid butt welding of large thickness naval steel. Metals. 2019; 9(1): 100. Available at: DOI:10.3390/met9010100

92. Huebla M. Investigation on laser-GMAW hybrid process in welding of structural beams. MSc thesis. Cranfield University; 2013.

93. Blecher J., Palmer T., Debroy T. Mitigation of Root Defect in Laser and Hybrid Laser-Arc Welding. Welding Research. 2015; 94(March): 73-s-82-s. Available at: https://www.researchgate.net/publication/279321301_Mitigation_of_Root_Defect_in_Laser_and_Hybrid_Laser-Arc_Welding

94. Ilar T., Eriksson I., Powell J., Kaplan A. Root humping in laser welding-an investigation based on high speed imaging. Physics Procedia. 2012; 39(December): 27–32. Available at: DOI:10.1016/j.phpro.2012.10.010

95. Hu J., Tsai HL. Effects of current on droplet generation and arc plasma in gas metal arc welding. Journal of Applied Physics. 2006; 100(5). Available at: DOI:10.1063/1.2337261

96. Xie J. Dual beam laser welding. Welding Journal (Miami, Fla). 2002; 81(10): 223–230. Available at: http://files.aws.org/wj/supplement/10-2002-XIE-s.pdf

97. Martukanitz RP. A critical review of laser beam welding. Industrial Lasers and Applications. 2005; 5706(March 2005): 11–24. Available at: DOI:10.1117/12.601655

98. Rubben K., Mohrbacher H., Leirman E. Advantages of using an oscillating laser beam for the production of tailored blanks. Lasers in Material Processing. 2010; 3097(August 1997): 228–241. Available at:

DOI:10.1117/12.281143

99. Joesbury AM. New approaches to composite metal joining. PhD thesis. Cranfield University; 2016.

Appendices

Appendix A Tensile test results

A.1 Tensile strength of HLAW and ALW process samples

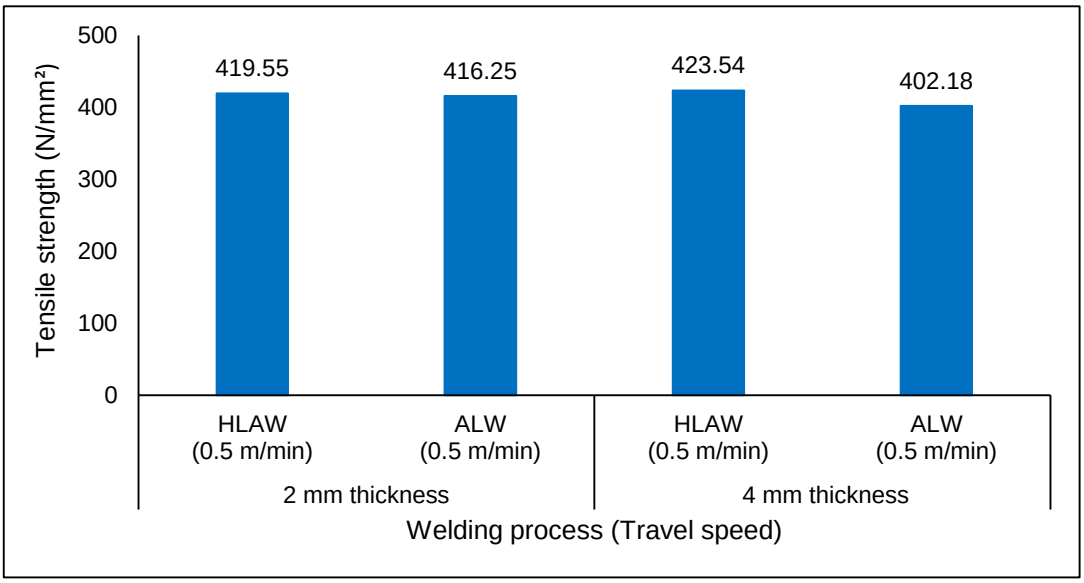

Figure A-1 Tensile strength of samples welded by HLAW and ALW processes at welding speed of 0.5 m/min

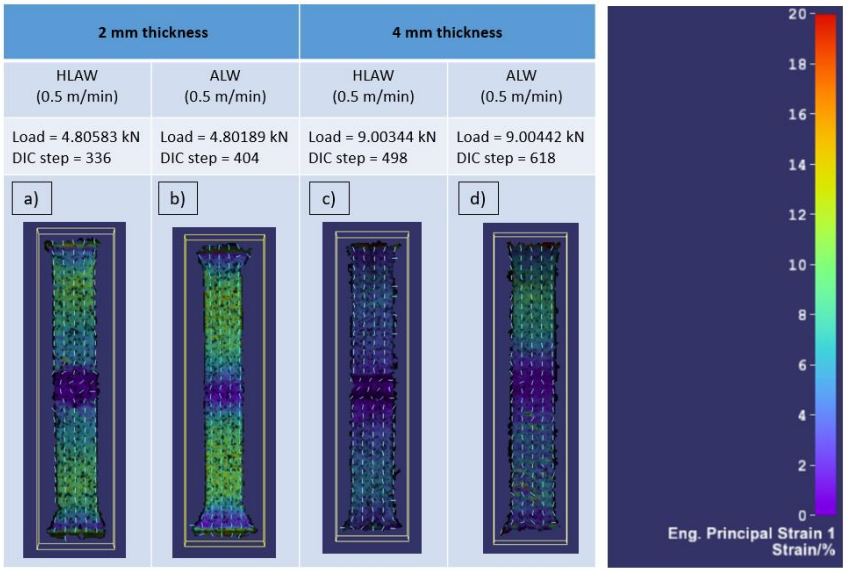

Figure A-2 Visual observation of strain by DIC in the samples welded by HLAW and ALW processes at welding speed of 0.5 m/min

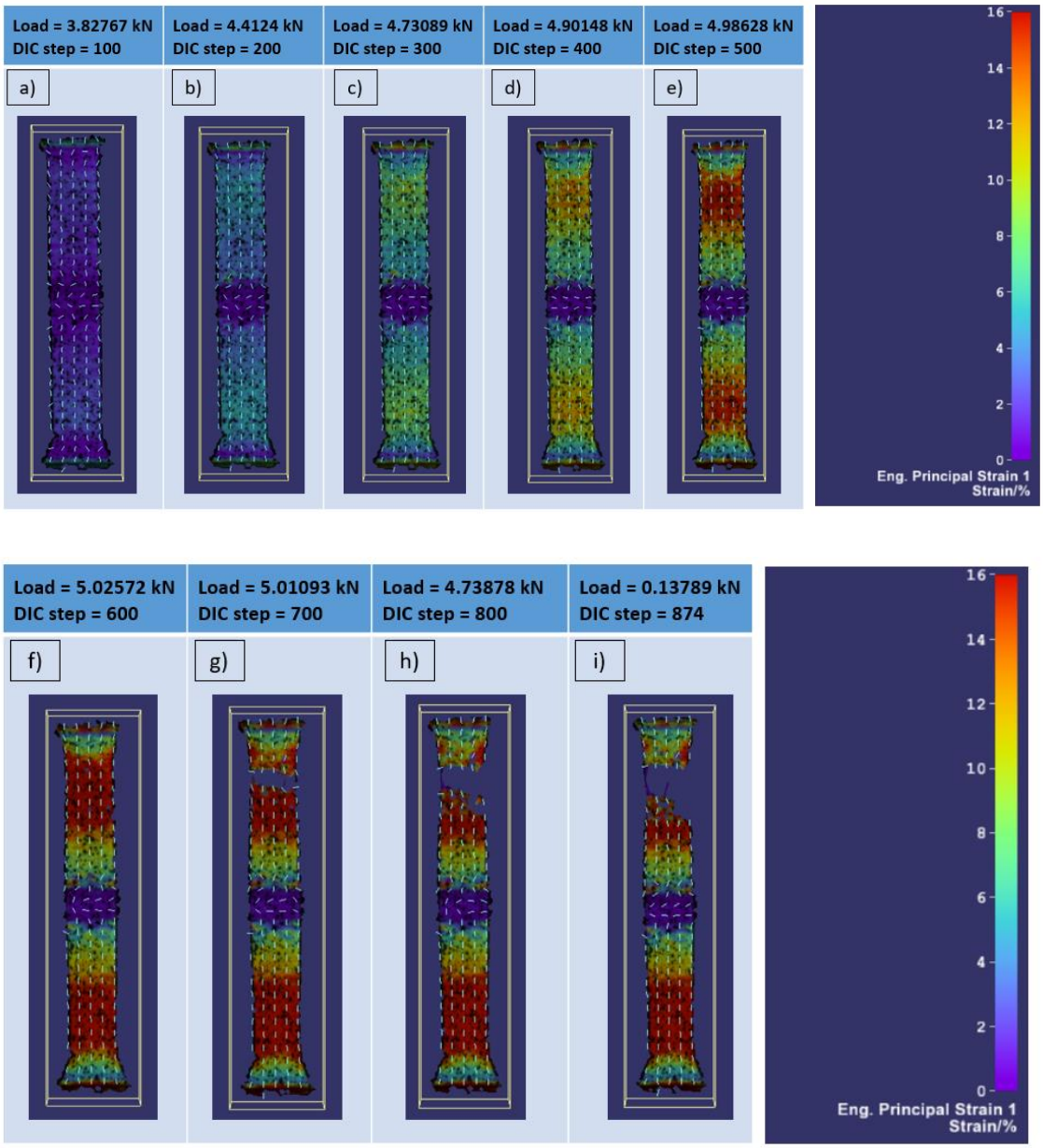

Figure A-3 Comparison of strain distribution at different load conditions in 2 mm thick sample welded by HLAW process at welding speed of 0.5 m/min

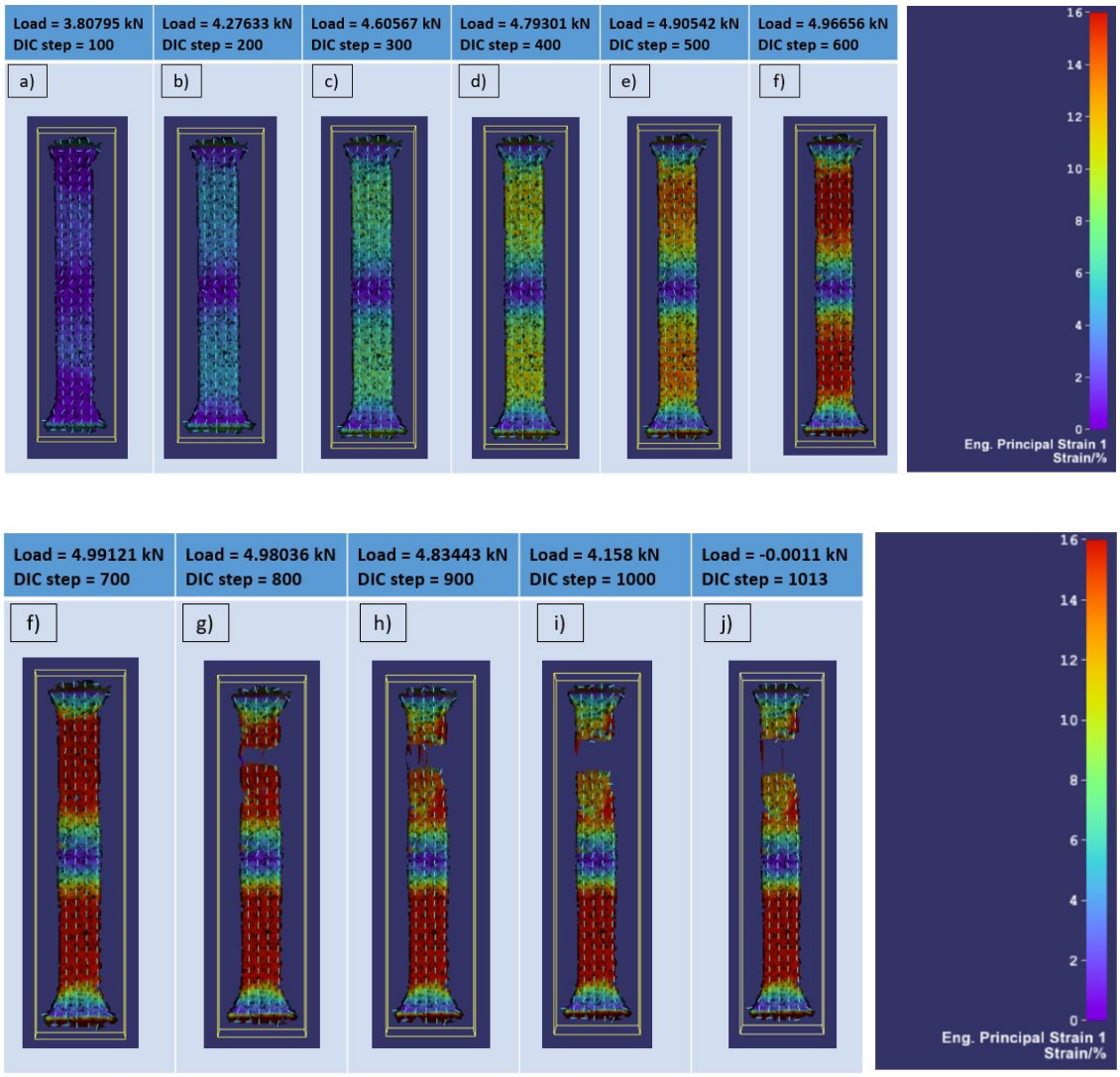

Figure A-4 Comparison of strain distribution at different load conditions in 2 mm thick sample welded by ALW process at welding speed of 0.5 m/min

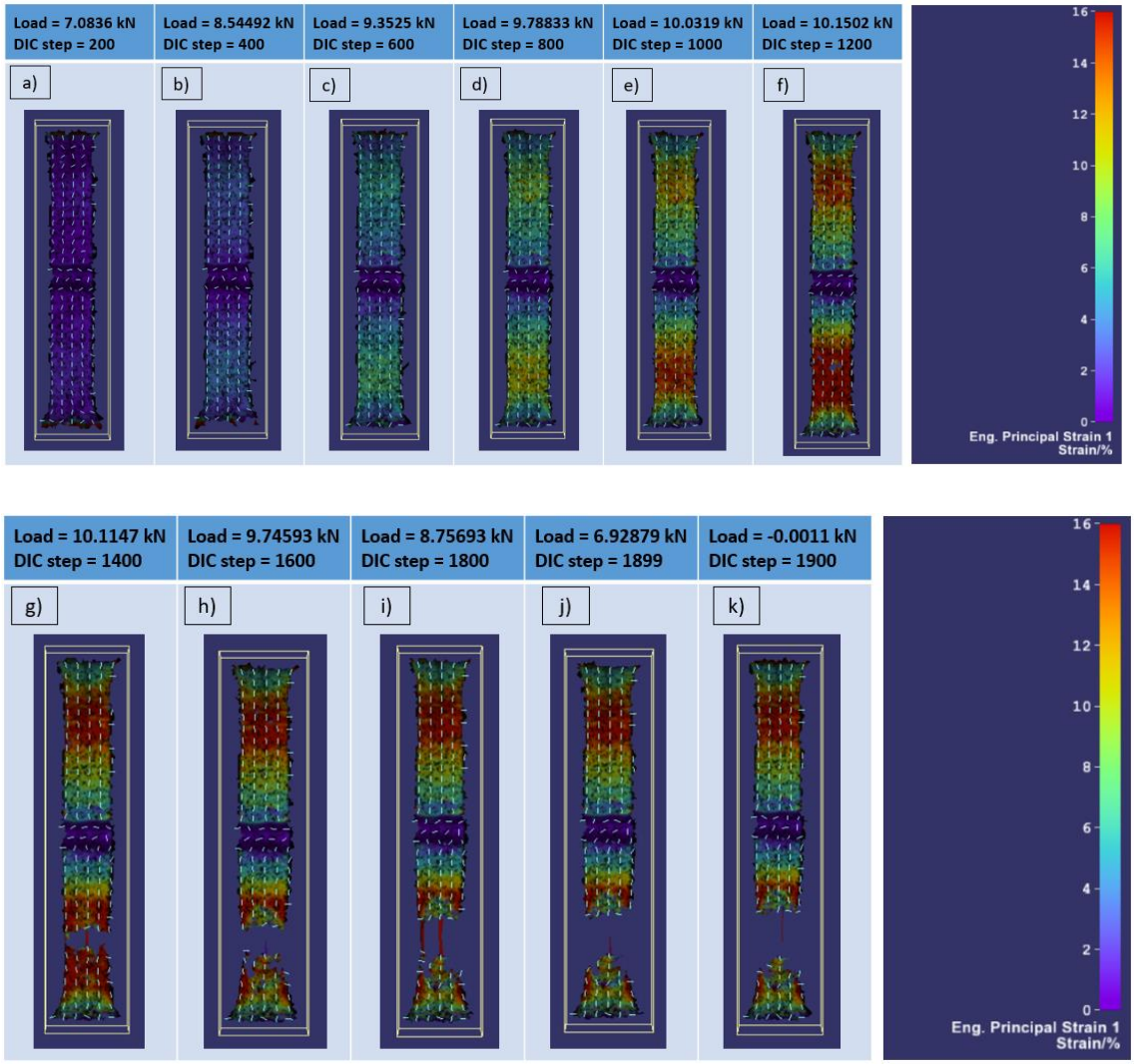

Figure A-5 Comparison of strain distribution at different load conditions in 4 mm thick sample welded by HLAW process at welding speed of 0.5 m/min (Captured at 2 fps)

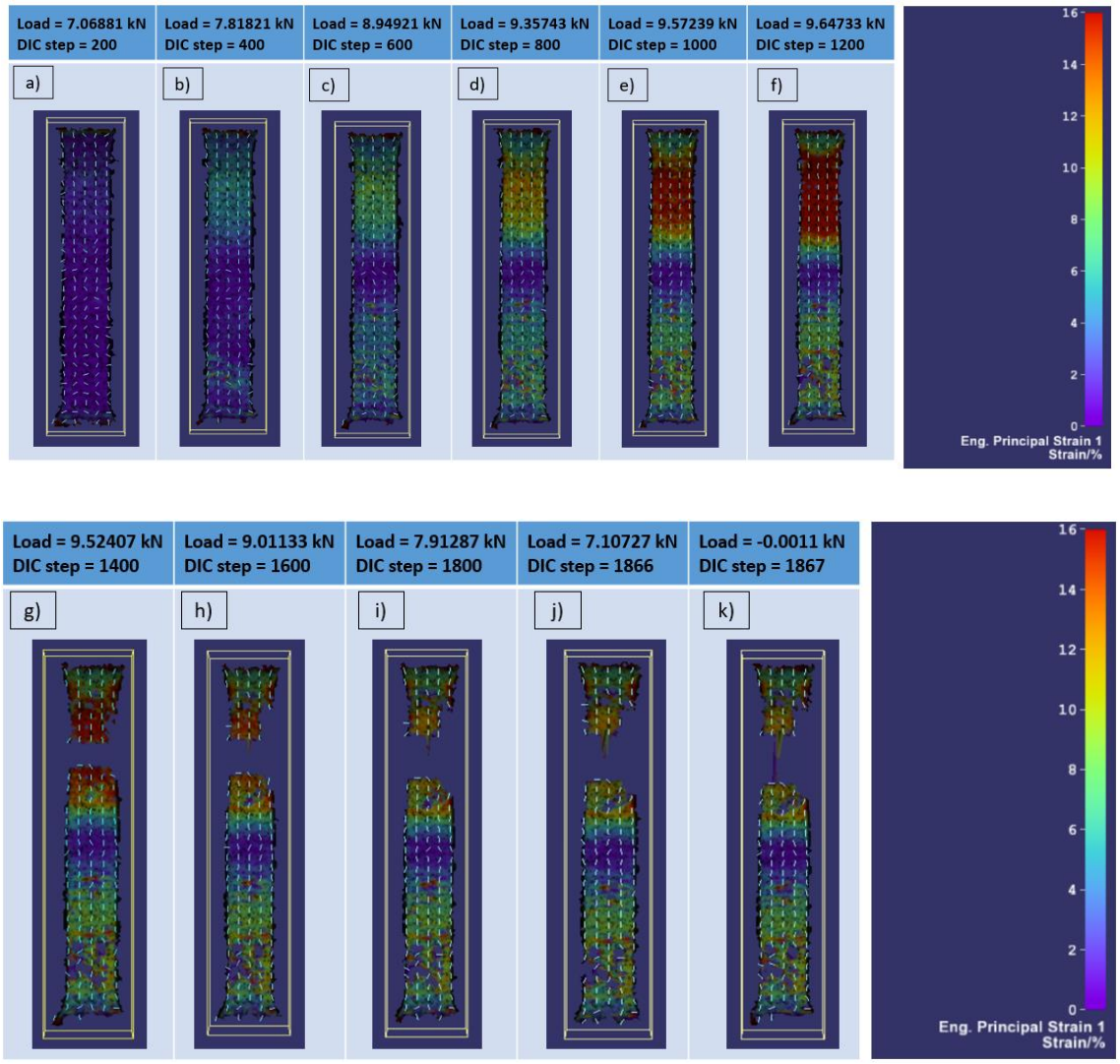

Figure A-6 Comparison of strain distribution at different load conditions in 4 mm thick sample welded by ALW process at welding speed of 0.5 m/min (Captured at 2 fps)

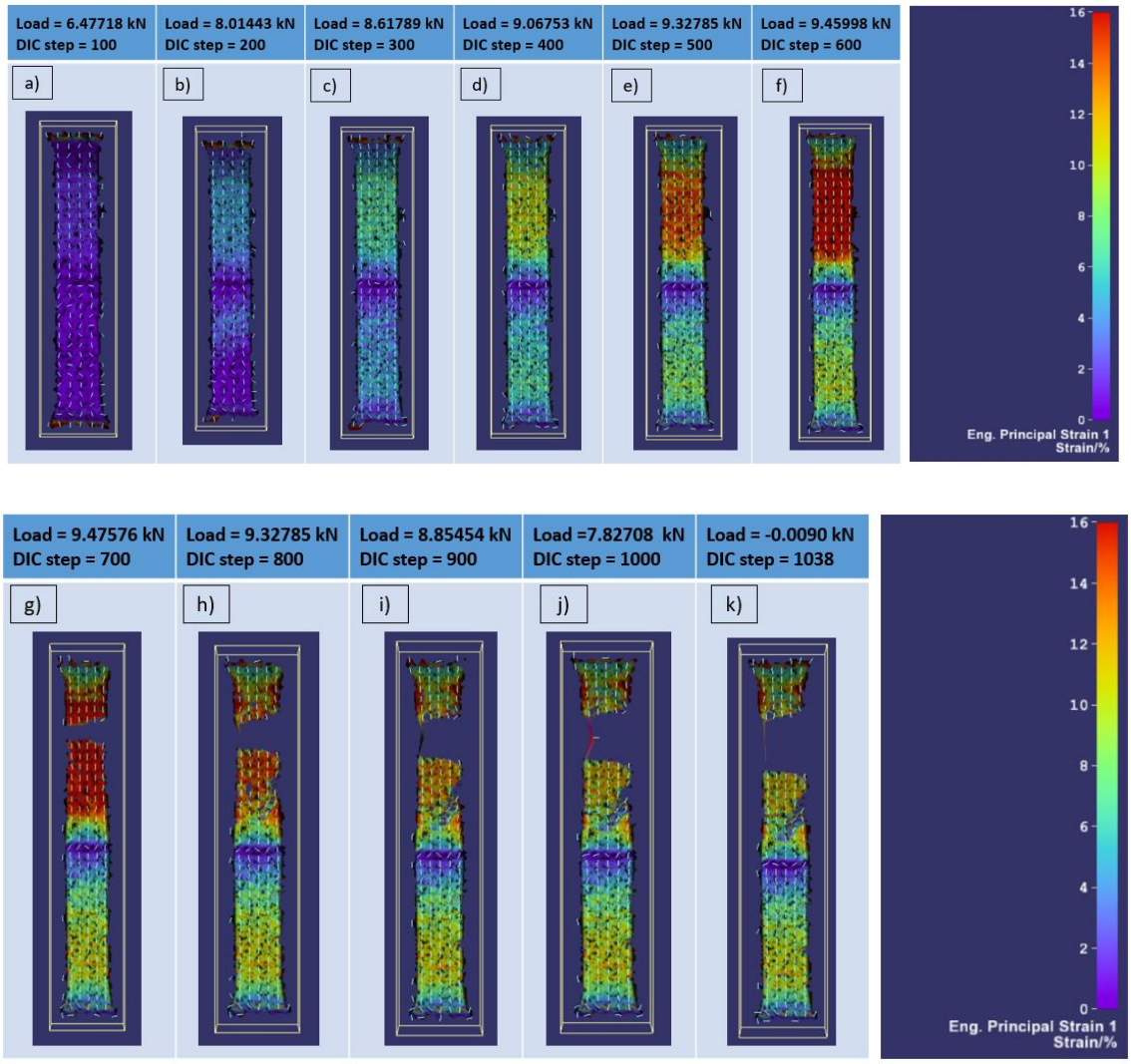

Figure A-7 Comparison of strain distribution at different load conditions in 4 mm thick sample welded by HLAW process at welding speed of 4 m/min

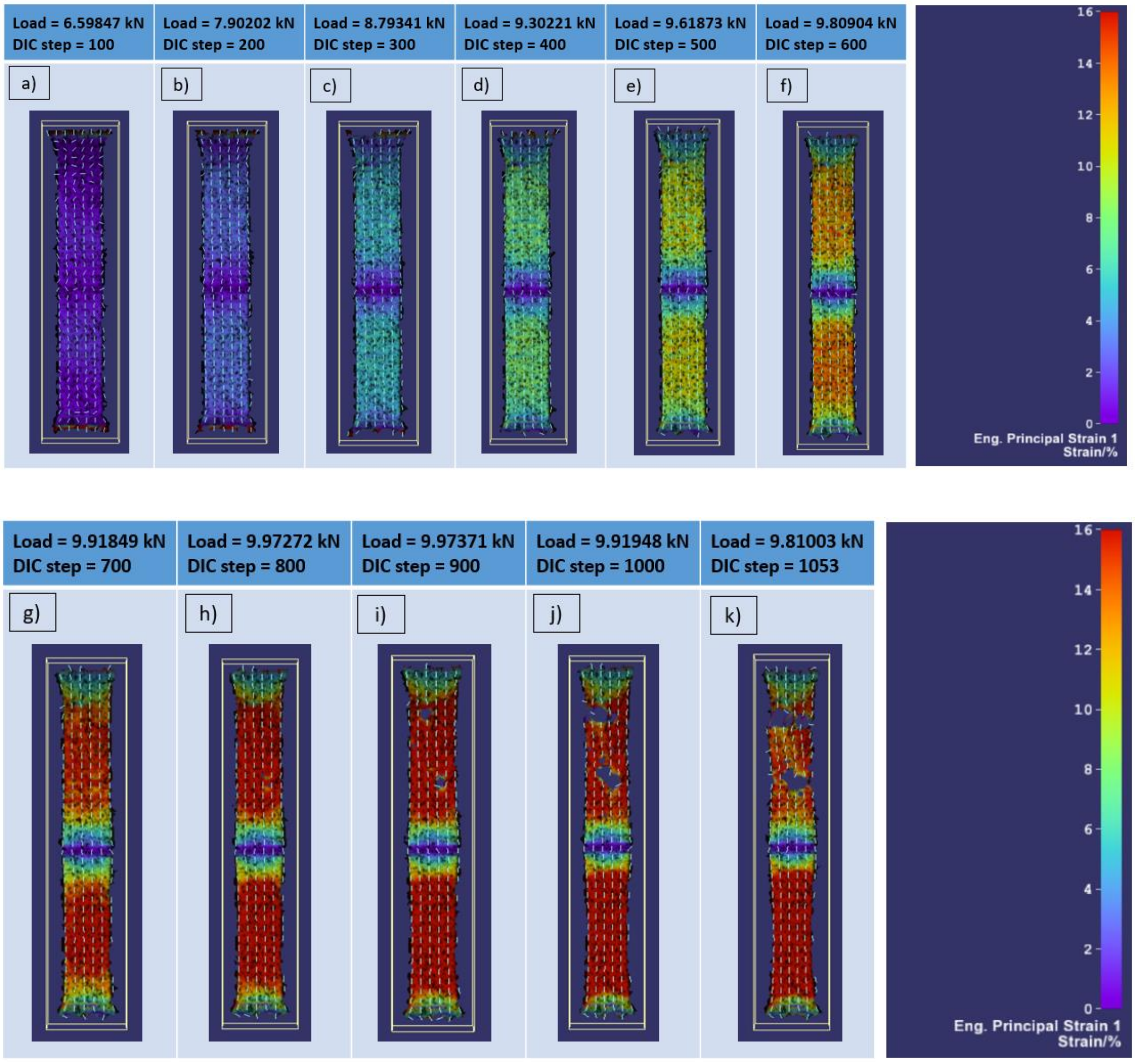

Figure A-8 Comparison of strain distribution at different load conditions in 4 mm thick sample welded by ALW process at welding speed of 4 m/min